
Damping properties and morphological characteristics of primary feathers

Dissertation

in fulfillment of the requirements for the degree “Dr. rer. nat”
of the Faculty of Mathematics and Natural Sciences
at Kiel University

submitted by

Kai Deng

Kiel, 2023

First examiner: Prof. Dr. Stanislav N. Gorb

Second examiner: Prof. Dr. Zhendong Dai

Date of the oral examination: 14.02.2024

Acknowledgments

First, I would like to express deepest gratitude to my supervisor, Prof. Dr. Stanislav N. Gorb. He offered me the opportunity to work in his research group with invaluable memories. Furthermore, he encouraged me to follow my ideas, supported me in many aspects, and kindly helped me in the most challenging times.

I am very grateful to Prof. Dr. Zhendong Dai, my second advisor at Nanjing University of Aeronautics and Astronautics (NUAA) in China, for his cooperation project, invaluable guidance, and constructive advice. Furthermore, his encouragement and recommendation of my German adventure significantly influenced me.

I sincerely thank Dr. Hamed Rajabi, Dr. Alexander Kovalev, and Dr. Clemens Schaber for their kind guidance, patient discussions, and availability of support in paper corrections. I owe them a particular debt of gratitude for their patience and every response.

I also thank my colleagues for their help. First, my special gratitude goes to Dr. Yoko Matsumura and Dr. Chuchu Li for the mental relaxation and valuable tips. Thanks to Dr. Emre Kizilkan, Dr. Chao Wan, Dr. Yun Ma, Dr. Shuto Ito, and Dr. Halvor Tramsen for their helpful comments, Dr. Ali Khaheshi, and Dr. Thies Büscher for their team support and encouragement, Ms. Angela Veenendaal for her kind helps on administration issues and daily warm smiles.

I express deep gratitude to my family for loving and supporting me in every critical moment. And thanks to my cats, Sascha and Kaiser, for their company.

I acknowledge the financial support of the Chinesisch-Deutsches Zentrum für Wissenschaftsförderung (Grant no. GZ1154 for SNG and ZDD) for my research at Kiel University.

Abstract

Flight provides to the birds efficient locomotion and occupation of various habitats. Wings and feathers sustain strong forces and vibration during flapping flight. Excessive vibration can lead to the stronger energy consumption, noise production and can therefore negatively impact the flight stability. Hence, it is reasonable to hypothesize that the primary feathers develop damping mechanisms to mitigate vibrations. Although feather microstructures have been well investigated, their damping properties still lack a systematic study. Here, this study shows that the primary flight feathers are capable of various damping mechanisms related to different structures.

In the shafts and barbs, the cortex and gradient foam support the mechanical bending and decay vibrations. The first indication of graded damping properties was related to the morphology of the shaft (foam cells size, area ratio of foam to cortex, and percentage of foam). In the vanes, there are three different types of structures related to the reduction of damping. First, we performed experiments to compare damping properties between feathers with vanes and the bare shaft without vanes. After trimming vanes, the damping ratio decreased by 38-60%. Second, the damping of zipped vanes and unzipped vanes was studied under normal air pressure. The results indicate that the zipped vanes have higher damping ratios. The planar surface of zipped vanes is responsible for aerodynamic damping, contributing 20% to 50% to the whole damping in a feather. Thirdly, the damping tests between zipped and unzipped vanes in vacuum were performed. Structural damping demonstrates 3.3 times (at vertical deflection) and 2.3 times (at horizontal deflection) difference in damping ratio between zipped and unzipped feathers in vacuum.

Kurzzusammenfassung

Die Fähigkeit zu fliegen ermöglicht Vögeln effiziente Fortbewegung und schnelle Anpassung in unterschiedlichen Lebensräumen. Flügel und Federn von Vögeln sind beim Schlagflug starken Kräften und Vibrationen ausgesetzt. Übermäßige Vibrationen können zu einem höheren Energieverbrauch, einer höheren Geräuschentwicklung und somit zu einer Beeinträchtigung der Flugstabilität führen. Deshalb ist anzunehmen, dass die Schwungfedern in ihrer Evolution verschiedene Dämpfungsmechanismen entwickelt haben, um die Vibrationen abzumildern. Obwohl die Mikrostrukturen von Federn bereits gründlich erforscht wurden, gibt es hinsichtlich der Dämpfungseigenschaften noch keine systematischen Analysen. Diese Studie zeigt, dass die Schwungfedern über verschiedene Dämpfungsmechanismen verfügen, die auf unterschiedliche Strukturen zurückzuführen sind.

Im Schaft und in den Fahnenstrukturen unterstützen Kortex und Gradientenschaum das mechanische Biegen und reduzieren die Vibration. Primär sind die Dämpfungseigenschaften abhängig von der Morphologie des Schaftes (Größe der Schaumzellen, Flächenverhältnis von Schaum und Kortex, und Schaumanteil). Bei der Fahne gibt es drei verschiedene Arten von Strukturen, die Einfluss auf die Dämpfungseigenschaften haben.

Zuerst wurde ein Vergleich zwischen den Dämpfungseigenschaften von Federn mit Fahnen und dem bloßen Schaft ohne Fahne durchgeführt. Nachdem die Fahnen entfernt wurden, hat sich das Dämpfungsverhältnis um 38-60% verringert. Danach wurde das Dämpfen von intakten und auseinandergezogenen Fahnen unter normalen Luftdruckverhältnissen untersucht. Die Resultate zeigen, dass die intakten Fahnen größere Dämpfungsverhältnisse haben. Die ebenen Flächen der intakten Fahnen sind für die aerodynamische Dämpfung verantwortlich. Sie tragen 20-50% zur gesamten Dämpfung der Feder bei. Zuletzt wurden Tests zwischen intakten und auseinandergezogenen Fahnen im Vakuum durchgeführt. Die strukturelle Dämpfung zeigt einen 3,3-fachen (vertikale Richtung) und 2,3-fachen (horizontale Richtung) Unterschied im Dämpfungsverhältnis zwischen intakten und auseinandergezogenen Fahnen im Vakuum im Vergleich zum Versuch unter normalen Luftdruckverhältnissen.

Table of Contents

1. Introduction	7
1.1 Flight related apparatus 7	
1.1.1 Avian body, respiratory system	7
1.1.2 Wings and tail	8
1.1.3 Flight feather.....	9
1.2 Feather: evolution, morphology, and mechanical characteristics 10	
1.4.1 Shaft	12
1.4.2 Vanes	16
1.4.3 Vibrations	19
2. The link between the morphology and damping properties of the foam-filled shaft of primary feathers	25
2.1 Introduction 26	
2.2 Materials and methods 28	
2.2.1 Sample preparation	28
2.2.2 Damping test.....	29
2.2.3 Feather morphology.....	30
2.2.4 Fitting of oscillation curves	30
2.3 Results and Discussion 31	
2.3.1 Damping properties of shaft segments	31
2.3.2 Feather shaft morphology	33
2.3 Effect of cortex and gradient foam structure 37	
2.4 Conclusions 38	
3. The function of vanes: a strategy to increase damping property in feathers.....	43
3.1 Introduction 44	
3.2 Materials and methods 47	
3.2.1 Morphological analysis.....	47
3.2.2 Damping tests	47
3.3 Results and Discussion 48	
3.3.1 Morphology	48
3.3.2 Damping behavior	49

3.3.3 Damping ratio	54
3.4 Conclusions	56
4. The significance of the zipped design in the vanes.....	62
4.1 Introduction	63
4.2 Materials and methods	65
4.2.1 Feather preparation and morphology observations.....	65
4.2.2 Damping test at the atmospheric pressure and in the vacuum condition.....	65
4.3 Results	67
4.3.1 Morphology	67
4.3.2 Damping behaviors	68
4.3.3 Vibration frequency	73
4.3.4 Damping in air	74
4.3.5 Damping in vacuum.....	75
4.4 Discussion and conclusion	76
5. Discussions.....	83
5.1 Morphology-damping relationship in the shaft	83
5.2 Damping of vanes	84
5.3 Damping of zipped vanes and unzipped vanes	85
5.4 Outlook	86
6. Conclusions	88

CHAPTER 1

Introduction

Flying ability can offer animals many benefits over non-flying animals of similar size. For example, flight affords more predator-escape routes and possible access to remote or higher locations (Alexander, 2015). The question ‘How do birds fly’ attracted so much attention over a long history of science. Avian flight triggered a long exploration from cave drawings to the technological revolution. Nowadays, we are still struggling to find more precise answers.

The basic laws enlightened the 17th and 18th centuries of physics explorers. The contributions of Daniel Bernoulli, Gottfried, Isaac Newton, and Leonhard Euler, set up the foundation of the mechanics of fluids (Videler, 2005). A century later, Otto Lilienthal tested his fly machines, and Osborne Reynolds provided insights into the different patterns in fluid flow (Videler, 2005). Finally, in the 20th century, the steady-state aerodynamic theory of fixed wings was established (Videler, 2005).

For so long, scientists and engineers have learned a lot from birds. They figured out how to generate the lift force and developed artificial flying devices. However, the flexibility and maneuverability are still far behind those of birds. To better understand avian flight, we further explore how birds’ flight apparatus meets the flying requirements, especially in vibration in each beating.

1.1 Flight-related apparatus

1.1.1 Avian body, respiratory system

Different types of flight and the related aerodynamic basis of the flight mechanism of birds have been investigated (Brown, 1963; Simpson, 1983). Birds must counteract gravity and deal with drag to be airborne (Bachmann, 2010). The avian bodies have cancellous bones, and fusion skeleton is reshaped to keep strong but lightweight (Sullivan et al., 2017). Birds possess a streamlined body with a rounded surface leading part and a pointed one at the trailing part (Alexander, 2015). Moreover, the

ratio between diameter and length is optimized to decrease drag. The largest diameter is at 1/3 of the length, and the ratio of diameter over length is between 1/4-1/5 (Videler, 2005). The neck and legs are expected to change their position and adjust the center of gravity during flight. The legs also help them to run, push off, and absorb energy when landing.

Flying birds can travel long distances, not only relying on body shape adaptations but also due to their respiratory and cardiovascular adaptations. The relationship between respiratory frequency, body temperature, and heart beat in different flights was studied and quantitatively analyzed in a wind tunnel (Butler et al., 1977).

1.1.2 Wings and tail

In birds, the wings are the most prominent flight-related parts of the body and receive the most scientists' attention. Wings are curved on the top, which forces the air to move fast and causes lift by low pressure, and the lift changes with the titling leading edge, camber, speed, and wing area (Alexander, 2015). Bird wings consist of an arm and a hand part, covered by feathers and connected by skeletal elements controlled by muscles (Kondo et al. 2018). Wings can be folded and stretched. They unfold and stretch at the onset of flight, flex during the upstroke, and extend before the downstroke. Significant variability of the wings has evolved among birds due to different demands by birds (Videler, 2005). Characteristics of the wing form were discussed, including the ratio of wing length to chord, overall size, weight divided by the wing and body area, sweep angles, camber and tip shape of wings, and so on (Weger, 2017). Wings must be strong enough during flapping by exchanging forces with the airflow and receiving the reactive forces. Simultaneously, wings must be light to reduce the inertial forces in the flapping cycles. Feathers are crucial elements for flight performance. They extend the shape of birds, especially that of the wings.

The tail comprises a few caudal vertebrae and pygostyle (Videler, 2005). The functional morphology study in the pigeon's tail (*Columba livia*) has been performed in detail (Baumel, 1988). Tail feathers, called rectrices, are attached to the tail and connected to the modified vertebrae. These rectrices differ in length and shape, which could form a variation of the tail shape (Videler, 2005). Furthermore, tail asymmetry

could be controlled by spreading and tilting angles of rectrices to meet the requirements of flight.

1.1.3 Flight feathers

Among the wings, feathers are essential for the flight performance (Weger, 2017): Several types of feathers are connected to a bird wing (Fig. 1). The primary flight feathers extend over the wing tip, and secondary flight feathers form a caudal wing part, while the covert feathers could change the thickness of cambered part of the wing.

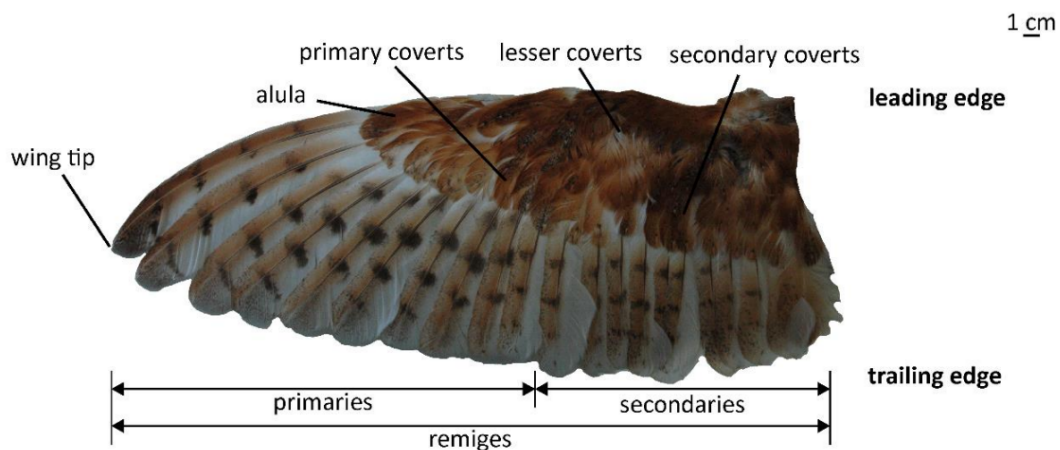


Fig.1 Wing and different feather types (*Tyto furcata pratincola*) (Weger, 2017)

The flight feathers create the aerodynamic surface of the wing to generate lift. As all main components of wings, primary feathers can withstand high cyclic loads and vibration during the flaps. Here the question raises: how primary feathers' design strategies prevent the potential instability caused by unwanted vibrations. This thesis aims to answer the above question. For this purpose, the author first conducted observations combining modern imaging techniques, including scanning electron microscopy and micro-computed tomography. Then, the damping tests were performed on primary feathers, to study the effect of different components of the shaft and vanes, which influence the feathers' damping behavior.

The thesis is subdivided into the following chapters. After this short introduction, I further provide a review of the literature regarding the structure and mechanical

properties of the wing feathers (Chapter 1). Chapter 2 presents the relationship between damping capability and the shaft microstructure, combined with a solid cortex and foamy medulla. We investigate the graded damping in the different locations in the shaft. In Chapter 3, the damping performance of feathers with and without vanes was characterised. In Chapter 4, the vane function in damping behavior was studied more thoroughly by comparing feathers in zipped and unzipped conditions in atmosphere and vacuum. In Chapter 5, a general discussion and outlooks are given. A short conclusion is presented in Chapter 6.

1.2 Bird feathers: evolution, morphology, and mechanical characteristics

During avian flight, their wings and feathers experience aerodynamic forces and resist vibrations (Bachmann et al., 2012; Schmitz et al., 2014; Harvey and Inman, 2022). Since flight feathers interact with the airflow, it is essential to understand the role of functional morphology in the damping property of primaries. This part summarizes the literature to date, covering the evolution of flight feathers, the morphology of the feather components and their impact on mechanical characteristics, and the potential impact of associated vibrations on flight performance.

Early evolution of flight is documented by fossil record of feathered dinosaurs in diverse intermediate feather forms (Zhang et al., 2006; Xu et al., 2012). Many theropod dinosaurs and early birds possessed feather-like structures, such as rachis, barbs, and vanes (Figs. 2-3) (Zhang et al., 2006). Feathers have been optimized in the course of evolution (150 million years) and evolved hierarchical branches (Prum, 1999). Avian feathers are considered one of the most complex integumentary structures (Bonser and Purslow, 1995).

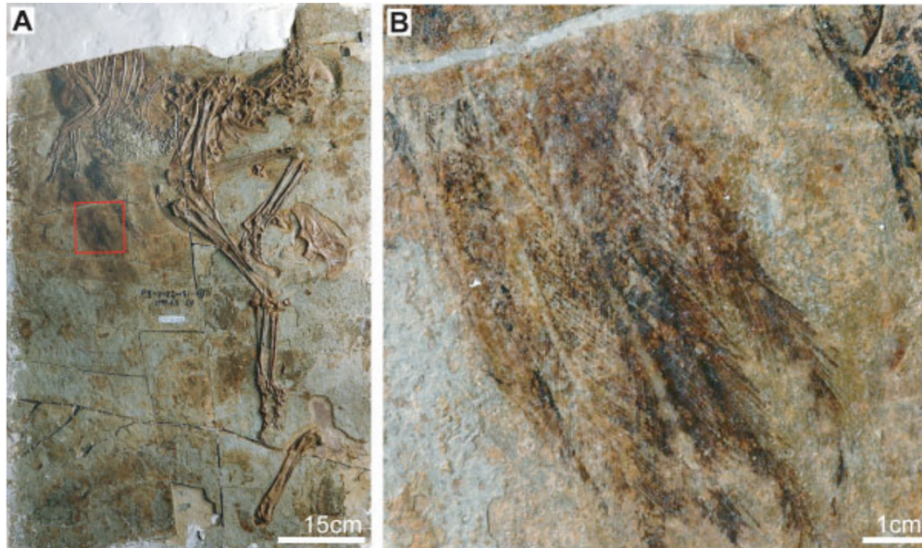


Fig. 2 (A) The image of theropod *Caudipteryx*; (B) Magnified view of complex integument structures similar to flight feathers of Mesozoic and extant birds (Zhang et al., 2006).



Fig. 3 Four types of feathers from Liaoning birds. (a) tail feather; (b) and (c) contour feathers imply their aerodynamic function by possessing a shaft, barbs, and barbules; (d) a strong and curved shaft with asymmetric vanes; (e) a weak shaft with long barbs (Zhang et al., 2006)

When seeking the evolutionary origin of the feathers, it is reasonable to put it into a morphological context. During the feather evolution, plumulaceous branches evolved for thermoregulation, water resistance, and pennaceous vanes for flight and display (Chen et al., 2012; Chang et al., 2019). These functions are based on the architecture composed of the shaft (rachis and calamus), barbs, and barbules (Chen et al., 2012). The flight feathers of the avian wings consist of a central foam-filled shaft and two vanes comprising barbs branching from the shaft and interlocking barbules branching from the barbs. The barbules adhere to neighboring via hook and grooved structures.

1.4.1 Shaft

As a lightweight multifunctional structure, feathers are composed of β -keratin and show remarkable regional specific types (Chen et al., 2012). The shaft extends the length of the feather and supports the herringbone-pattern barbs. In the center of the shaft, the cellular foam is surrounded by the cortex (Fig. 4), and this sandwich-like construction offers a maximum flexural-strength-to-weight ratio (Chen et al., 2012).

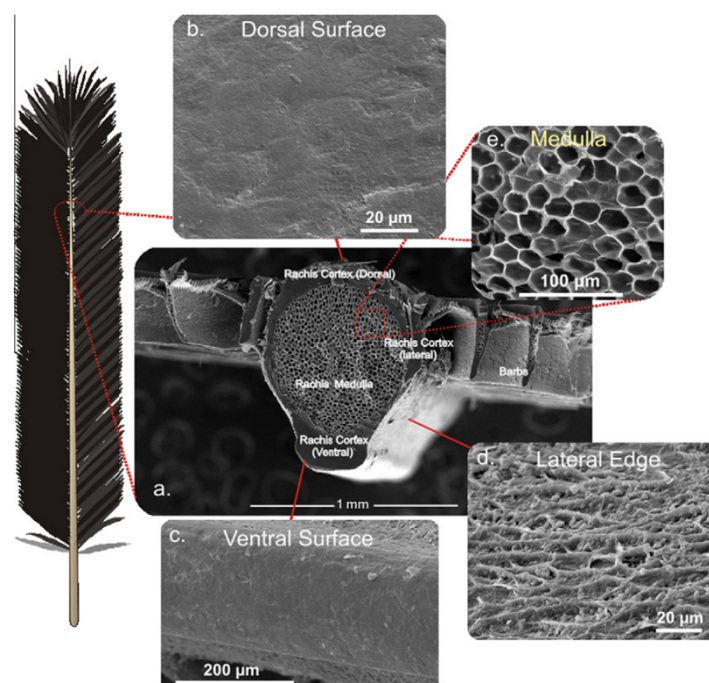


Fig.4 Hierarchical structure in the feather (*Toco toucan*). (a) SEM of the cross section of a distal rachis; (b) dorsal and (c) ventral cortical rachis keratin is smooth, which is expected to decrease the drag; (d) lateral cortical rachis keratin is fibrous (Chen et al., 2012)

The mechanical properties of biological materials show a wide variation due to their heterogeneous and composite nature (Chen et al., 2012). Biomechanics of feathers has been subject to scrutiny in the last decades. Wing kinetic energy is transferred to the air by a mechanism involving stored energy in the bent shafts of feathers (Fig. 5) (Pennycuick and Lock, 1976). The dorso-ventral flexural stiffness is higher than the lateral one to support the greater force in the downstroke during flapping (Fig. 6) (Purslow and Vincent, 1978). The flexural stiffness of the shaft varies along the length of feathers (Fig. 7) in different primary positions and species (Bonser and Purslow, 1995). The characteristics of the shaft and vanes were investigated; in the downward flap, the wider vanes are kept against the neighboring feathers shafts, forming a gas-impermeable surface that allows the secondary feathers to change the airfoil geometry with increasing angle of attack, while in the upward flap when the air pressure on the upper side becomes more significant than that on the lower side, the vanes are detached from the shafts of the neighboring feathers (Bostandzhiyan et al., 2008).

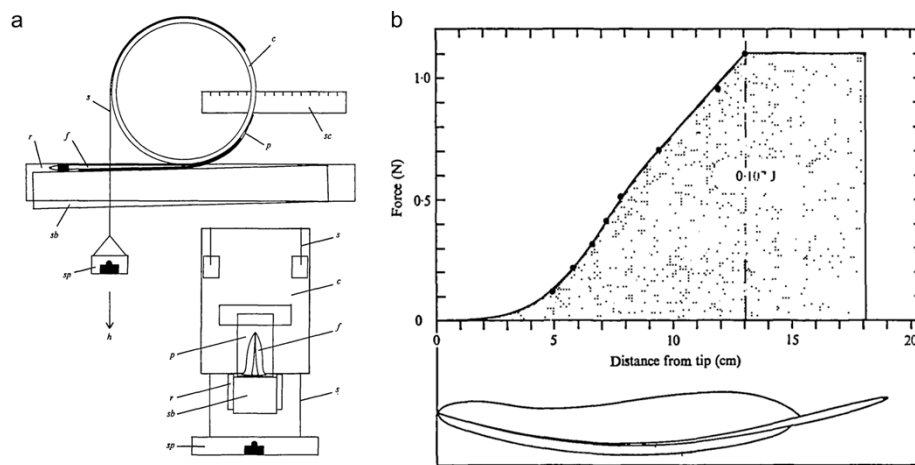


Fig. 5 (a) Apparatus for measuring bending feathers by a given radius of curvature. (b) Work diagram from an experiment of primary rolled a cylinder radius of 3.8 cm, 13 cm from the tip (Pennycuick and Lock, 1976)

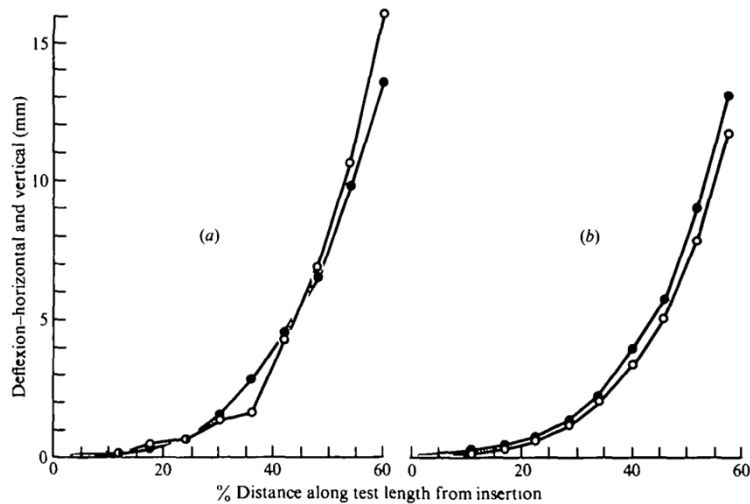


Fig. 6 Deflexions under load applied at distances along the shaft from a bird of 300g. (a) the outmost feather and (b) the feather immediately proximal to it. \circ = dorso-ventral bending, and \bullet = lateral bending (Purslow and Vincent, 1978)

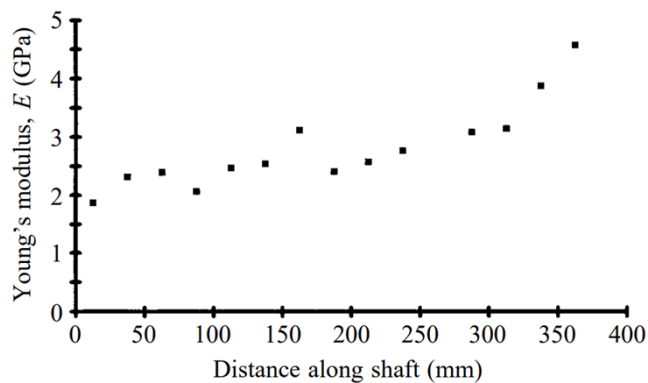


Fig. 7 Variation of Young's modulus along the length of primary feather from a mute swan (Bonser and Purslow, 1995)

Considering the weather condition, the influence of hydration on the structural properties of feathers also triggered some interest. Usually, the stiffness and strength of wet keratin were much lower than that of dry ones (Bonser, 2002). The failure properties and moduli of the feathers in tension were presented, and it was proved that a high-water content led to decreased stiffness, but to increased strain (Taylor et al., 2004).

The relationship between geometry and the mechanics of the shaft is well studied. Significant differences between proximal and distal feather regions show that the geometry influenced their Young's modulus and flexural stiffness in owls and pigeons, (Fig. 8) (Bachmann et al., 2012). The geometry and mechanical properties vary along the length have been examined on the shaft of a peacock's tail feather, and

lower strength and Young's modulus were confirmed under wet conditions compared with dry conditions (Liu et al., 2015).

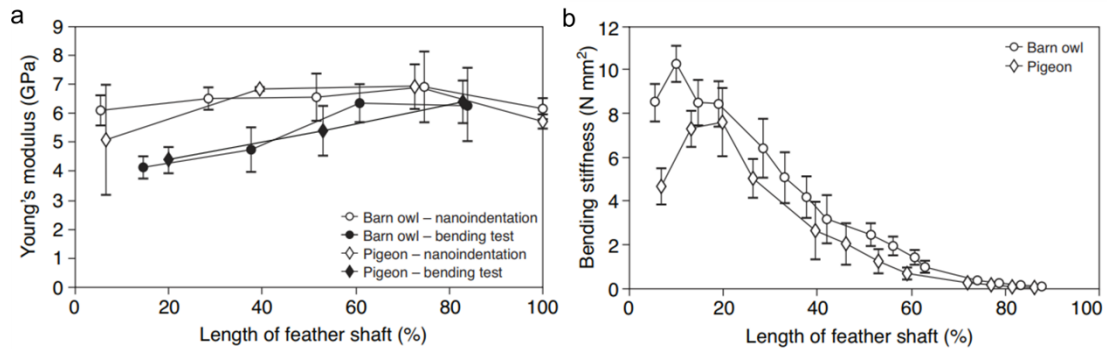


Fig. 8 (a) Young's modulus of feather rachis along the longitudinal length. (b) The bending stiffness of rachis along the longitudinal length, from 5th primaries from barn owls and pigeons (Bachmann et al., 2012)

A schematic drawing of the feather material with a detailed fiber orientation is based on microbial biodegradation (Fig. 9) (Lingham-Soliar et al., 2009). The shaft, as a multilayer fibrous composite with varying laminar properties, was examined by the nano-indentation tests. The CT scan validates the link between the stress values and the orientations of the laminae (Laurent et al., 2014). Later, the shape factor and layer-fiber structure were found in the cortex: the shape change allowed different bending rigidities and twists, and the dorsal and ventral cortex regions consisted of longitudinal and circumferential fibers (Wang and Meyers, 2016a).

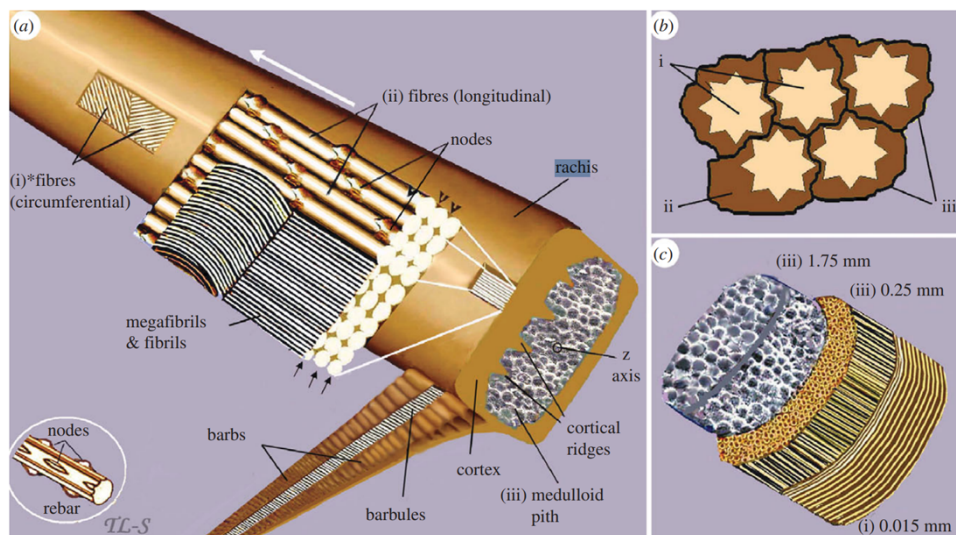


Fig.9 A schematic view of feather rachis. (a) i. superficial layer of fibers, circumferential around the rachis. ii. The major fiber parallel extends to the axis. iii. the medulloid pith is composed of air-filled foam structures. (b) Schematic cross-section of fibers and biodegraded

matrix, i fibers; ii residual cytosol of keratinocytes; iii integrating plasma membrane of original keratinocytes. (c) 3-dimensional cross-section of rachis showing approximate thickness. i. circumferential and ii longitudinal fiber of the cortex and iii polyhedral of medulloid pith (Lingham-Soliar et al., 2009)

Inside the cortex, the medulla foam was confirmed to have a minimal effect on stiffness and strength (Bonser, 1996). After medulla removal, the shaft was 16% less stiff (Bonser, 2001). Furthermore, the mean Young's modulus of foam (15.18 Mpa) with its mean density (0.061g cm^{-3}) was obtained from the compression test (Fig. 10) (Bonser, 2001). Although the foam within the shaft is less stiff than the cortex, it may be stiff enough to delay the buckling under compression (Bonser 2001) and bending conditions (Purslow and Vincent 1978), since the stress is transferred from the cortex to the medulla. Foam structures are used to enhance mechanical stability and increase energy absorption (Bonser and Purslow 1995; Gao et al. 2014). The dissipation energy of the foam medulla presumably also contributes to the feathers' damping properties.

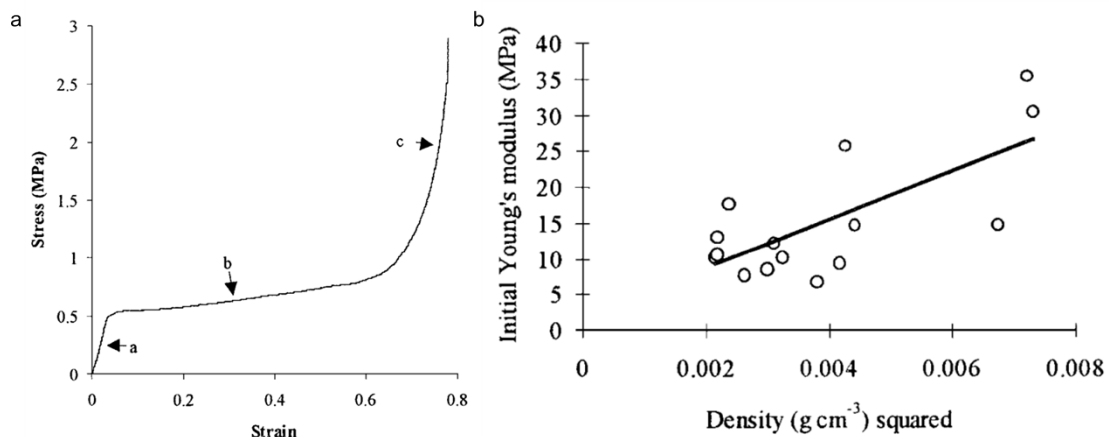


Fig.10 (a) Typical stress-strain curve for medullary foam. After an initial steep, linear portion reaches plateau stress, where strain increases rapidly, and finally, the foam cells collapse, causing densification. (b) Young's modulus of samples against their density. (Bonser, 2001)

1.4.2 Vanes

During feather evolution, pennaceous vanes evolved for functions of flight and display, while fluffy plumulaceous evolved for thermoregulation (Chang et al. 2019). Typical flight feathers consist of a shaft and two vanes. The primary feathers usually have symmetric vanes: a narrow one (outer vane) at the leading edge, and a wider one

(inner vane) at the trailing edge (Videler, 2005). The architecture of the vanes is linked with the advantage of aerial locomotion during evolution (Alibardi, 2007).

The microstructure of vanes was first observed in the goose feather (Hooke, 1665). The vanes consist of numerous barbs oriented in parallel but at some angle to the shaft (Prum and Williamson, 2001). The barbs carry a similar array of barbules, second-level branches, on either side (Kovalev et al., 2013). Moreover, two types of barbules have been described (Fig.11): the barbules on the distal barb with hooks interlocking with grooves situated on the proximal barbules of the next barb (Ennos et al., 1995).

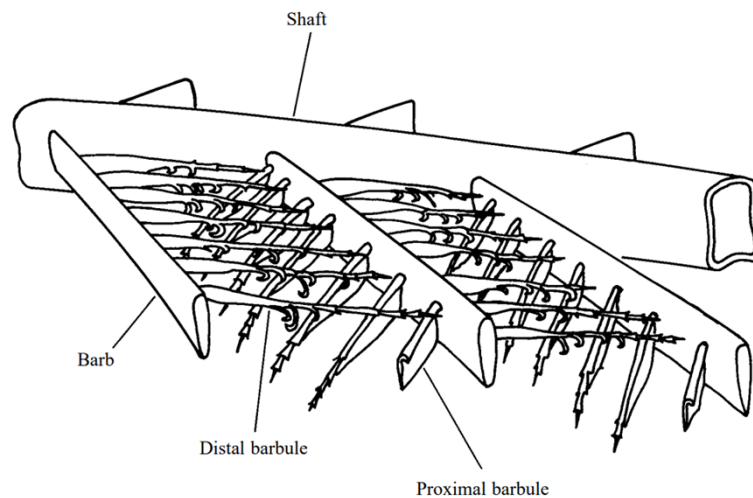


Fig.11 Structure of a primary flight feather, with the mechanism of attachment of adjacent barbs, hooked distal barbules grip grooved proximal barbules (Ennos et al., 1995)

A theory of the growth of feathers has been presented and simulated with a model based on six parameters: i. absolute barb and rachis ridge growth rate; ii. angle of helical growth of barb ridges; iii. initial barb ridge number; iv. new barb ridge addition rate; v. barb ridge diameter, and vi. the angle of barb ramus expansion following emergence from the sheath (Prum and Williamson, 2001). It is confirmed that the barb length determines the vane's asymmetry, and the barb angle varies with the vane function, which could influence their aerodynamic performance (Feo et al., 2014).

Concerning the mechanical properties of feather barbs, a micro-tensile test was performed at a speed of $0.02\mu\text{m/s}$ to get Young's modulus range of 3.13-3.66 GPa in flight feathers. (Gao et al., 2013). In addition, Young's modulus, the bending

stiffness, and the barb separation forces of feathers have been investigated in four species with different flight styles (Schmitz et al., 2014).

The overlapping and interlocking barbs in the vanes also attracted the researcher's attention. The mechanism of interlocking of the barbs and their reestablishment was studied and summarized in a numerical model by Kovalev et al. (2013) (Fig. 12). In addition, the separation force of single hooklets (14 μ N) and arrays of hooklets (1.74 mN in 20 arrays) was measured (Kovalev et al., 2013). The robustness and flaw-tolerance of the barbule structures have been explained by an analytical model based on small- and large-beam deflections (Chen et al., 2016).

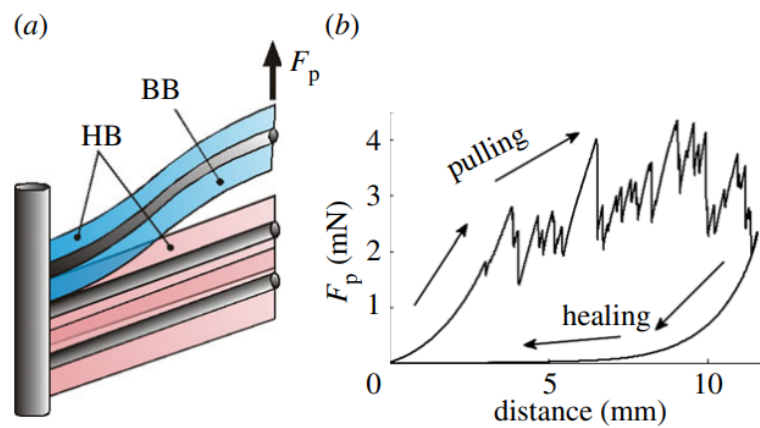


Fig.12 (a) Scheme of the experimental set-up. The feather was separated at the interface using a micromanipulator with a force transducer. The separation caused hook barbules (HB) detachment from bow barbules (BB). (b) The force and distance curve obtained from the measurement (Kovalev et al., 2013)

It was assumed that the membranous flaps of overlapping barbules of feathers are impervious to air (Dyck, 1985). The vane's permeability is based on the effect of barb dimensions and the degree of their mechanical interlocking (Sullivan et al., 2017). Furthermore, mechanical adhesion of 3D printed hooks and grooves, which have been simplified and scaled up the hook design of vanes, was performed, and the effects of thickness and shape have been investigated (Fig. 13) (Sullivan et al., 2017).

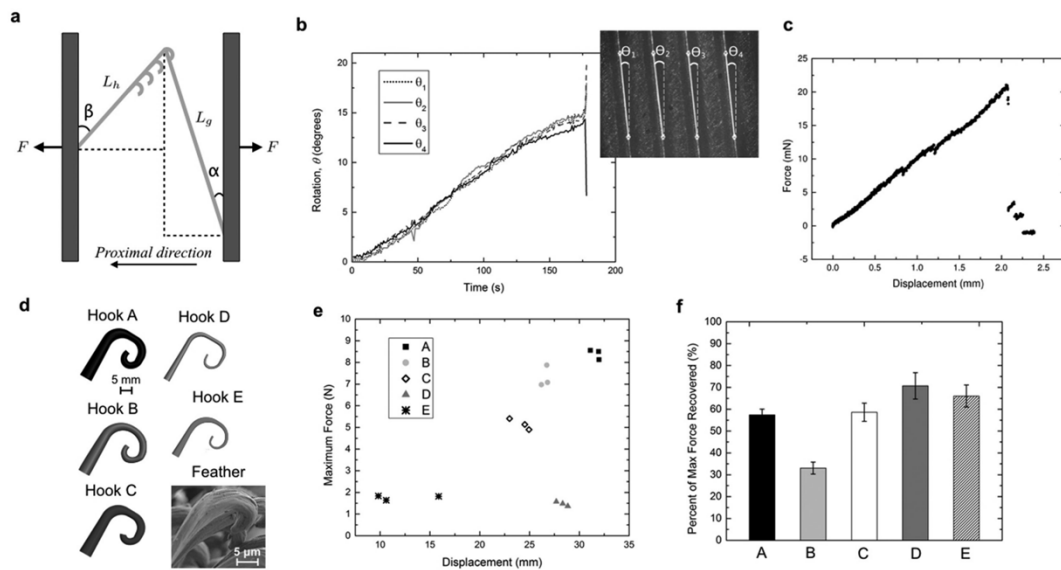


Fig.13 In-plane tension tests performed in the vanes. (a) A schematic of the lengths and angles of the hooked and grooved barbules. The proximal rotation was triggered by a greater moment applied to grooved barbules. (b) Barbules maintain attached as barbs rotate proximally at an angle θ throughout the test before failure. The angle is in the right image, where dashed lines mark the original barbs' position, and the solid lines mark the ending barbs' position. (c) A measured force displacement reveals that the feathers exhibit failure when unzipped. (d) Different hooks (A–E) were 3D printed. (e) The maximum force versus displacement for the tension of the hooked structures. Note that sample A has the maximum mechanical adhesion force. (f) Hooks D and E have the highest percentage of maximum recovered force measured in repeated adhesion tests. (Sullivan et al., 2017)

1.4.3 Vibrations

During flapping, wings undergo continuous oscillations (Greenwalt, 1960). Unwanted oscillations can negatively influence the performance of dynamic systems, such as giant reeds (Speck and Spatz, 2004), wings of dragonflies and damselflies (Rajabi et al., 2016; Lietz et al., 2021), and insect antennae (Rajabi et al., 2018). Damping alters the system response in oscillations, enhancing stability and controllability (De Silva, 1999). The loss factor is the ratio between the loss modulus and storage modulus, representing a system's viscoelasticity and damping capacity. The loss factor is in the range of 0.03 to 0.07 for the bending of the shaft of swan feathers (Bonser and Purslow, 1995) and 0.896 ± 0.238 for the shafts of pigeon feathers (Gao et al., 2014).

The vibration-related silent flight of owls has been described since the early 20th century. The reduction of noise in flight provides two advantages for their hunting: firstly, it enables better detection of acoustic signals from the prey, and secondly, it

makes it more difficult for the potential detection of owls (Weger and Wagner, 2017). Several studies confirmed that the noise emission of owls is diminished, especially at higher frequencies (Geyer et al., 2014). The reduced noise in many owl species is achieved by their wing and feather morphology. For example, barn owl wings show a shape optimized to lower flight speeds, like an anteriorly thickened, highly cambered proximal wing and a thinner, low-cambered distal part (Bachmann, 2010). Furthermore, its noise-reduced function was explained by inner vane fridges of feathers, combined with the morphometric (seen Fig.14) (Weger and Wagner, 2017) and air-flow studies (Bachmann et al., 2012;). Furthermore, the flight of the owl was compared to that of the common buzzard, revealing that the leading-edge serration and trailing-edge fringe in owls led to the lower noise emission (Chen et al., 2012).

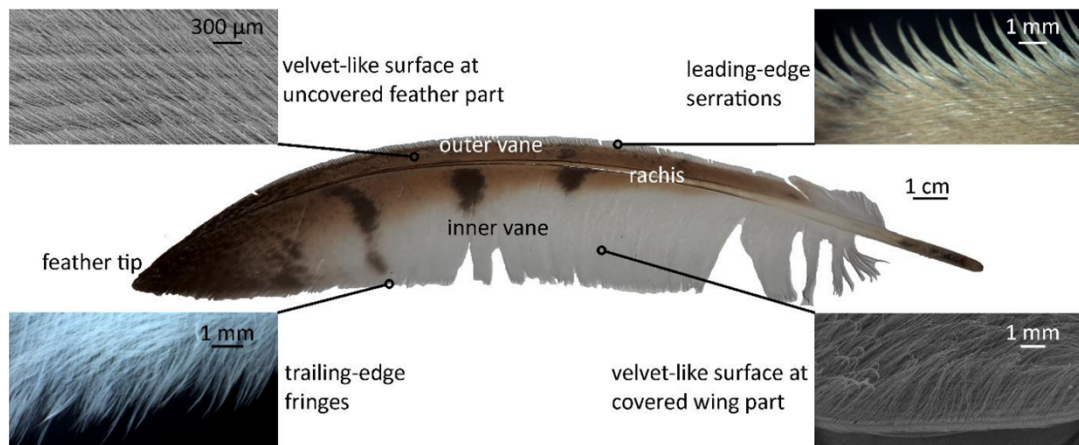


Fig.14 The specializations in the outmost primary feather of the owl (*T. furcata pratincola*). Serrations (upper right) can be found at the leading edge only on specific feathers. Two types of velvet structures: one in uncovered feather parts (upper left) and one in covered parts (lower right). And the trailing edge exhibits fringes (lower left) (Wegner and Wagner, 2017)

The other acoustics investigations in birds have also been carried out. Sound classified as pressure waves is generated by vibrating structures that induce the vibration (Gao et al., 2015). In courtship display, peacock feathers perform the train-rattling using a range of vibration frequencies (22–28 Hz); higher damping of feathers broadens the resonant peaks and has the advantage of damping out oscillations (Dakin et al., 2016). In addition to the flight performance, the various acoustic communication functions are served by pressure waves when birds flap their wings (Hightower et al., 2021). Male Club-winged Manakins produce tonal sounds with specialized feathers, and the resonant properties were determined that the feathers

exhibit unusually high Q-values (Bostwick et al., 2010). The communication sounds generated in the wing and tail are mainly attributable to three mechanisms: flutter, percussion, and wing whirring (Clark et al., 2015). Pigeons produce tonal sounds during the downstroke when barbs of the inner vane of the outermost primary flutters (Niese and Tobalske, 2016). The modified feather of crested pigeons produces a specific tonal sound as an alarm sonation (Murray et al., 2017).

In summary, previous studies indicate that the feather's mechanical properties and morphology are rather well investigated. However, the damping behavior and mechanisms responsible for it are still missing as a systematic study. In the following chapters, we aim to address this question. We hypothesize that the primary feathers possess several damping mechanisms to mitigate vibrations. This study shows that the primary flight feathers have various damping mechanisms related to different feather structures, from the shaft to the vanes and hooked structures in the vanes.

References

- Alexander DE (2015). On the wing. Insects, pterosaurs, birds, bats and the evolution of animal flight. UK: Oxford University Press.
- Alibardi L (2007) Cell organization of barb ridges in regenerating feathers of the quail: implications of the elongation of barb ridges for the evolution and diversification of feathers. *Acta Zoologica*. 88, 101-117.
- Bachmann T (2010) Anatomical, morphometrical and biomechanical studies of barn owls' and pigeons' wings. PhD Thesis, RWTH Aachen.
- Bachmann T, Emmerlich J, Baumgartner W, Schneider JM and Wagner H (2012) Flexural stiffness of feather shafts: Geometry rules over material properties. *J. Exp. Biol.* 215 (3): 405-415.
- Bachmann T, Wagner H and Tropea C (2012) Inner vane fringes of barn owl feathers reconsidered: morphometric data and functional aspects. *J. Anat.* 221, 1-8.
- Baumel JJ (1988) Functional morphology of tail apparatus of the pigeon (*Columba livia*). *Adv. Anat. Embryol. Cell Biol.*, 110, 1-115.
- Bonser RHC (1996) The mechanical properties of feather keratin. *J. Zool. Lond.* 239, 477-484.
- Bonser RHC and Purslow PP (1995) The Young's modulus of feather keratin. *J. Exp. Biol.* 198, 1029-1033.
- Bonser RHC (2001) The mechanical performance of medulla foam from feathers. *J. Mater. Sci. Lett.* 20: 941-942.

-
- Bonser RHC (2002) Hydration sensitivity of ostrich claw keratin. *J. Mater. Sci. Lett.* 21, 1563-1564.
- Bostandzhiyan SA, Bokov AV and Shteinberg AS (2008) Flexural characteristics and aerodynamic aspects of design of the bird feather shaft. *Dokl. Phys.* 53, 9, 476-479
- Bostwick KS, Elias DO, Mason A and Montealegre-Z F (2010) Resonating feathers produce courtship song. *Proc. R. Soc. B.* 277, 835-841.
- Brown RHJ (1963) The flight of birds. *Biol. Rev.* 38, 460-489
- Butler PJ, West NH and Jones DR (1977) Respiratory and cardiovascular responses of the pigeon to sustained level flight in a wind tunnel. *J. Exp. Biol.* 71, 7-26.
- Chang W, Wu H, Chiu Y, Wu P, Juan W and Chuong C (2019) The making of a flight feather: Bio-architectural principles and adaption. *Cell* 179, 1409-1423
- Chen K, Liu Q, Liao G, Yang Y, Ren L, Yang H and Chen X (2012) The sound suppression characteristics of wing feather of Owl (*Bubo bubo*). *J. Bionic. Eng.* 9, 192-199
- Chen P, Mckittrick J and Meyers MA (2012) Biological materials: function adaptations and bioinspired designs. *Prog. Mater. Sci.* 57, 1492-1704.
- Chen Q, Gorb SN, Kovalev A, Li Z and Pugno N (2016) An analytical hierarchical model explaining the robustness and flaw-tolerance of the interlocking barb-barbule structure of bird feathers. *Europhys Lett.* 116 (2): 24001.
- Clark CJ and Prum RO (2015) Aeroelastic flutter of feathers, flight and the evolution of non-vocal communication in birds. *J. Exp. Biol.* 218, 3520-3527.
- Dakin R, McCrossan O, Hare JF, Montogomerie R and Kane AS (2016). Biomechanics of the peacock's display: How feather structure and resonance influence multimodal signaling. *PLoS One.* 11(4), e0152759.
- De Silva, CW (1999) *Vibration: fundamentals and practice.* Boca Raton, USA.
- Deng K, Kovalev A, Rajabi H, Schaber CF, Dai ZD and Gorb SN. (2022) The damping properties of the foam-filled shaft of primary feathers of the pigeon *Columba livia*. *Sci. Nat.*, DOI:10.1007/s00114-021-01773-7.
- Dyck J (1985) The evolution of feathers. *Zool. Scrip.* 14, 2, 137-154.
- Ennos AR, Hickson JRE and Roberts A (1995) Functional morphology of the vanes of the flight feathers of the pigeon *Columba livia*. *J. Exp. Biol.* 198, 1219-1228.
- Gao JL, Zhang GQ, Guan L, Chu JK, Kong DY and Bi YT (2013) Structure and mechanical property of *Asio otus* feather barbs. *Key Eng. Mater.* 562-565: 914-919.
- Gao JL, Chu JK, Guan L, Shang HX and Lei ZK (2014) Viscoelastic characterization of long-eared owl flight feather shaft and the damping ability analysis. *Shock Vib.* 709367.
- Gao JL, Chu JK, Shang HX and Guan L (2015) Vibration attenuation performance of long-eared owl plumage. *Bioinspir. Biomim.* Nan. 4, BBN3.
- Geyer T, Sarradj E and Fritzsche C (2014) Measuring owl flight noise. In *INTER-NOISE and NOISE-CON Congress and Conf. Proc.*, 183-198.

-
- Greenewalt CH (1960) The wings of insects and birds as mechanical oscillators. Proc. Amer. Phil. Soc. 104, 6, 605-611.
- Hansen C (2018) Foundations of vibroacoustics. Boca Raton, USA.
- Harvey C and Inman D (2022) Gull dynamic pitch stability is controlled by wing morphing. PNAS, 119, 37, e2204847119.
- Hightower BJ, Wijnings PWA, Scholte R, Ingersoll R, Chin DD, Nguyen J, Shorr D and Lentink D (2020) How hummingbirds hum: oscillating aerodynamic forces explain timbre of humming sound. <https://doi.org/10.48550/arXiv.2009.01933>.
- Hooke, R. (1665) Micrographia: or some physiological descriptions of minute bodies made by magnifying glasses with observations and inquiries thereupon. London, UK.
- Kondo M, Sekine T, Miyakoshi T, Kitajima K, Egawa S, Seki R, Abe G and Tamura K (2018) Flight feather development: its early specialization during embryogenesis. Zool. Lett. 4 (1): 2.
- Kovalev A, Filippov AE, Gorb SN (2013) Unzipping bird feathers. J. R. Soc. Interface 11: 20130988.
- Laurent CM, Palmer C, Boardman RP, Dyke G and Cook RB (2014) Nanomechanical properties of bird feather rachises: exploring naturally occurring fibre reinforced laminar composites. J. R. Soc. Interface 11: 20140961.
- Lietz, C., Schaber, C. F., Gorb, S. N. and Rajabi, H. (2021) The damping and structural properties of dragonfly and damselfly wings during dynamic movement. Commun. Biol. 4, 737.
- Lingham-Soliar T, Bonser RHC, Wesley-Smith J. (2009) Selective biodegradation of keratin matrix in feather rachis reveals classics bioengineering. Proc. R. Soc. B. 227, 1161-1168.
- Liu ZQ, Jiao D, Meyers MA and Zhang ZF (2015) Structure and mechanical properties of naturally occurring lightweight foam-filled cylinder: The peacock's tail coverts shaft and its components. Acta Biomater. 17, 137-151.
- Murray TG, Zeil J and Magrath RD (2017) Sounds of modified flight feathers reliably signal danger in a pigeon. Curr. Biol. 27, 3520-3525.
- Niese R and Tobalske BW (2016) Specialized primary feathers produce tonal sounds during flight in rock pigeons (*Columba livia*). J. Exp. Biol. 219, 2173-2181.
- Pennycuik CJ and Lock A (1976) Elastic energy storage in primary feather shafts. J. Exp. Biol. 64, 677-689
- Prum RO (1999) Development and evolutionary origin of feathers. J. Exp. Zool. 285 (4): 291-306.
- Prum RO, Williamson S (2001) Theory of the growth and evolution of feather shape. J. Exp. Zool. 291 (1): 30-57
- Purslow PP and Vincent JFV (1978) Mechanical properties of primary feathers from the pigeon. J. Exp. Biol. 72 (1): 251-260.
- Rajabi H, Shafiei A, Darvizeh A, Dirks JH, Appel E and Gorb SN (2016) Effect of microstructure on the mechanical and damping behaviour of dragonfly wing veins. R. Soc. Open Sci. 3, 160006.

-
- Rajabi H, Shafiei A, Darvizeh A, Gorb SN, Dürr V, and Dirks JH (2018) Both stiff and compliant: morphological and biomechanical adaptations of stick insect antennae for tactile exploration. *J. R. Soc. Interface*, 15(144), 20180246.
- Schmitz A, Ponitz B, Bruecker C, Schmitz H, Herweg J, and Bleckmann (2015) Morphological properties of the last primaries, the tail feathers, and the alulae of *Accipiter nusus*, *Columba livia*, *Flaco peregrinus*, and *Falco tinunculus*. *J Morphol.* 276, 1, 33-46.
- Simpson SF (1983) The flight mechanism of the pigeon *Columbia livia* during take-off. *J. Zool. Lond.* 200,435-443.
- Speck O and Spatz HS (2004) Damped oscillations of the giant reed *Arundo donax* (Poaceae). *Am. J. Bot.* 91: 789-796.
- Sullivan TN, Wang B, Espinosa HD and Meyers MA (2017) Extreme lightweight structures: avian feathers and bones. *Mater. Today* 20 (7): 377-391.
- Taylor AM, Bonser RHC and Farrent JW (2004) The influence of hydration on the tensile and compressive properties of avian keratinous tissues. *J. Mater. Sci.* 39: 939-942.
- Videler JJ (2005). *Avian flight*. Oxford, UK: Oxford University Press.
- Vincent JFV and Owers P (1986) Mechanical design of hedgehog spines and porcupine quills. *J. Zool.* 210 (1): 55-75.
- Wang B and Meyers MC (2016) Light like a feather: A fibrous natural composite with a shape changing from round to square. *Adv. Sci.* 4 (3): 1600360.
- Weger M (2017) Morphological and functional investigations on feather specializations of owls (Strigiformes). PhD Thesis, RWTH Aachen.
- Weger M and Wagner (2017) Distribution of the characteristics of barbs and barbules on barn owl wing feathers. *J. Anat.* 230: 734-742.
- Xu X, Wang K, Zhang K, Ma Q, Xing L, Sullivan C, Cheng S and Wang S (2012) A gigantic feathered dinosaur from the Lower Cretaceous of China. *Nature* 92, 484, doi:10.1038.
- Yang W, Chao C and McKittrick J (2013) Axial compression of a hollow cylinder filled with foam: A study of porcupine quills. *Acta Biomater.* 9 (2): 5297-5304.
- Zhang F, Zhou Z and Gareth D (2006) Feathers and 'Feather-like' integumentary structure in Liaoning birds and dinosaurs. *Geol. J.* 41:395-404.

CHAPTER 2

The link between the morphology and damping properties of the foam-filled shaft of primary feathers

Summary:

Bird wings endure cycles of dynamic loading during their flap. Primary feathers are subjected to mechanical force, further experiencing vibrations that result from the airflow. The unwanted vibration may lead to the instability and noise of feathers. As an essential feather component, the foam-filled shaft showed a gradient structure. Here, we collected quantitative data to investigate the damping properties in the three locations of the shaft. The morphological-damping relationship of the shaft is found.

The damping properties of the foam-filled shaft of primary feathers of the pigeon *Columba livia*

K. Deng¹, A. Kovalev¹, H. Rajabi², C. F. Schaber¹, Z. D. Dai³ and S. N. Gorb¹

1. Functional Morphology and Biomechanics, Institute of Zoology, Kiel University, Kiel, Germany

2. School of Engineering, London South Bank University, London, England

3. Institute of Bioinspired Structure and Surface Engineering, Nanjing University of Aeronautics and Astronautics, Nanjing, China

Published by:

The Science of Nature (2022) 109:1

<https://doi.org/10.1007/s00114-021-01773-7>

Abstract

The avian feather combines mechanical properties of robustness and flexibility while maintaining a low weight. Under periodic and random dynamic loading, the feathers sustain bending forces and vibrations during flight. Excessive vibrations can increase noise, energy consumption and negatively impact flight stability. However, damping can alter the system response, resulting in increased stability and reduced noise. Although the structure of feathers has already been studied, little is known about their damping properties. In particular, the link between the structure of shafts and their damping is unknown. This study aims at understanding the structure-damping relationship of the shafts. For this purpose, Laser Doppler vibrometry (LDV) was used to measure the damping properties of the feather shaft in three segments selected from the base, middle, and tip. A combination of scanning electron microscopy (SEM) and micro-computed tomography (μ CT) was used to investigate the gradient microstructure of the shaft. The results showed the presence of two fundamental vibration modes, when mechanically excited in the horizontal and vertical directions. It was also found that the base and middle parts of the shaft have higher damping ratios than the tip, which could be attributed to their larger foam cells, higher foam/cortex ratio, and a higher percentage of foam. This study provides the first indication of graded damping properties in feathers.

Keywords

Bird, vibration, biomechanics, Laser Doppler Vibrometry, frequency, flight.

2.1 Introduction

Flight has given the animals survival advantages, by providing efficient locomotion and various habitats (Clark 2013). In avians, wings consisted of the flight feathers needed to sustain the dynamic force and vibration during the flapping (Greenewalt 1960). Excessive vibrations can lead to more consumed energy, noise and negatively impact flight stability. Therefore, it is reasonable to hypothesize that feathers of wings have undergone adaptations to develop several mechanisms to mitigate vibrations.

Feathers originated in theropod dinosaurs as simple filaments of varying lengths and diameters (Clark 2013). Feathers of modern birds, in contrast, evolved into complex hierarchically organized epidermal structures (Prum 1999; Bragulla and Hirschberg 2003). During feather evolution, pennaceous vanes for flight and display, and fluffy plumulaceous branches evolved for thermoregulation (Chang et al. 2019). Typical bird flight feathers consist of a shaft and two vanes (Fig. 1). The shaft is composed of a rigid outer shell and an inner foam-like structure, which shows a longitudinal gradient of cell sizes (Bonser and Purslow 1995). The vane consists of numerous barbs aligned parallel to each other, but at some angle to the shaft (Prum 1999; Clark 2013). The barbs are loosely connected by the elaborate system of hooklets and, when separated by an external force, they can easily re-establish their connections (Ennos et al. 1995; Butler and Johnson 2004; Kovalev et al. 2013; Gao et al. 2013; Chen et al. 2016; Sullivan et al. 2016).

Similar to other flyers such as dragonfly and damselfly, oscillations might negatively influence the stability (Rajabi et al. 2011; Rajabi et al. 2016). Hence, damping or energy dissipation is present in such a dynamic system. Damping alters the response of the system and results in desirable effects, such as stability and enhanced controllability (De Silva 1999). Therefore, it is plausible to hypothesize that there are structural mechanisms that enhance the damping properties of feathers and, thereby, reduce unwanted oscillations during flight.

Concerning the feather shaft, damping-related loss factors ($\tan \delta$) of swan, eagle, owl, and pigeon have been previously measured (Bonser and Purslow 1995; Gao et al. 2014). Loss factor, the ratio of loss modulus to storage modulus, is a parameter that presents the viscoelasticity and the damping capacity. For a small damping ratio, the loss factor is twice the damping ratio, $\tan \delta = 2 \zeta$ (Hansen 2018). A low damping ratio ranging from 0.015 to 0.035 has been revealed for bending of the swan feathers (Bonser and Purslow 1995), while the damping ratio of owl flight shafts has been estimated to be 0.804 ± 0.119 , which is larger than those of gold eagle 0.543 ± 0.037 and pigeon 0.448 ± 0.041 (Gao et al. 2014). However, a systematic understanding of the relationship between gradient structure and damping property of feathers is still far from being achieved.

Feather, as a mechanical structure, is lightweight and combines this feature with specific robustness and flexibility (Raspert 1960; Prum 1999). This combination is supposed to be the result of the specific hierarchical organization at the macro-, micro-, and nano-scales (Yang et al. 2013). It has been suggested that the mechanical properties of the shaft are mainly dominated by the properties of the outer cortex (Purslow and Vincent 1978; Bachman et al. 2012). Inside of the cortex, foams are known to be a design strategy to enhance mechanical stability by energy absorption (Bonser and Purslow 1995; Banhart and Baumeister 1998; Bonser 2001; Gao et al. 2014).

In this study, we aimed to understand the contribution of the gradient foam-filled shaft to the damping behavior of primaries. Measurements, using Laser Doppler Vibrometry (LDV), were performed on specimens selected from different shaft regions, to study variations of damping properties along the shafts. A combination of Scanning Electron Microscopy (SEM) and Micro-Computed Tomography (μ CT) was used to explore the correlation between the shaft morphology, its microstructure, and measured damping properties.

2.2 Materials and methods

2.2.1 Sample preparation

Adult female pigeons *Columba livia* were taken from the collection of the Zoological Institute of Kiel University, Germany. Preliminary experiments showed the presence of more than one oscillatory mode in vibrations of deflected feather shafts after release. Hence, to facilitate the data analysis, we introduced a simple manipulation to the system: the oscillations were studied with a mass attached to the free distal end of each segment. In this way, only two resonance frequencies were observed in the deflected shafts after release.

For further studies, the primary flight feathers were cut out from the wing (Fig. 1a). Primary feathers 1-6 (165-180 mm length) were sectioned, and 18 shaft specimens were used for damping tests. Vanes were cut from the feathers using a razor blade. The shaft was transversely sectioned in 50 mm long intervals from the tip, dividing the shaft into three parts (Fig. 1b). The most basal part of the shaft, the calamus, was

excluded from the experiments. The basal part of the specimens was embedded in epoxy resin and then mechanically fixed (Fig. 2b, black triangles). Primary feather 7 (160 mm length) was used for μ CT analysis.

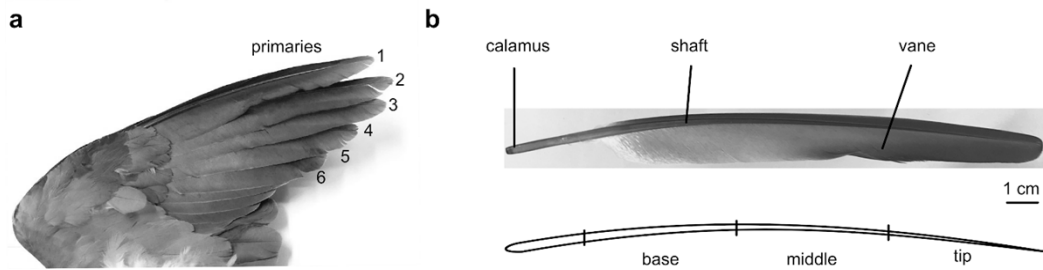


Fig. 1 Primary feathers of the rock pigeon *Columba livia* used in the study (ventral view). (a) Location of primary feathers. (b) An intact primary feather. (b) Scheme of the shaft segments

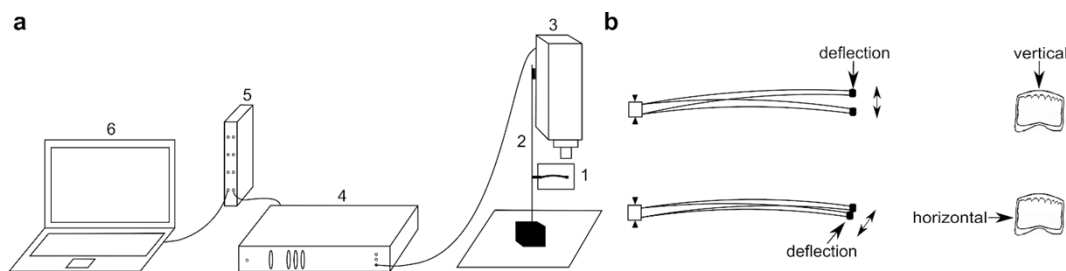


Fig. 2 Damping measurements. The oscillation of the shaft specimen was measured using a velocity-sensitive laser Doppler vibrometry (LDV). (a) Experimental setup: feather specimen (1), support (2), objective lens (3), video monitor (4), waveform analysis equipment (5), and software control (6). (b) Excitation of oscillations of the feather shaft segments by its tip deflection and abrupt release vertically (upper panel) perpendicularly to the vane, and horizontally in the plane of the vane (lower panel)

2.2.2 Damping test

In this study, damping tests were performed under room temperature 20°C-22°C and humidity 40%-45%. Damping tests were conducted on the basal, middle, and tip segments of the shaft. The test specimens were mechanically fixed at their basal parts in a 3D micromanipulator. To reduce the oscillation decay and to simplify the frequency analysis, as mentioned earlier, an extra mass (of 2.015 g) was attached at the free distal end of the specimens. The specimens were excited to oscillate by releasing from an initial deflection of 15 mm. The oscillations were excited in the vertical (perpendicular to the vane) and horizontal (parallel to the vane) directions (Fig. 2b). The decaying oscillation velocity was measured using a Laser Doppler Vibrometer (Polytec, Waldbronn, Germany) (Fig. 2a). The experimental setup including the mechanical supporters holding the feather specimen and the laser

displacement sensor is shown in Fig. 2a. The oscillation velocity was recorded with a sampling rate of 5 kHz and observed in one direction, perpendicular or parallel to the vane plane. The original experimental recordings were then converted from the analysis software package Spike2 (CED, version 4.24) (Cambridge Electronic Design Limited, Cambridge, England) to the software Origin Pro 8.0 (OriginLab, Massachusetts, USA).

2.2.3 Feather morphology

An SEM Hitachi S-4800 (Hitachi High-Technology, Tokyo, Japan) was used at an acceleration voltage of 3 kV to study the feather microstructure at different levels of the shaft. Dry samples were attached to aluminum stubs using adhesive tape and then sputter-coated with 8 nm gold-palladium using a Leica EM SCD 500 (Leica Microsystems, Mannheim, Germany).

Skyscan 1172 μ CT (Bruker microCT, Kontich, Belgium) was used for three-dimensional scanning of shaft specimens (1 primary feather, 8 segments). The X-ray voltage and current were set to 40 kV and 250 μ A, respectively. The NRecon software (SkyScan, Kontich, Belgium) was used to reconstruct structures from the 3D data of μ CT scans. The segmentation was performed using the image analysis software Amira (FEI Visualization Sciences Group, Bordeaux, France).

2.2.4 Fitting of oscillation curves

In this study, the equation of under-damped oscillations was employed to describe the damping behavior of the shaft. For shaft segments with a terminal mass, the oscillations behavior is under-damped. The motion of the shaft end can be described by the following equation (Rao 2010):

$$X = A e^{-\beta t} \cos(\omega t + \varphi) \quad (1)$$

where X and t are the displacement and time, β is the damping coefficient, A is the initial amplitude, ω is the circular frequency, and φ is the phase angle. The presence of two vibration modes (frequencies) was observed in experiments on oscillating shaft

segments. Therefore, a second term for the second vibration mode as well as an offset, A_0 , was added to Eqn. 2:

$$X = A_0 + A_1 e^{-\beta_1 t} \cos(\omega_1 t + \varphi_1) + A_2 e^{-\beta_2 t} \cos(\omega_2 t + \varphi_2) \quad (2)$$

where indices 1 and 2 refer to the first and second vibration modes. To perform the fit of experimental curves with Eqn. 2, the initial values of the fit parameters were determined as follows. Fast Fourier Transformation (FFT) was employed to estimate the first (ω_1) and second (ω_2) frequencies and initial phases φ_1 and φ_2 of the shaft segments. Initial amplitudes A_1 and A_2 were taken equal to half of the peak value in the experimental velocity-time curve.

However, the damping coefficient β , is related to the frequency (Beards 1996), while the damping ratio ζ , is frequency independent. The damping ratio was calculated using Eqn. 3:

$$\zeta = \beta/\omega \quad (3)$$

To compare our results with those previously reported in the reference (Bonser and Purslow 1995; Gao et al. 2014), the damping ratios will be further presented.

2.3 Results and Discussion

2.3.1 Damping properties of shaft segments

After deflecting the free end of the shaft specimens, they started to oscillate. The velocity of the oscillations decreased over time until they stopped. The oscillations of all shaft segments showed typical characteristics of an under-damped regime (Fig. 3). The decay times of the shaft specimens are roughly 1 s at the base, 3 s in the middle, and 12 s at the tip. The power spectra of the velocity-decay time curves calculated using Fast Fourier Transform (FFT) are illustrated in Fig. 3b,d,f. Two frequencies were observed in all segments: 54.66 ± 17.37 Hz and 66.62 ± 9.91 Hz at the base, 29.46 ± 1.75 Hz and 38.14 ± 4.16 Hz in the middle, 6.46 ± 0.40 Hz and 8.16 ± 1.41 Hz at the tip of the shaft.

The comparison of damping ratios of the shaft segments in the horizontal and vertical deflections (as Fig. 2b) is illustrated in Fig. 4. Under both deflections, the damping ratios of the 1st mode at the base are higher than those in the middle and tip segments.

In the 2nd mode, in contrast, the maximum values of the damping ratios were observed in the middle segment. The damping ratio in the horizontal direction was higher than that in the vertical direction.

As seen, the damping ratios of primary feather shafts from the pigeon range from 0.268 to 0.034 in the 1st mode, 0.127 to 0.032 in the 2nd mode (Fig. 4). Our results are lower than the previous data obtained from a uniaxial tensile test (Gao et al. 2014), where the of the pigeon shafts was found to be 0.448. This difference can be due to the use of different specimens and measurement techniques.

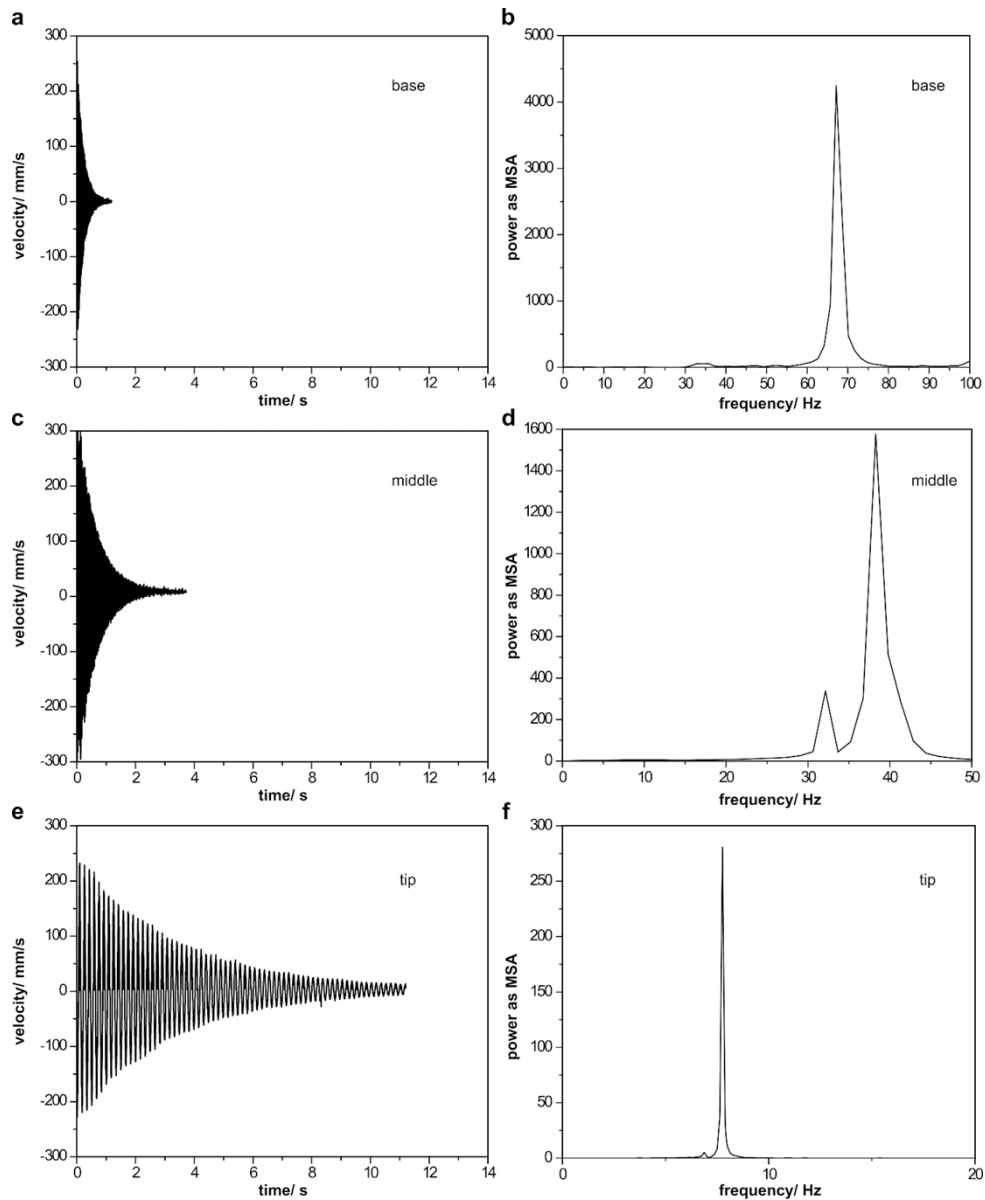


Fig. 3 Typical oscillation curves for the base (a), middle (c), and tip (e) segments of the feather shaft with corresponding power spectra for the base (b), middle (d), and tip (f) segments representing velocity mean square amplitude (MSA)

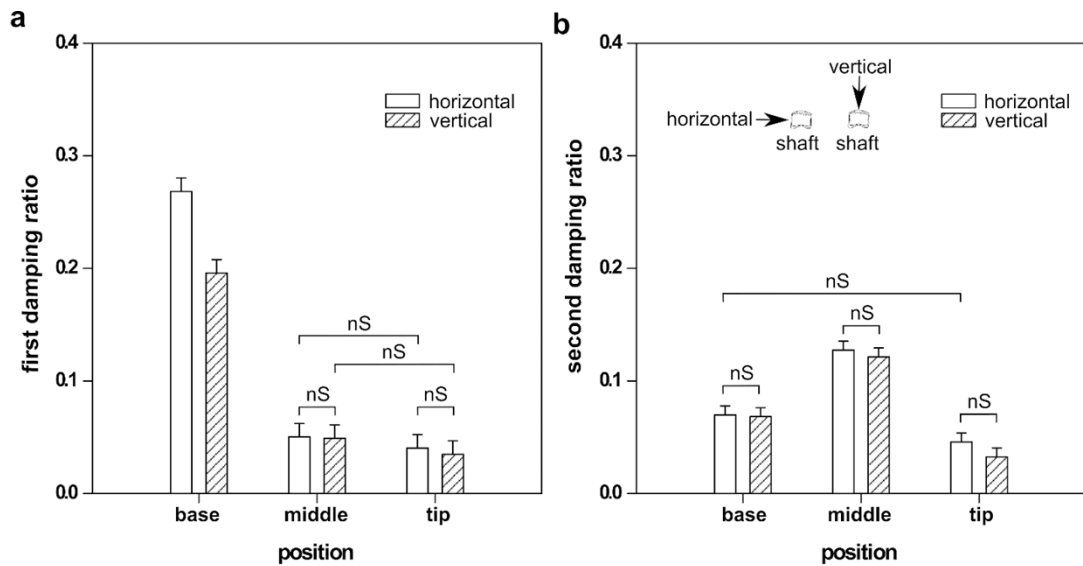


Fig. 4 Damping ratios of (a) the 1st (lower) frequency and (b) the 2nd (higher) frequency oscillations in different segments of the feather shaft under vertical and horizontal deflections. Measurements were performed for 6 feather shafts, 18 segments, and repeated three times. nS indicates no significant difference according to the results of the two-way ANOVA test

2.3.2 Feather shaft morphology

2.3.2.1 Cortex morphology

The three-dimensional reconstructions based on μ CT data show structural variations of the cortex (Fig. 5). The diameter and the cross-sectional area decrease continuously from the feather base towards its tip. The shape of the cortex varies from an almost circular shape at the base, to a rectangle in the middle, and finally to an ellipse at the tip. It is known that, given the same cross-sectional area, square cross-sections show higher bending rigidity and are superior in maintaining the original shape under deformation, in comparison to circular sections, which become oval-shaped upon flexing (Prum and Williamson 2001; Wang and Meyers 2016). The square shape with a high area moment of inertia, using a larger amount of material, would be mechanically favorable in bending, but also heavier. Taking into account that feathers are anchored to the bone, the circular base has grown from cylindrical feather follicles perhaps providing better mechanical connectivity (Prum and Williamson 2001; Wang and Meyers 2016). However, to achieve improved resistance to forces applied to the feather during flight at a minimal weight, the cross-sectional shape of the feather transforms to a square in the middle, and then to a more elliptical shape at the tip.

In the interior dorsal surface of the cortex, ridges are running from 1/4 to 3/4 of the feather length (Fig. 5). At the base of the shaft, next to the calamus, two dorsal ridges are present. In the middle of the feather, four ridges appear. The ridges transform into a serrated structure and disappear at the tip. The ridges are likely to contribute to a tight bonding between the stiff cortex and flexible medulla by increasing the interfacial area (Zhang et al. 2012).

Along the shaft, the thickness of the cortex changes (Fig. 6). This decreasing thickness may enhance the damping performance, as shown for the stick insect antenna with a longitudinal thickness gradient (Rajabi et al. 2011). The feather cortex has also a radial gradient of the thickness in cross-section. The cortex is thicker on the dorsal and ventral sides if compared with the lateral sides (Table 1). This difference could be explained by a potential need to resist higher levels of stress experienced by the dorsal and ventral bending during flight (Sullivan et al. 2016). The mechanical behavior of the shaft is mainly determined by the cortex (Bonser and Purslow 1995; Lingham-Soliar et al. 2010; Liu et al. 2015). The flexural stiffness depends on the second moment of the area and Young's modulus, which in turn depends on the keratin bundles formed in the cortex (Lingham-Soliar et al. 2010; Liu et al. 2015).

Table 1. The thickness of the cortex in three segments of feather shafts

location	dorsal thickness /mm	ventral thickness /mm	lateral thickness /mm
base	0.135 ± 0.021	0.153 ± 0.013	0.0718 ± 0.003
middle	0.124 ± 0.006	0.147 ± 0.007	0.0325 ± 0.005
tip	0.103 ± 0.011	0.107 ± 0.014	0.045 ± 0.003

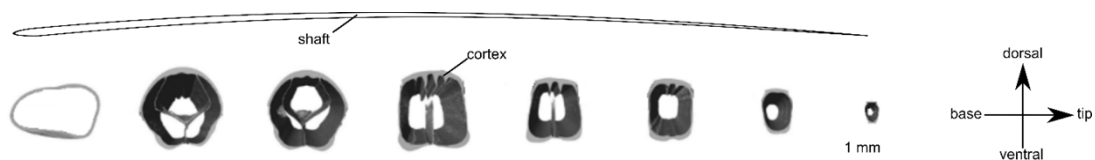


Fig. 5 Cross-sections of shaft segments were obtained from the μ CT scans. Segments were taken from the primary feather No.7 (separated into 8 segments). the morphology of the cortex within the shaft is shown from the calamus to the distal tip. The shape and diameter changes of the shaft are visible

2.2.2.2 Medullary foam structure

The shaft is filled with foam cells. The shape and morphology of foam cells demonstrate a gradient (Figs. 6, 7). At the base, the foam cells are relatively large with a diameter of about $27.09 \pm 1.08 \mu\text{m}$. Their size decreases to $21.35 \pm 0.40 \mu\text{m}$ in the middle, and to $18.21 \pm 0.46 \mu\text{m}$ at the tip (a decrease of $\sim 15\%$ and $\sim 32\%$, respectively). The cells are polyhedrally- or spherically-shaped, and the walls (membranes) are very thin ($\sim 0.08 \mu\text{m}$ thickness). The SEM analysis also revealed that the walls and struts are closely packed in the septa. The fragmentary or columnar struts interconnect the foam cells and strengthen the cell interfaces. The continuous wall likely serves as the primary load supporter increasing the stability of the foams. The cell walls are made of irregularly orientated and curved weaving fibers (Fig. 6 j-l). The fibers of cells merge with the fibrils composing the cortex, which enhance the mechanical stiffness of the medulla foam.

Bird wings in general and feathers, in particular, are simultaneously robust and light enough to meet the mechanical demands to generate aerodynamic forces (Pennycuik 1968). The shaft is an important part, which consists of medullary foam and cortex (Sullivan et al. 2017). The tubular structure is perhaps the simplest solution to maximize the stiffness at a minimal weight (Bonser 2001). However, a tubular structure is likely to fail by buckling (Bonser 2001). The foam-like lightweight medulla within the shaft is much less stiff than the cortex but also contributes to the mechanical performance of the shaft (Purslow and Vincent 1978; Bonser 2001; Lingham-Soliar et al. 2010). It has been previously shown that the removal of the medulla reduces the stiffness of the shafts by 16% (Bonser 2001). The estimated Young's modulus of the foam showed considerable variation, ranging from 5 MPa to 1.58 GPa (Bonser 2001). The foam is expected to delay the onset of buckling under compression (Bonser 2001) and bending (Purslow and Vincent 1978) by transferring the stress from the cortical layer to medulla foams. The foams are also likely to dissipate energy and, thereby, contribute to the damping properties of the feathers.

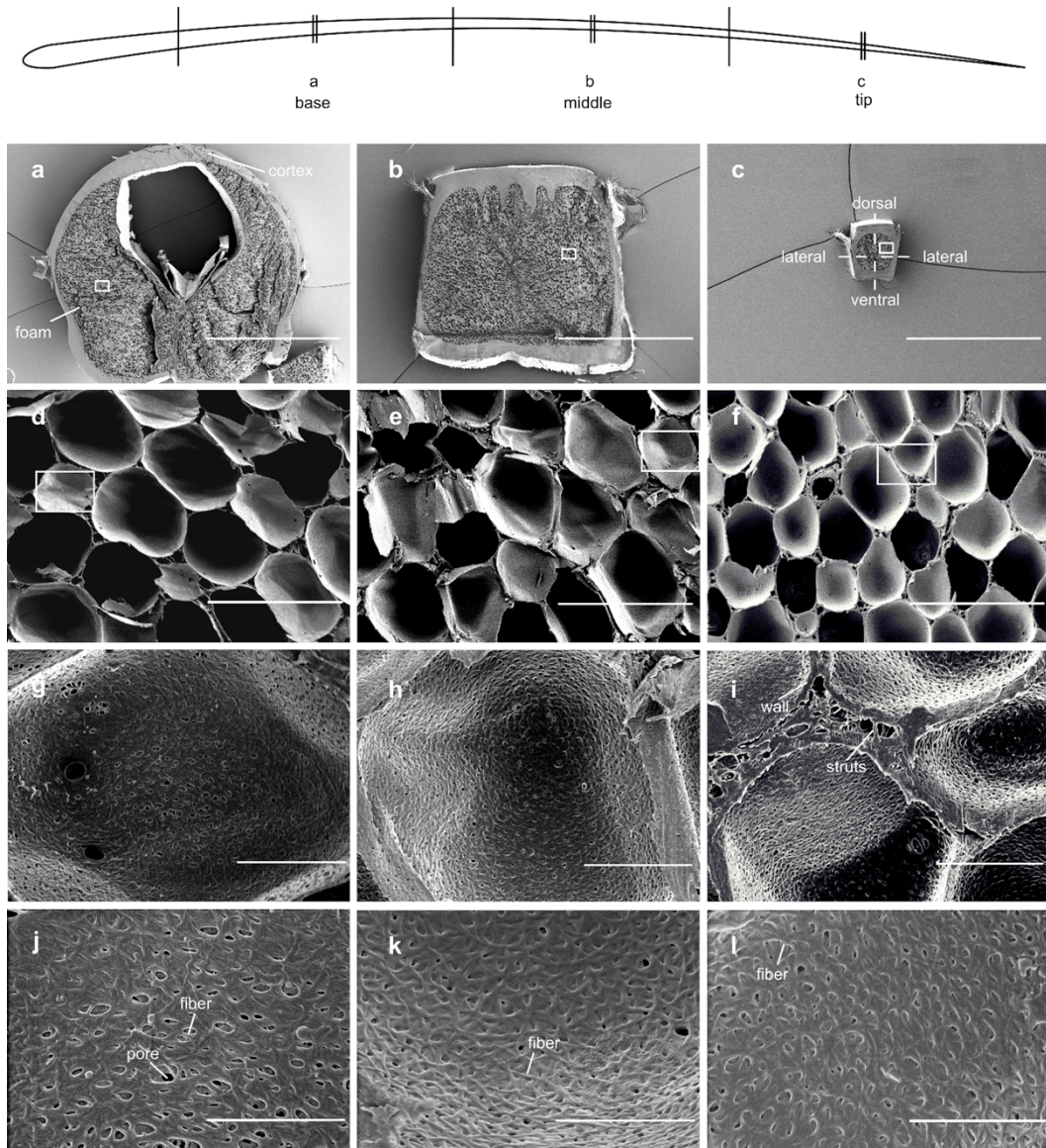


Fig. 6 SEM images of transverse sections of shaft segments taken at 150 mm-100mm (base), 100 mm-50mm (middle), and 50 mm-0mm (tip) away from the tip. (a, d, g, j) Basal region. (b, e, h, k) Middle region. (c, f, i, l) Tip of the shaft. (a-c) Scale bars: 1 mm. (d-f) Scale bars: 100 μ m. (g-i) Scale bars: 10 μ m. (j-l) Scale bars: 5 μ m

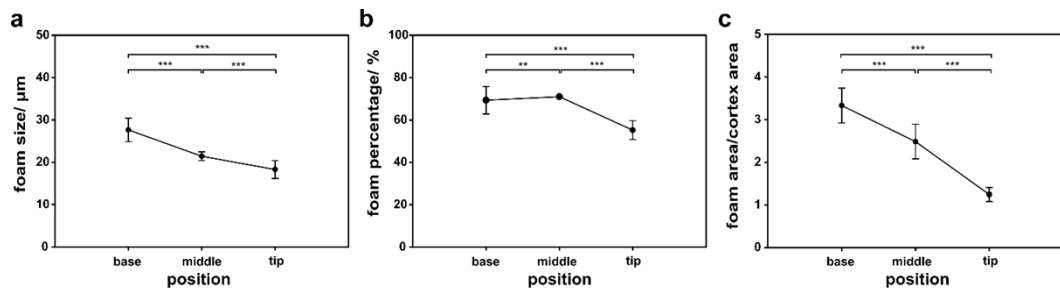


Fig. 7 The foam morphology and relationship between medulla and cortex. (a) Size of foam cells in the base, middle, and tip regions. (b) The relationship between the foam area and shaft segments. (c) The ratio between the medullar foam area and the cortex area along the shaft

2.3 Effect of cortex and gradient foam structure

Similar to other dynamic systems, unwanted oscillations could reduce the aerodynamic performance in flying animals (Rajabi et al. 2011; Alexander 2015; Rajabi et al. 2016). It is known that bird wings have vibration-sensitive mechanoreceptors, either at the follicle or Herbst corpuscles (Bruecker et al. 2016). Apart from the active control of energy-consuming muscles and neural systems (Alexander 2015), the feathers with damping capability could help to passively minimize undesirable vibrations. The flight feathers are anchored to the ulna and metacarpals/phalanges, where they are supplemented with muscles and sensors (Kondo et al. 2018). The higher damped base of the shaft assures the stability of the wing bone under oscillations.

A gradient of damping properties is present in the shaft. The observed structural gradients, both of the cortex wall and foams, are assumed to be responsible for the different damping properties of the three segments of the shaft. The cortex consists of multiple layers of aligned collagen fibers (Liu et al. 2015). It is plausible to assume that friction between these fibers and layers may contribute to the damping properties. The presence of ridges increases the cortex-foam interface and therein leads to increased friction between them. The filled medulla, which occupies a large part of the shaft's cross-section, is assumed to strongly contribute to the damping properties of the shaft. The damping ratio following the size of foam cell and area ratio of the foam/cortex change in the 1st vibration mode (Figs. 4a and 7a,c). It means that the larger foam cells and the higher area ratio between foam and cortex are, the higher is the damping ratio. The higher percentage of foam structure is proportional to the higher damping ratio in the 2nd vibration mode (Figs. 4b and 7b).

Bending, shear and buckling are the main deformation modes in the foam structure (Vincent and Owers 1986; Gibson et al. 1989; Gibson and Ashby 1997). During shaft bending, the cells situated remote from the central axis experience the highest stress (Nillsson and Nillsson 2002). At small strains, the walls elastically bend, the foam cells/struts undergo the shear deformation, and cell walls may experience no stretching. At large strains, beyond a critical value, the cells may collapse by elastic buckling and plastic yielding or even fracture. At higher strains, the cells collapse and

undergo densification with rapidly increasing stiffness (Triantafillou et al. 1989; Gibson and Ashby 1997). Several mechanisms participate in the energy dissipation in foams (Schwaber 1973). Foams dissipate deformation energy across layers, reduce possible crack propagation and delay the local buckling (Vincent and Owers 1986; Bonser 2001). The cell walls which are composed of curved weaving fibrils, absorb energy known as intrinsic damping (Andersson et al. 2010). The fiber-composite cells dissipate energy by fiber pullout (Gibson and Ashby 1997). The difference under the two deflections may depend on the anisotropy of the cortex and foam-like medulla structure. The cell sizes, relative density, and anisotropy have proven to be important parameters governing the mechanical properties of the foam (Gibson and Ashby 1997).

Consequently, the combination of the cortex and the gradient foam makes the feather shaft a lightweight structure with varied damping properties. The higher damped base anchored to the bone assures the wing stability under oscillations. To decay the oscillations in flapping, avian feathers have reached certain levels of damping due to their specialized macro- and microstructures.

2.4 Conclusions

The feather shaft represents natural gradient material with damping properties that have been previously oversimplified in the literature. This paper provides the first indication of the graded damping properties of the shaft in feathers. Under horizontal and vertical deflections, the damping ratios at the base are highest in the 1st mode, and the maximum values were observed in the middle of the shaft in the 2nd mode. The higher damping of the base and the middle of the shaft close to the bone assures the stability of the wing under oscillations. SEM and μ CT analyses were used to investigate the gradient microstructure of the shaft. The closed-cell medulla is based on curved weaving fibrils with hierarchical levels of porosity. The energy dissipation of the shaft is likely due to the deformations and the densification of foam cells. The higher damping properties are influenced by the larger foam cells, higher area percentage of the foam, and higher area ratio between the foam and cortex. This study represents the first step in exploring damping mechanisms in bird feathers. It also

offers an interesting design that may inspire technical structures with adjustable damping properties.

Acknowledgments The authors would like to thank all the related members of the Institute of Functional Morphology and Biomechanics at Kiel University, Germany, and the Institute of Bioinspired Structure and Surface Engineering at Nanjing University of Aeronautics and Astronautics, China.

Authors' contributions S.N.G. designed and coordinated the study; K.D., A.K., H.R., C.F.S., and S.N.G. designed the experiment; K.D. performed the experiment, carried out the statistical analysis, and wrote the manuscript; All authors analyzed the data, discussed the results, edited the manuscript, and gave final approval for publication.

Funding Open Access funding enabled and organized by Projexkt DEAL. This work was financially supported by Chinesisch-Deutsches Zentrum für Wissenschaftsförderung to SNG and ZDD (Grant no. GZ1154).

Declarations

Competing interests The authors declare no conflict of interest.

Open Access This article is licensed under a Creative Commons Attribution 4.0 International License, which permits use, sharing, adaptation, distribution and reproduction in any medium or format, as long as you give appropriate credit to the original author(s) and the source, provide a link to the Creative Commons licence, and indicate if changes were made. The images or other third party material in this article are included in the article's Creative Commons licence, unless indicated otherwise in a credit line to the material. If material is not included in the article's Creative Commons licence and your intended use is not permitted by statutory regulation or exceeds the permitted use, you will need to obtain permission directly from the copyright holder. To view a copy of this licence, visit <http://creativecommons.org/licenses/by/4.0/>.

References

- Alexander DE (2015) *On the wing: Insects, pterosaurs, birds, bats and the evolution of animal flight*. Oxford, UK
- Andersson A, Lundmark S, Magnusson A, Maurer FHJ (2010) Vibration and acoustic damping of flexible polyurethane foams modified with a hyperbranched polymer. *J Cell Plast* 46 (1): 73-93
- Bachmann T, Emmerlich J, Baumgartner W, Schneider JM, Wagner H (2012) Flexural stiffness of feather shafts: Geometry rules over material properties. *J Exp Biol* 215 (3): 405-415
- Banhart J, Baumeister J (1998) Deformation characteristics of metal foams. *J Mater Sci* 33: 1431-1440
- Beards CF (1996) *Structural vibration: Analysis and damping*. London, UK
- Bonser RHC, Purslow PP (1995) The Young's modulus of feather keratin. *J Exp Biol* 198: 1029-1033
- Bonser RHC (2001) The mechanical performance of medulla foam from feathers. *J Mater Sci Lett* 20: 941-942
- Bragulla H, Hirschberg RM (2003) Horse hooves and bird feathers: Two model systems for studying the structure and development of highly adapted integumentary accessory organs - the role of the dermo-epidermal interface for the micro-architecture of complex epidermal structures. *J Exp Zool B Mol Dev Evol* 298 (1): 140-151
- Bruecker C, Schlegel D, Triep M (2016) Feather vibration as a stimulus for sensing incipient separation in falcon diving flight. *Nat Resour J* 7 (7): 411-422
- Butler M, Johnson AS (2004) Are melanized feather barbs stronger? *J Exp Biol* 207 (2): 285-293
- Chang WL, Wu H, Chiu YK, et al (2019) The making of a flight feather: Bio-architectural principles and adaptation. *Cell* 179 (6): 1409-1423
- Chen Q, Gorb SN, Kovalev A, Li Z, Pugno N (2016) An analytical hierarchical model explaining the robustness and flaw-tolerance of the interlocking barb-barbule structure of bird feathers. *Europhys Lett* 116 (2): 24001
- Clarke J (2013) Feathers before flight. *Science* 340 (6133): 690-692
- De Silva CW (1999) *Vibration: Fundamentals and practice*. Boca Raton, USA
- Ennos AR, Hickson JRE, Roberts A (1995) Functional morphology of the vanes of the flight feathers of the pigeon *Columba livia*. *J Exp Biol* 198 (5): 1219-1228
- Gao JL, Zhang GQ, Guan L, Chu JK, Kong DY, Bi YT (2013) Structure and mechanical property of *Asio otus* feather barbs. *Key Eng Mater* 562-565: 914-919
- Gao JL, Chu JK, Guan L, Shang HX, Lei ZK (2014) Viscoelastic characterization of long-eared owl flight feather shaft and the damping ability analysis. *Shock Vib* 709367

-
- Gibson LJ, Ashby MF, Zhang J, Triantafillou TC (1989) Failure surfaces for cellular materials under multiaxial loads - I. Modeling. *Int J Mech Sci* 31 (9): 635-663
- Gibson LJ, Ashby MF (1997) *Cellular solids: Structure and properties*. Cambridge, UK
- Greenewalt CH (1960) The wings of insects and birds as mechanical oscillators. *Proceedings of the American Philosophical Society* 104 (6): 605-611
- Hansen C (2018) *Foundations of vibroacoustics*. Boca Raton, USA
- Kondo M, Sekine T, Miyakoshi T, Kitajima K, Egawa S, Seki R, Abe G, Tamura K (2018) Flight feather development: its early specialization during embryogenesis. *Zoological Lett* 4 (1): 2
- Kovalev A, Filippov AE, Gorb SN (2013) Unzipping bird feathers. *J R Soc Interface* 11: 20130988
- Lingham-Soliar T, Bonser RHC, Wesley-Smith J (2010) Selective biodegradation of keratin matrix in feather rachis reveals classic bioengineering. *Proc R Soc B* 277: 1161-1168
- Liu ZQ, Jiao D, Meyers MA, Zhang ZF (2015) Structure and mechanical properties of naturally occurring lightweight foam-filled cylinder- The peacock's tail coverts shaft and its components. *Acta Biomater* 17: 137-151
- Nilsson E, Nilsson AC (2002) Prediction and measurement of some dynamic properties of sandwich structure with honeycomb and foam cores. *J Sound Vib* 251 (3): 409-430
- Pennycuik CJ (1968) Power requirements for horizontal flight in the pigeon *Columba livia*. *J Exp Biol* 49 (3): 527-555
- Prum RO (1999) Development and evolutionary origin of feathers. *J Exp Zool* 285 (4): 291-306
- Prum RO, Williamson S (2001) Theory of the growth and evolution of feather shape. *J Exp Zool* 291 (1): 30-57
- Purslow PP, Vincent JFV (1978) Mechanical properties of primary feathers from the pigeon. *J Exp Biol* 72 (1): 251-260
- Rajabi H, Moghadami M, Darvizeh A (2011) Investigation of microstructure, natural frequencies and vibration modes of dragonfly wing. *J Bionic Eng* 8 (2): 165-173
- Rajabi H, Shafiei A, Darvizeh A, Dirks JH, Appel E, Gorb SN (2016) Effect of microstructure on the mechanical and damping behaviour of dragonfly wing veins. *R Soc Open Sci* 3: 160006
- Rao SS (2010) *Mechanical vibrations*. New Jersey, USA
- Raspel A (1960) Biophysics of bird flight. *Science* 132 (3421): 191-200
- Schwaber DM (1973) Impact behavior of polymeric foams: A review. *Polymer-Plast Technol Eng* 2 (2): 231-249
- Sullivan TN, Pissarenko A, Herrera SA, Kisailus D, Lubarda VA, Meyers MA (2016) A lightweight biological structure with tailored stiffness: the feather vane. *Acta Biomater* 41: 27-39

Sullivan TN, Wang B, Espinosa HD, Meyers MA (2017) Extreme lightweight structures: avian feathers and bones. *Mater Today* 20 (7): 377-391

Triantafillou TC, Zhang J, Shercliff TL, Gibson LJ, Ashby MF (1989) Failure surfaces for cellular materials under multiaxial loads – II. Comparison of models with experiment. *Int J Mech Sci* 31 (9): 665-678

Vincent JFV, Owers P (1986) Mechanical design of hedgehog spines and porcupine quills. *J Zool* 210 (1): 55-75

Wang B, Meyers MC (2016) Light like a feather: A fibrous natural composite with a shape changing from round to square. *Adv Sci* 4 (3): 1600360

Yang W, Chao C, McKittrick J (2013) Axial compression of a hollow cylinder filled with foam: A study of porcupine quills. *Acta Biomater* 9 (2): 5297-5304

Zhang YM, Yao H, Oritz C, Xu JQ, Dao M (2012) Bio-inspired interfacial strengthening strategy through geometrically interlocking designs. *J Mech Behav Biomed Mater* 15: 70-77

Publisher's note Springer Nature remains neutral with regard to jurisdictional claims in published maps and institutional affiliations.

CHAPTER 3

The function of vanes: a strategy to increase damping property in feathers

Summary:

As a lightweight structure, a feather possesses a shaft and two vanes that resist unwanted vibration during flapping. In this part, the damping results demonstrate vanes' significant influence on the feathers in vibration.

The Role of Vanes in the Damping of Bird Feathers

Kai Deng^{1,*}, Hamed Rajabi², Alexander Kovalev¹, Clemens F. Schaber¹, Zhendong Dai³ and Stanislav N. Gorb¹

¹ Functional Morphology and Biomechanics, Institute of Zoology, Kiel University, Kiel, 24098, Germany

² School of Engineering, London South Bank University, London, SE1 0AA, U. K.

³ Institute of Bioinspired Structure and Surface Engineering, Nanjing University of Aeronautics and Astronautics, Nanjing, 210026, China

* Corresponding author

Kai Deng

E-mail: kdeng@zoologie.uni-kiel.de

Published by:

Journal of Bionic Engineering, 2023

<https://doi.org/10.1007/s42235-022-00329-3>

Abstract

Bird feathers sustain bending and vibrations during flight. Such unwanted vibrations could potentially cause noise and flight instabilities. Damping could alter the system response, resulting in improving quiet flight, stability, and controllability. Vanes of feathers are known to be indispensable for supporting the aerodynamic function of the wings. The relationship between the hierarchical structures of vanes and the mechanical properties of the feather has been previously studied. However, still little is known about their relationship with feathers' damping properties. Here, the role of vanes in feathers' damping properties was quantified. The vibrations of the feathers with vanes and the bare shaft without vanes after step deflections in the plane of the vanes and perpendicular to it were measured using high-speed video recording. The presence of several main natural vibration modes was observed in the feathers with vanes. After trimming vanes, more vibration modes were observed, the fundamental frequencies increased by 51-70%, and the damping ratio decreased by 38-60%. Therefore, we suggest that vanes largely increase feather damping properties. Damping mechanisms based on the morphology of feather vanes are discussed. The aerodynamic damping is connected with the planar vane surface, the structural damping is related to the interlocking between barbules and barbs, and the material damping is caused by the foamy medulla inside barbs.

Keywords: bird, feather, vibrations, damping, bionic

3.1 Introduction

Flight gives an animal a very potent predator-escape route, and the privilege to reach remote or for non-flying animals inaccessible locations [1]. Through the evolution over millions of years, remarkable flight abilities have developed with complex modes of locomotion [2]. The evolution of aerial locomotion was accompanied by the acquisition of anatomical and physiological adaptations in flapping flying [3, 4, 5]. The adaptations in birds include the fusion of parts of the skeleton, the pneumaticity of bones, and equipment of wings with strong yet lightweight feathers [6].

Bird wings consist of arm and hand parts that can be easily stretched and folded [7]. Primary flight feathers are attached to the metacarpal and phalangeal bones [8]. The balance between the robustness, flexibility, and lightweight properties of the feathers is supposed to be the result of specific materials and the particular organization of their macro-, micro-, and nanostructures [9]. Feathers of recent birds have evolved from simple keratinous filaments to fascinating outer coverings and complex epidermal structures of varying lengths and diameters [10, 11, 12, 13].

Typical flight feathers consist of a shaft and asymmetrical vanes on two sides. The shaft is composed of a rigid outer cortex and the inner foam-like medulla [14]. The vanes consist of numerous barbs oriented in parallel but at some angle to the shaft [15]. The architecture of the vanes is linked with advancements in aerial locomotion during evolution [16]. The microstructure of goose vanes was first observed by Hooke [17], and two types of barbules were described by Ennos et al. [18]. The barbules on the distal barb with hooks interlock with grooves situated on the proximal barbules of the next barb (Fig. 1). The mechanism of interlocking of the barbs, its ease of reestablishment after separation, and the separation forces of hooklets have been experimentally studied by Kovalev et al. [19] and finally summarized in a dynamical mathematical model. The robustness and flaw-tolerance of the interlocking barbs have been explained using an analytical model based on small- and large-beam deflections by Chen et al. [20].

During the flight, wings undergo continuous vibrations [21]. At a particular orientation, a feather becomes a driven oscillator when air velocity exceeds a threshold [22]. Unwanted vibrations can influence flight stability and make noise, as have been previously studied in other flying animals [23, 24]. Concerning the shaft, a damping ratio ranging from 0.015 to 0.035 has been revealed for the bending of swan feathers [25], while the damping ratio of shafts in pigeons has been estimated to be 0.448 ± 0.041 [26]. The loss factor of single pigeon primary feathers (0.1573, 0.093 vertically, and 0.0912, 0.0709 parallelly) and single barb (0.0790 vertically, and 0.1234 parallelly) [27]. The different shaft regions of the pigeon feathers under deflections were investigated, and graded damping properties from base to tip were found (from 0.268 to 0.034) [28].

The investigations of sound are also closely related to vibration. Sound classified as

pressure waves is generated by vibrating structures that can induce the vibration [27]. In courtship display, peacock feathers perform the train-rattling using a range of vibration frequencies (22 - 28 Hz); higher damping of feathers broadens the resonant peaks and has the advantage of quickly damping out oscillations [29]. In addition to furnishing flight, the various acoustic communication functions are served by pressure waves when birds flap their wings [30]. The flag model was used to explain the fluttering and accompanying sound by the outermost tail feathers, that subtle changes in shape tune the produced sound frequency [31]. The distinctive flight sound is produced by wings in hummingbirds, enabled via morphological changes of primaries [32]. Male Club-winged Manakins produce tonal sound with specialized feathers, and the resonant properties were determined that the feathers exhibit unusually high Q-values [33]. The aeroacoustic behavior of hummingbird tail feathers that vary in shape over a range of air velocities in a wind tunnel was examined [12]. The communication sounds generated in the wing and tail are mainly attributable to 3 mechanisms: flutter, percussion, and wing whirring [22]. Aeroelastic flutter results from the dynamic coupling of aerodynamic forces with the feather's geometry and stiffness to produce a limited cycle vibration of a feather [22]. Pigeons produce tonal sounds (700 ± 50 Hz) during the downstroke when a small region of long, curved barbs on the inner vane of the outermost primary flutters [34]. The modified feather P8 of crested pigeons produces a specific tonal sound that acts as an alarm sonation [35].

However, it remains unclear how different feather parts contribute to their damping properties. Despite the important aerodynamic function of the vanes, its damping significance in vibration lacks a systematic study. To support the feathers' aerodynamic function, the vanes form an airfoil stabilized by the interlocked barbules, which may strongly contribute to the feather damping. We hypothesize that vanes help to enhance the damping of primary flight feathers. To examine the effects of vanes removal on feathers' damping, in this study the underdamped vibrations (parallel and perpendicular to the vane plane) were studied on feathers with the vanes and bare shafts without the vanes. The role of the vanes in the damping behavior of feathers was quantified and analyzed in combination with their morphological characteristics.

3.2 Materials and methods

3.2.1 Morphological analysis

Outermost primary flight feathers (Nos. 1-5, Fig. 1) were taken from the wings of an adult male pigeon (*Columba livia*). They were imaged using an iPhone X camera (Apple, California, USA). A Scanning Electron Microscope (SEM) Hitachi S-4800 (Hitachi, Chiyoda, Japan) was used to examine the vanes microstructure. The middle section of the shaft and vanes were cut. The specimens were then mounted on a vertical SEM stub. SEM samples were coated with 8 nm gold-palladium using a sputter coater EM SCD500 (Leica, Wetzlar, Germany) before SEM observation and examined at an acceleration voltage of 3.0 kV.

3.2.2 Damping tests

In this study, damping tests were performed under room temperature of 18°C-20°C and humidity of 40%-45%. The intact feather with the vanes was fixed horizontally at their calamus part in a micromanipulator. Feather vibrations were excited by vertical (perpendicular to the vanes) and horizontal (parallel to the vanes) step deflections (10 mm). Five flight feathers (Nos. 1-5) were tested under two deflection directions, repeated three times for each feather and each direction. Then the vanes were removed from the shaft of the feathers using a razor blade and the damping tests were repeated on the shafts without the vanes.

The feather vibrations were recorded using a digital high-speed video system (Olympus, I-Speed 3). The videos were recorded at a 1280 × 1024 pixels resolution, 3000 fps, and a shutter time of 0.667 μs. To facilitate tracking, the distal tips of feathers were marked with white markers point (compared to feather mass is low enough and can be ignored) before experiments. The video recordings were transformed into single-frame stacks in the JPG image format. The motion of the feather tip was analyzed using the image analysis software ImageJ (version 1.48; Wayne Rasband, National Institute of Health, USA.). The tracking positions of the tip (horizontal position, X and vertical position, Y) were determined using the MJTrack function (version 1.48; Wayne Rasband, National Institute of Health, USA), an ImageJ plugin for motion tracking in a single frame.

Fast Fourier Transformation (FFT) with the rectangular window was employed to obtain the natural frequencies of the feathers with the vanes and the shaft without the vanes using the software Origin (OriginLab, Massachusetts, USA). For visualization purposes, the first main fundamental frequency (vibration modes) of the feathers was separated using a bandpass filter.

The equation of under-damped vibrations was employed to define the vibrations of the first main frequency. The displacement (X) and the decay time (t) satisfy the under-damped condition with the following equation

$$X = Ae^{-\beta t} \cos(\omega t + \varphi), \quad (1)$$

where β is the damping coefficient, A is the initial amplitude, ω is the frequency, and φ is the phase angle. The damping coefficient β was obtained by the curve fitting with the frequency ω being gained earlier by FFT analysis. For statistics, two-way Analysis of Variance (ANOVA) was used for the damping data, including the Turkey test for multiple comparisons by the software SigmaPlot 12.0 (SPSS Inc, Chicago, USA). The damping ratios were normalized by rank cases using the software IBM SPSS Statistics 25 (SPSS Inc, Chicago, USA). To compare our results with those obtained in previous studies, the damping ratios ζ were calculated from the damping coefficient using the following equation

$$\zeta = \frac{\beta}{\omega}. \quad (2)$$

3.3 Results and Discussion

3.3.1 Morphology

The arrangement of the primary feathers in the spread and the folded wing is shown in Fig. 1 a. In the primaries, the shaft is asymmetrically surrounded by the vanes on the two sides (Fig. 1 b). In the vanes, barbs, barbules, and hooklets responsible for the integrity of the vanes are easily recognizable in the SEM images (Fig. 1 c, d). The barbs are arranged at angles of approximately 30° - 40°, decreasing from the base towards the tip. These branching angles are smaller at the leading edge in comparison to the trailing edge. Additionally, the barbs have asymmetrical and cambered cross-sections. The barbules can be divided into two types [18]: (i) the distal barbules,

which branch out towards the tip and have hooklets on their underside, and (ii) the proximal barbules with rounded ridges on the upper side. The hooklets of the distal barbules overlap with the proximal barbules of adjacent barbs and keep them in parallel (Fig. 1 d). Many of the outstanding properties of feathers are linked to this interlocking mechanism [16, 19, 26]. The uniformly overlapping barbules prevent an increase in the distance between the barbs and their separation. However, these overlapping structures allow for a decrease in the distance between the barbs during the compression in the vane plane. In vibrating feathers, this behavior of the overlapping barbs should potentially affect the damping behavior of the vanes in different deflection directions differently.

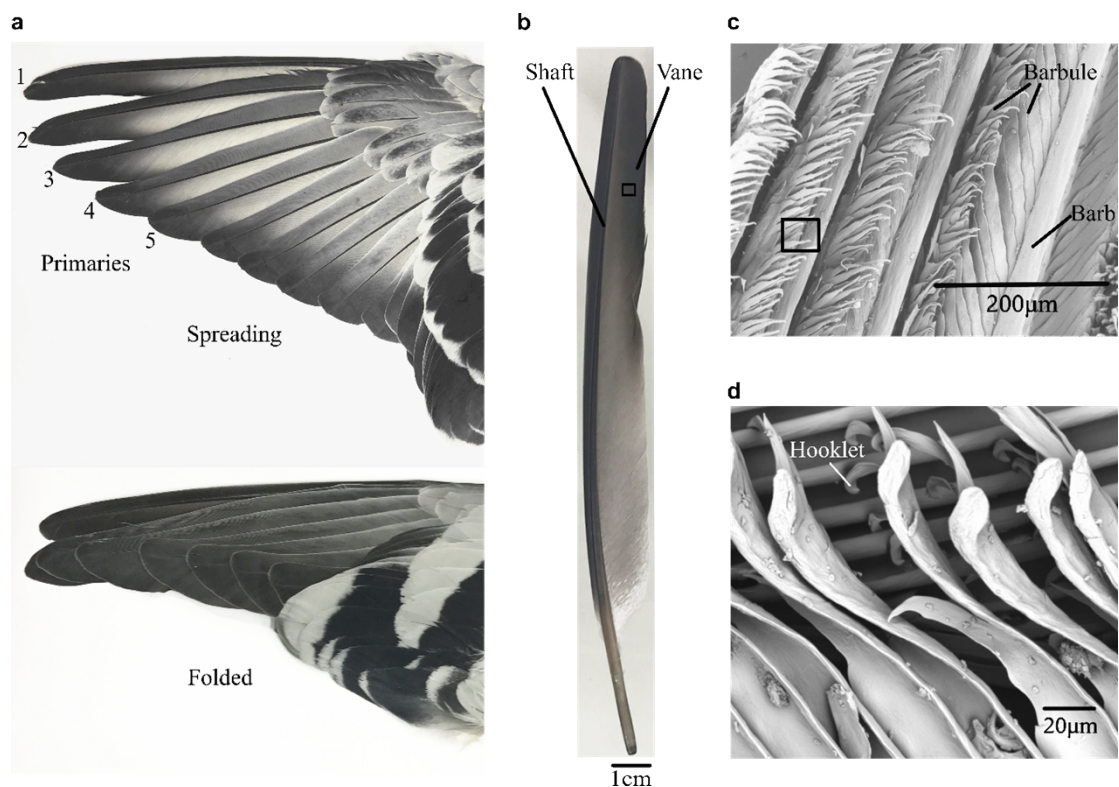


Fig. 1. Morphology of the primary flight feathers (PFF). (a) The wing of the pigeon, with spread (upper image) and folded (lower image) primaries. (b) The primary feather is composed of the main shaft and vanes (No.1 PFF). (c) Barbs of the vane branch from the shaft, and barbules branch from barbs. (d) Hooklets at the tip of distal barbules interlock with the proximal barbules on the neighboring barbs

3.3.2 Damping behavior

Damping tests were conducted to investigate a possible difference in the damping behavior of the intact feathers with vanes and the shafts without vanes in two

deflection directions, parallel and perpendicular to the vanes. The shapes of the trajectories, excursion of amplitudes, and the directionality of the vibrations varied regarding with or without the feather vanes and deflection direction (Fig. 2). Compared to feathers with the vanes (Fig. 2 a, b), the vibrations of the shafts without vanes have more complex trajectories (Fig. 2 c, d).

The trajectories were further separated into the X and Y amplitudes by time (Fig. 3). Vibration amplitudes in the direction of their excitation continuously decreased from their maximum at the first oscillation. However, vibration amplitudes observed perpendicular to their excitation direction first increased. Compared to the intact feather, the vibrations of the shaft without vanes showed more harmonics and possible phase shifts. After removing the vanes, the varied vibrations may be due to the decreased mass, the changed stiffness distribution, and the asymmetric shape of the shaft.

The frequency spectra obtained by FFT of the $X(t)$ and $Y(t)$ curves are shown in figure 4. Although flat plates with a uniform cross-sectional area and constant elastic modulus have easily predicted orders of frequencies and mode shapes, it is difficult to apply these models that do not have uniform cross-section area or elastic moduli [36]. A related aspect of flutter in airflows was described that feathers may exhibit a dozen or more modes, and can abruptly switch from one mode to another [12]. To simplify the frequency analysis, the first main frequencies of the vibrations in horizontal (f_x) and vertical (f_y) directions (PFF1, Fig. 4) and summarized in Table 1. After trimming the vanes, the fundamental frequencies of the bare shaft increased by 51 – 70%.

Table 1. First main frequencies of feathers at two deflection directions ($n=60$)

feather status	deflections / relative to the vanes	f_x / Hz	f_y /Hz
with vanes	vertical / perpendicular	43.14 ± 5.32	42.32 ± 6.27
with vanes	horizontal / parallel	41.82 ± 4.85	44.38 ± 6.47
without vanes	vertical / perpendicular	65.12 ± 4.25	72.09 ± 10.69
without vanes	horizontal / parallel	70.82 ± 6.78	70.21 ± 8.88

The feathers with vanes had significantly lower fundamental vibration frequencies $f(x)$ and $f(y)$ than the shafts without vanes ($P < 0.001$). Interestingly, the frequency $f(x)$ of

the vibrations in the shafts is significantly lower at vertical excitations than at horizontal excitation ($P=0.024$). Reasons for this difference could be the influence of the zipped vanes plane. The excited vibrations perpendicular to the vanes will trigger the vibrations parallel to the vanes as driven vibrations or crosstalk because of the shaft twisting.

Summed up, the vibrations of the feathers with vanes decayed faster than those of the bare shafts. The loss of mass, different stiffness distribution and the increased air friction of the vanes may explain the increased frequencies of the shaft after trimming the vanes.

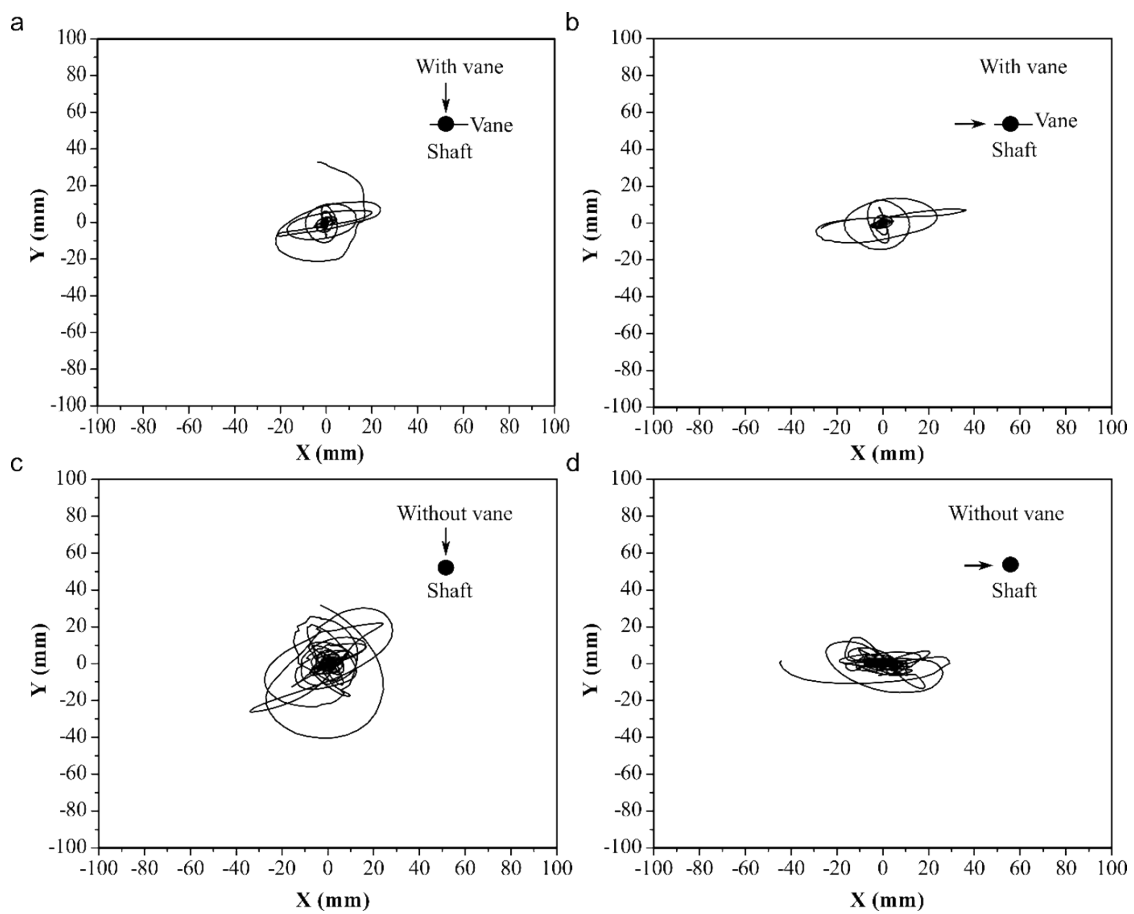


Fig. 2. Exemplary trajectories of the primary flight feather's (no. 1) tip vibrations were observed perpendicular to the shaft. Feather with vane after (a) vertical and (b) horizontal excitation. Feather shaft without vane after (c) vertical and (d) horizontal excitation. The top-right icon indicates the feathers and the deflection direction

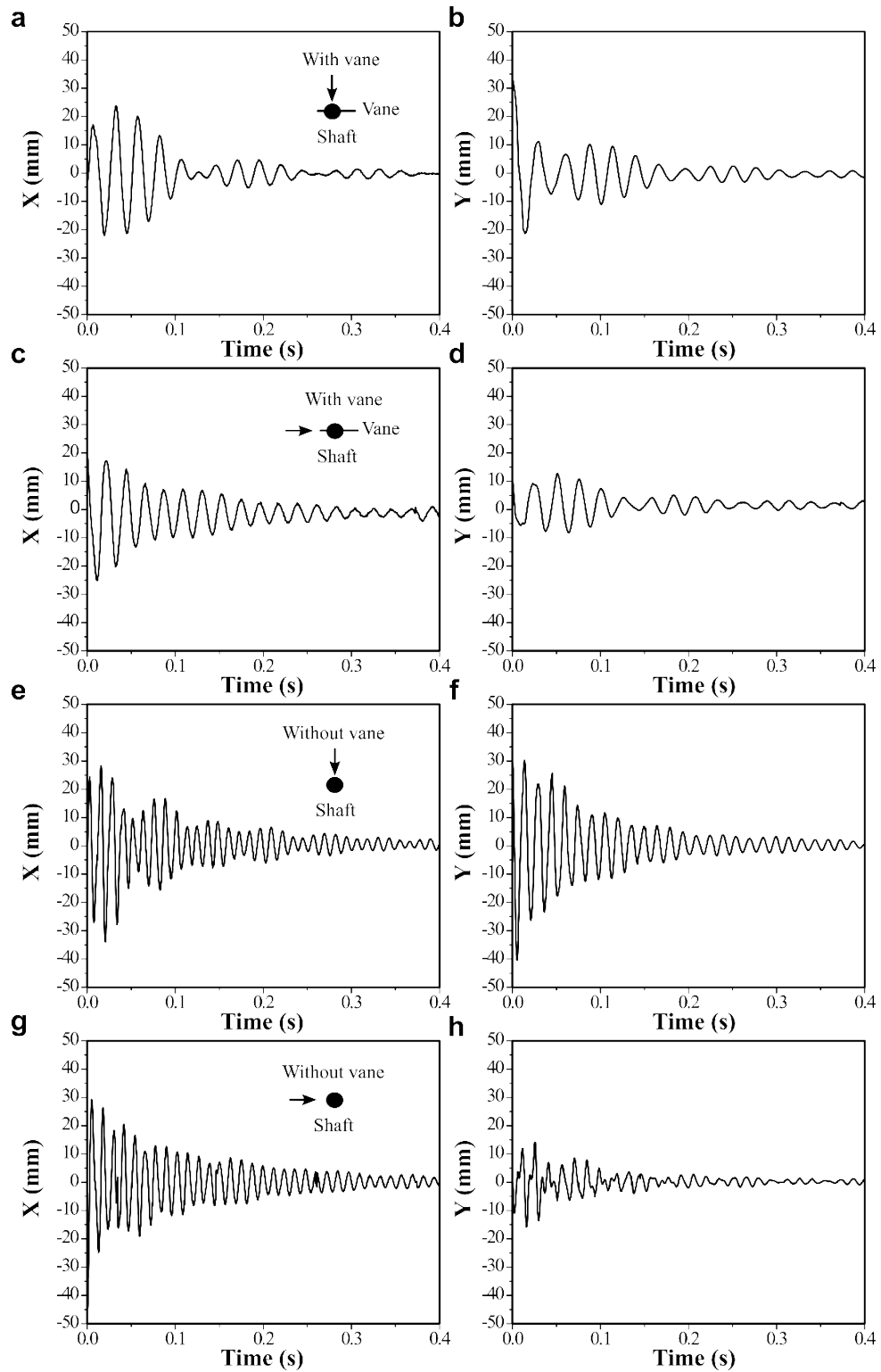


Fig. 3. Amplitudes of damped vibrations as a function of time. (a, b) X- and Y- vibrations of the feather with vane at vertical deflection; (c, d) X- and Y- vibrations of the feather with vane at horizontal deflection; (e, f) X- and Y- vibrations of the shaft without vane at vertical deflection; (g, h) X- and Y- vibrations of the shaft without vane at horizontal deflection

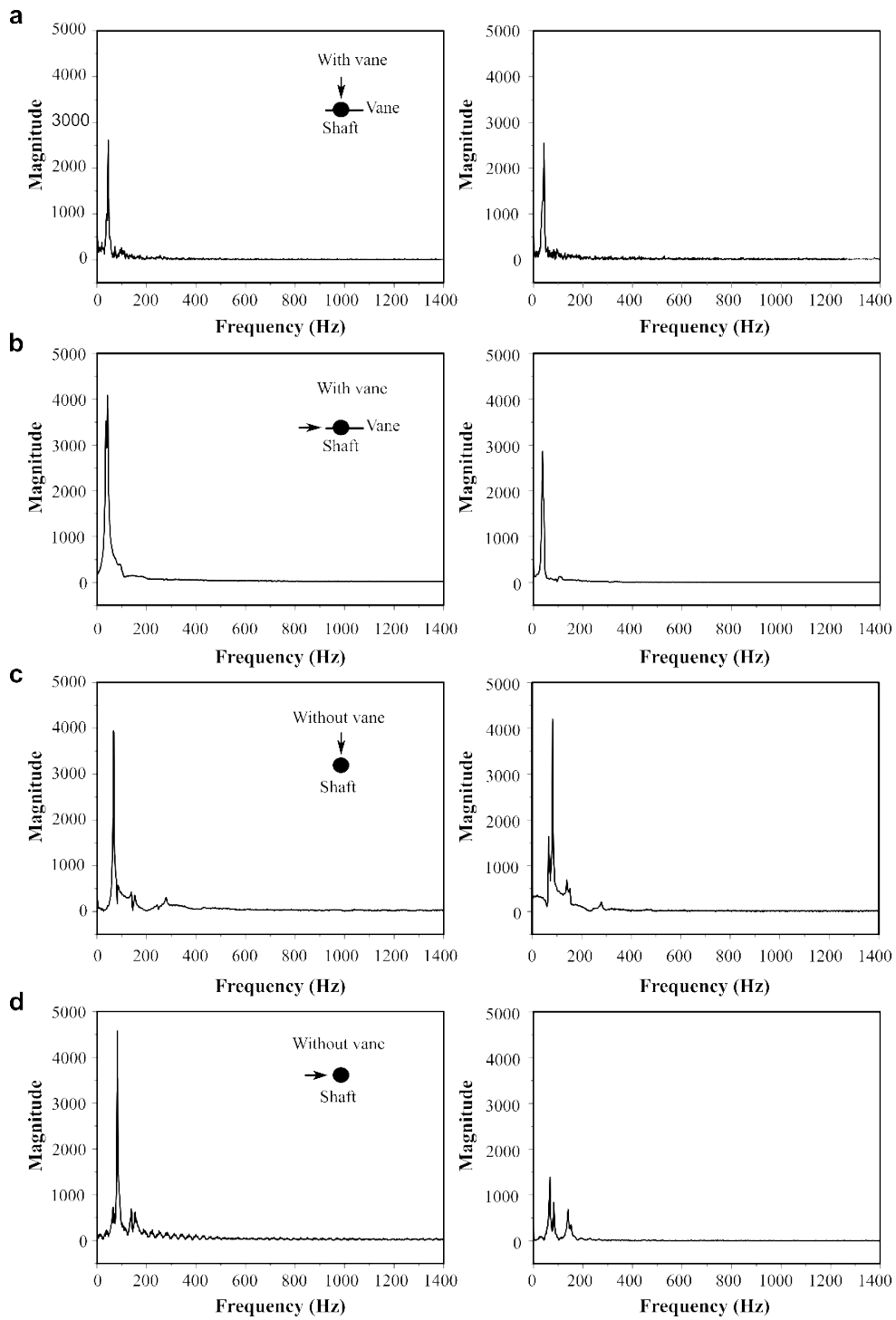


Fig. 4. Typical power spectra and natural frequencies of feather vibrations. (a) Frequencies of X- and Y- vibrations in the feather with vane at the vertical deflection; (b) Frequencies of X- and Y- in the feather with vane at the horizontal deflection; (c) Frequencies of X-, Y- in the shaft without vane at the vertical deflection; (d) Frequencies of X-, Y- in the shaft without vane at the horizontal deflection

3.3.3 Damping ratio

Bird feathers are known to be coupled to vibration-sensitive nerves allowing birds to sense and respond to mechanical changes [37, 38]. Besides nerve and muscle control, the structure could also help. The developed serrations along the leading edges were investigated in different owl species [39]. And the specialized feather velvet in owls was confirmed to reduce the sound produced [40]. The damping significance of vanes was exhibited by damping ratios. The damping ratios were determined for the first natural vibration frequencies. In all preparations and excitation directions, the damping ratios of feathers with the vanes compared to those of shafts without the vanes were significantly higher ($P < 0.001$, $n=60$) (Fig. 5). For feathers with vanes, the damping ratios for excitations parallel and perpendicular to the vanes also differed significantly ($P=0.010$, $n=30$). In the shafts without vanes, the damping ratios significantly differed only for vibrations perpendicular to the vane plane ($P<0.001$, $n=30$). Remarkably, in the feathers with vanes and the shafts without vanes, the damping ratio for vibrations perpendicular to the vane plane was the highest at vertical excitation. Compared to the intact feathers, the damping ratios are decreased by 38-60% after trimming the vanes. Possible damping mechanisms of the vanes are listed below.

I. *Aerodynamic damping*. During the flight, the feathers are practically air-impermeable by the pressure gradient in the overlapping inner and outer vanes [41]. Airflow may aerodynamically damp vibrations of an airfoil [42]. Wingbeat frequencies of the pigeon *Columba livia* were measured to be 6.5 ± 0.2 Hz in paired flight and 5.5 ± 0.2 Hz in solo flight [43]. In homing flights, the maximum airspeed of *C. livia* was $23.0 \text{ m}\cdot\text{s}^{-1}$ with a mean value of $19.9 (\pm 2.6 \text{ s.d.}) \text{ m}\cdot\text{s}^{-1}$ [44]. At such high wingbeat frequencies and airspeeds, the air friction especially perpendicular to the vanes by beating wing will strongly affect the damping of feathers. In addition, the passive structure responses of flexible membranes with the flow could alter the aerodynamic characteristic of simple flat-plate wings confirmed [45], which makes the motion of zipped vanes surface result in an aerodynamic benefit.

II. *Structural damping*. At low speeds, structural damping is also a significant factor [46]. Under loading, the feather barbules and hooklets move, generating friction at

these interfaces and bending, generating energy storage in structural deformations. At a certain load, the hooked anchoring separates, the energy stored in the structural deformation releases, and the vibration energy dissipates. The collective effect of neighboring barbs allows the accumulation of more elastic energy and, in this way, further enhances energy dissipation [19]. Vibrations excited perpendicular to the vanes can be effectively transferred to vibrations in the vane plane. Other mechanisms, which are not discussed in detail here, could be the vibrations transferred to the surrounding feathers and tissues (skin, bones).

III. *Material damping.* Material damping refers to inherent energy dissipation during material deformation [42]. The shaft and vanes elements of the feather are filled with a foam medulla, which was shown to effectively damp vibrations [28].

The interesting feature of the interlocking mechanism in the vanes not only increases the damping ratio but transfers the vibrations excited perpendicular to the vanes to vibrations in the vane plane. This transfer shortens decay time and quickly stabilizes the feather, due to the stronger energy dissipation caused by friction, deformations of hooks, and additional vibrations caused by neighboring barbs in the vanes.

This intricate design of multidirectional damping capability in the feather vanes also contributes to the efficiency of bird flight. During flapping, forces and stresses are higher on the dorsal and ventral sides, and the main vibrations of feathers are excited vertically, perpendicular to the vanes. The higher damping ratios of feathers under vertical deflection contribute to the stronger stability of the wing.

The vane features examined here may inspire more efficient lightweight aerospace materials with tailored damping properties and directional differences. The damping ratio of artificial wings or their parts could be potentially adjusted by layers of zipped structures in unmanned aerial vehicles.

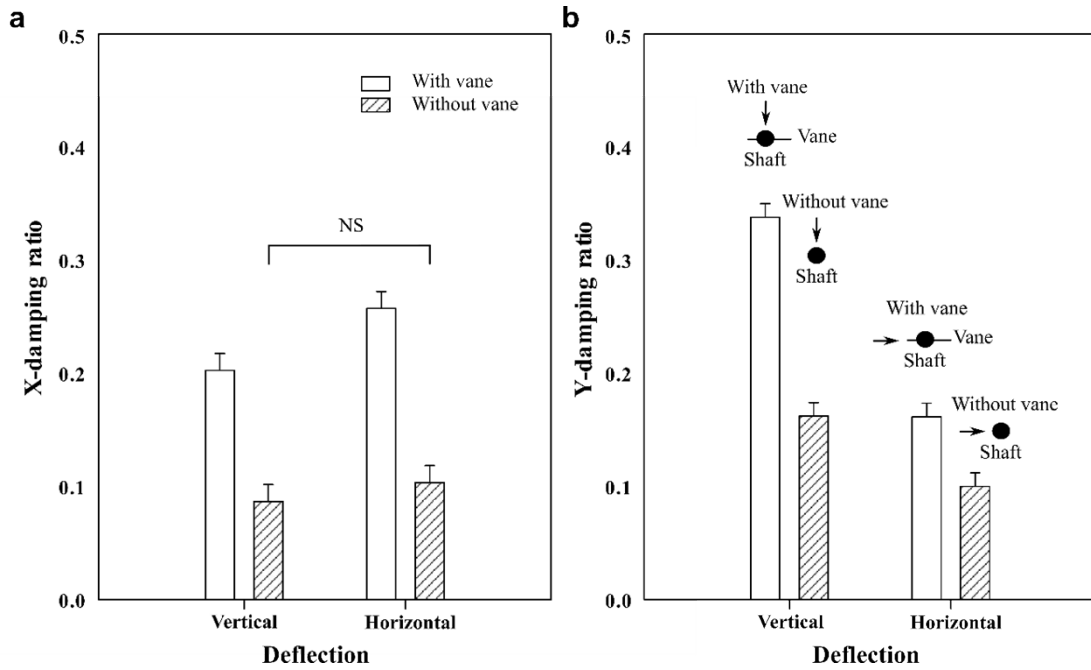


Fig. 5. Damping ratios of the feathers with vane (open bars) and the shafts without vane (hatched bars). ζ_x and ζ_y were calculated for vibrations in X (a, parallel to the vane)- and Y (b, perpendicular to the vane) directions. Here, the results are presented for two deflections. 'NS' means no significant difference

3.4 Conclusions

Unwanted vibrations of bird wings and feathers may lead to instability during flight. To exclude specific functions related to alarm signal and courtship, high damping is desirable to attain low vibration and low noise. In this study, vanes have been confirmed to enhance the damping of feathers. The presence of vanes decreases the number of vibration modes and the first natural vibration frequency and increases damping ratios independent of the excitation direction (horizontal or vertical). Feathers with vanes are likely to be adapted to have the highest damping ratio perpendicular to the vanes at vertical deflections. The aerodynamic resistance of the vanes' planar surface, the movement of the numerous hooklets and barbules, and the foam-filled shaft and barbs are likely to be the mechanisms responsible for the enhanced damping properties of the feathers.

Acknowledgments The authors would like to thank Dr. Oleksii Vodka (National Technical University "Igor Sikorsky Kyiv Polytechnic Institute," Kiev, Ukraine) for his idea of separating the vibration modes. Also, thanks to all related members of the

Functional Morphology and Biomechanics, at Kiel University, Germany, and the Bioinspired Structure and Surface Engineering, at Nanjing University of Aeronautics and Astronautics, China.

Authors' contributions S.N.G. designed and coordinated the study; K.D., A.K., H.R., C.F.S., and S.N.G. designed the experiment. K.D. experimented, carried out the statistical analysis, and wrote the manuscript. All authors discussed the results, edited the manuscript, and gave final approval for publication.

Funding This work was financially supported by Sino-German Center for Research Promotion (Grant no. GZ1154).

Data availability statement The data that support the findings of this study are available from the corresponding author upon request.

Declarations

Conflict of Interests The authors declare that there is no conflict of interest regarding the publication of this paper.

Open Access This article is licensed under a Creative Commons Attribution 4.0 International License, which permits use, sharing, adaptation, distribution and reproduction in any medium or format, as long as you give appropriate credit to the original author(s) and the source, provide a link to the Creative Commons licence, and indicate if changes were made. The images or other third party material in this article are included in the article's Creative Commons licence, unless indicated otherwise in a credit line to the material. If material is not included in the article's Creative Commons licence and your intended use is not permitted by statutory regulation or exceeds the permitted use, you will need to obtain permission directly from the copyright holder. To view a copy of this licence, visit <http://creativecommons.org/licenses/by/4.0/>.

References

1. Alexander, D. E. (2015). *On the wing. Insects, pterosaurs, birds, bats and the evolution of animal flight*. Oxford University Press, Oxford, UK.

2. Clark, C. J., Elias, D. O., & Prum, R. O. (2013). Hummingbird feather sounds are produced by aeroelastic flutter, not vertex-induced vibration. *Journal of Experimental Biology*, **216**, 3395-3403.
3. Makovicky, P. J., & Zanno, L. E. (2011). Theropod diversity and the refinement of avian characteristics. In Dyke, G., & Kaiser, G. (Eds) *Living dinosaurs: the evolutionary history of modern birds* (pp. 9-29). John Wiley & Sons, Ltd, Oxford, UK.
4. Liu, X., Hefler, C., Shyy, W., & Qiu, H. (2021). The importance of flapping kinematic parameters in the facilitation of the different flight modes of dragonflies. *Journal of Bionic Engineering*, **18**, 419-427.
5. Shen, H., Ji, A., Li, Q., Wang, W., Qin, G., & Han, Q. (2021). The unique strategies of flight initiation adopted by butterflies on vertical surface. *Journal of Bionic Engineering*, **18**, 840-856.
6. Feo, T. J., Field, D. J., & Prum, R. O. (2015). Barb geometry of asymmetrical feathers reveals a transitional morphology in the evolution of avian flight. *Proceedings of the Royal Society B*. **282**, 20142864.
7. Videler, J. J. (2005). *Avian flight*. Oxford University Press, Oxford, UK.
8. McLelland, J. (1990) *A color atlas of avian anatomy*. Wolfe Publishing Ltd, London, UK.
9. Yang, W., Chao, C., & McKittrick, J. (2013). Axial compression of a hollow cylinder filled with foam: A study of porcupine quills. *Acta Biomaterialia*, **9**, 5297-5304.
10. Prum, R. O. (1999). Development and evolutionary origin of feathers. *Journal of Experimental Zoology Part B: Molecular and Developmental Evolution*, **285**, 291-306.
11. Bragulla, H., & Hirschberg, R. M. (2003). Horse hooves and bird feathers: Two model systems for studying the structure and development of highly adapted integumentary accessory organs-the role of the dermoepidermal interface for the microarchitecture of complex epidermal structures. *Journal of Experimental Zoology Part B: Molecular and Developmental Evolution*, **298**(1), 140-151.
12. Clark, C. J., Elias, D. O., Girard, M. B., & Prum, R. O. (2013). Structural resonance and mode of flutter of hummingbird tail feathers. *Journal of Experimental Biology*, **216**, 3404-3413.
13. Sullivan, T. N., Pissarenko, A., Herrera, S. A., Kisailus, D., Lubarda, V. A., & Meyers, M. A. (2016). A lightweight biological structure with tailored stiffness: the feather vane. *Acta Biomaterialia*, **41**, 27-39.
14. Liu, Z. Q., Jiao, D., Meyers, M. A., & Zhang, Z. F. (2015). Structure and mechanical properties of naturally occurring lightweight foam-filled cylinder: The peacock's tail coverts shaft and its components. *Acta Biomaterialia*, **17**, 137-151.
15. Prum, R. O., & Williamson, S. (2001). Theory of the growth and evolution of feather shape. *Journal of Experimental Zoology Part B: Molecular and Developmental Evolution*, **291**, 30-57.

-
16. Alibardi, L. (2007). Cell organization of barb ridges in regenerating feathers of the quail: implications of the elongation of barb ridges for the evolution and diversification of feathers. *Acta Zoologica*, **88**, 101-117.
 17. Hooke, R. (1665). *Micrographia: or some physiological descriptions of minute bodies made by magnifying glasses with observations and inquiries thereupon*. Royal Society, London, UK.
 18. Ennos, A. R., Hickson, J. R. E., & Roberts, A. (1995). Functional morphology of the vanes of the flight feathers of the pigeon *Columba livia*. *Journal of Experimental Biology*, **198**, 1219-1228.
 19. Kovalev, A., Filippov, A. E., & Gorb, S. N. (2013). Unzipping bird feathers. *Journal of Royal Society Interface*, **11**, 20130988.
 20. Chen, Q., Gorb, S. N., Kovalev, A., Li, Z., & Pugno, N. (2016). An analytical hierarchical model explaining the robustness and flaw-tolerance of the interlocking barb-barbule structure of bird feathers. *Europhysics Letters*, **116**, 24001.
 21. Greenewalt, C. H. (1960). The wings of insects and birds as mechanical oscillators. *Proceedings of the American Philosophical Society*, **104**(6), 605-611.
 22. Clark, C. J., & Prum, R. O. (2015). Aeroelastic flutter of feathers, flight and the evolution of non-vocal communication in birds. *Journal of Experimental Biology*, **218**, 3520-3527.
 23. Rajabi, H., Shafiei, A., Darvizeh, A., Dirks, J. H., Appel, E., & Gorb, S. N. (2016). Effect of microstructure on the mechanical and damping behavior of dragonfly wing veins. *Royal Society Open Science*, **3**, 160006.
 24. Lietz, C., Schaber, C. F., Gorb, S. N., & Rajabi, H. (2021). The damping and structural properties of dragonfly and damselfly wings during dynamic movement. *Communications Biology*, **4**, 737.
 25. Bonser, R. H. C., & Purslow, P. P. (1995). The Young's modulus of feather keratin. *Journal of Experimental Biology*, **198**, 1029-1033.
 26. Gao, J. L., Chu, J. K., Guan, L., Shang, H. X., & Lei, Z. K. (2014). Viscoelastic characterization of long-eared owl flight feather shaft and the damping ability analysis. *Shock and Vibration*, 709367.
 27. Gao, J. L., Chu, J. K., Shang, H. X., & Guan, L. (2015). Vibration attenuation performance of long-eared owl plumage. *Bioinspired, Biomimetic and Nanobiomaterials*, **4**(3), 187-198.
 28. Deng, K., Kovalev, A., Rajabi, H., Schaber, C. F., Dai, Z. D., & Gorb, S. N. (2022). The damping properties of the foam-filled shaft of primary feathers of the pigeon *Columba livia*. *The Science of Nature*, **109**(1). 10.1007/s00114-021-01773-7.
 29. Dakin, R., McCrossan, O., Hare, J. F., Montogomerie, R., & Kane, S. A. (2016). Biomechanics of the peacock's display: How feather structure and resonance influence multimodal signaling. *Plos One*, **11**(4). 10.1371/journal.pone.0152759.
 30. Hightower, B. J., Wijnings, P. W. A, Scholte, R., Ingersoll, R., Chin, D. D., Nguyen, J., Shorr, D., & Lentink, D. (2021). How oscillating aerodynamic forces

explain the timbre of the hummingbird's hum and other animals in flapping flight. *ELife*. <https://doi.org/10.7554/eLife.63107>.

31. Clark, C. J., & Feo, T. J. (2008). The Anna's hummingbird chirps with its tail: a new mechanism of sonation in birds. *Proceedings of the Royal Society B Biological Sciences*, **275**, 1637. 10.1098/rspb.2007.1619.
32. Clark, C. J. (2008). Fluttering wing feathers produce the flight sounds of male streamertail hummingbirds. *Biology Letters*, **4**(4), 341-34.
33. Bostwick, K. S., Elias, D. O., Mason, A., & Montealegre-Z, F. (2010). Resonating feathers produce courtship song. *Proceedings of the Royal Society B Biological Sciences*, **277** (1683), 835-841.
34. Niese, R., & Tobalske, B. W. (2016). Specialized primary feathers produce tonal sounds during flight in rock pigeons (*Columba livia*). *Journal of Experimental Biology*, **219**(14), 2173-2181.
35. Murray, T. G., Zeil, J., & Magrath, R. D. (2017). Sounds of modified flight feathers reliably signal danger in a pigeon. *Current Biology*, **27**(20), 3520-3525.
36. Clark, C. J., Mountcastle, A. M., Mistick, E., & Elias, D. O. (2017). Resonance frequencies of honeybee (*Apis mellifera*) wings. *Journal of Experimental Biology*, **220**(15), 2697-2700.
37. Bruecker, C., Schlegel, D., & Triep, M. (2016). Feather vibration as a Stimulus for sensing incipient separation in falcon diving flight. *Natural Resources*, **7**(7), 411-422.
38. Kane, S. A., Beveren, D. V., & Dakin, R. (2018). Biomechanics of the peafowl's crest reveals frequencies tuned to social displays. *Plos One*. 10.1371/journal.pone.0207247.
39. Weger, M., & Wagner, H. (2016). Morphological variations of leading-edge serrations in Owls (*Strigiformes*). *Plos One*. **11**(3), e0149236.
40. LePiane, K., & Clark, C. J. (2020). Evidence that the dorsal velvet of barn owl wing feathers decreases rubbing sounds during flapping flight. *Integrative & Comparative Biology*, **60**(5), 1068-1079.
41. Mueller, W., & Patone, G. (1998). Air transmissivity of feathers. *Journal of Experimental Biology*, **201**(18), 2591-2599.
42. Akay, A., & Carcaterra, A. (2014). Damping mechanisms. In Hagedorn P., Spelsberg-Korspeter G. (Eds) *Active and passive vibration control of structures* (pp. 259-299). CISM International Centre for Mechanical Sciences, Springer, Vienna.
43. Taylor, L. A., Taylor, G. K., Lambert, B., Walker, J. A., Biro, D., & Portugal, S. J. (2019). Birds invest wingbeats to keep a steady head and reap the ultimate benefits of flying together. *Plos Biology*, **17**(6), e3000299.
44. Garde, B., Wilson, R. P., Lempidakis, E., Boerger, L., Portugal, S. J., Hedenstroem, A., Dell'Omo G., Quetting, M., Wikelski, M., & Shepard, E. L. C. (2021). Fine-scale changes in speed and altitude suggest protean movements in homing pigeon flights. *Royal Society Open Science*, **8**(5), 210130.

-
45. Timpe, A., Zhang, Z., Hubner, J., & Ukeiley, L. (2013). Passive flow control by membrane wings for aerodynamic benefit. *Experiments in Fluids*, **54**, 1471.
 46. Sun, J. (2012). *Vibration characteristics and structural damping of rotating compressor blades*. KTH Royal Institute of Technology, Stockholm, Sweden.

CHAPTER 4

The significance of the zipped design in the vanes

Summary:

The interlocked barbules of vanes play a key role in flight by supporting feathers' aerodynamic function. However, the exact mechanisms that determine the damping properties of the vanes remain elusive. In this part, the damping results indicate the advantage of zipped vanes compared with unzipped vanes in atmosphere and in vacuum. The planar surface in zipped vanes is responsible for aerodynamic damping. Other mechanisms, structural damping and material damping, were also discussed.

Aerodynamic vs. frictional damping in primary flight feathers of the pigeon *Columba livia*

K. Deng^{1, *}, C. F. Schaber¹, A. Kovalev¹, H. Rajabi², Z. D. Dai³ and S. N. Gorb¹

¹ Functional Morphology and Biomechanics, Institute of Zoology, Kiel University, Kiel, Germany

² School of Engineering, London South Bank University, London, U. K.

³ Institute of Bioinspired Structure and Surface Engineering, Nanjing University of Aeronautics and Astronautics, Nanjing, China

* Corresponding author

Kai Deng

E-mail: kdeng@zoologie.uni-kiel.de

Published by:

Applied Physics A, 2023, 129:121

<https://doi.org/10.1007/s00339-023-06395-6>

Abstract

During flight, vibrations potentially cause aerodynamic instability and noise. Besides muscle control, the intrinsic damping in bird feathers helps to reduce vibrations. The vanes of the feathers play a key role in flight, and they support feathers' aerodynamic function through their interlocked barbules. However, the exact mechanisms that determine the damping properties of the vanes remain elusive. Our aim was to understand how the structure of the vanes on a microscopic level influences their damping properties. For this purpose, scanning electron microscopy (SEM) was used to explore the vane's microstructure. High-speed videography (HSV) was used to record and analyze vibrations of feathers with zipped and unzipped vanes upon step deflections parallel or perpendicular to the vane plane. The results indicate that the zipped vanes have higher damping ratios. The planar surface of the barbs in zipped vanes is responsible for aerodynamic damping, contributing 20% to 50% to the whole damping in a feather. To investigate other than aerodynamic damping mechanisms, the structural and material damping, experiments in vacuum were performed. High damping ratios were observed in the zipped vanes, even in vacuum, because of the structural damping. The following structural properties might be responsible for high damping in feathers: (i) the intact planar surface, (ii) the interlocking of barbules, and (iii) the foamy inner material of the barb's medulla. Structural damping is another factor demonstrating 3.3 times (at vertical deflection) and 2.3 times (at horizontal deflection) difference in damping ratio between zipped and unzipped feathers in vacuum. The shaft and barbs filled with gradient foam are thought to increase the damping in the feather further.

Keywords bird, feather, vane, zipped, unzipped, vacuum, damping ratio

4.1 Introduction

The flight of birds is believed to have originated from dinosaurs' jumping, gliding, and eventually flapping powered flight [1]. Through evolution, birds have transformed the challenging act of flight into a complex mode of locomotion [2].

Aerial locomotion was accompanied by numerous anatomical and physiological adaptations [3]. These avian adaptations include wing stroke efficiency, the fusion of skeleton parts, and strong yet lightweight feathers [3, 4]. In addition, the bird feathers are linked to the musculoskeletal and soft tissues and can create efficient aerodynamic force [5].

During flapping, wings undergo continuous oscillations [6]. Unwanted oscillations can negatively influence the performance of dynamic systems, such as giant reeds [7], wings of dragonflies [8] and damselflies [9], and insect antennae [10]. In oscillations, damping alters the response of the system and results in stability and enhanced controllability [11]. The loss factor is the ratio of the loss modulus to the storage modulus and represents a system's viscoelasticity and damping capacity. For small damping ratios, the loss factor is twice the damping ratio [12]. The loss factor is in the range of 0.03 to 0.07 for the bending of the shaft of swan feathers [13] and 0.896 ± 0.238 for the shafts of pigeon feathers [14]. The damping ratios of pigeon feather shaft regions gradually decreased from the base to the tip from 0.268 to 0.034 [15].

A typical primary feather consists of a shaft and vanes. The shaft has a rigid outer cortex and an inner foam-like medulla [16]. The vanes consist of numerous barbs aligned parallel to each other but at a certain angle to the shaft [17]. The architecture of the vane is closely linked with advancements in aerial locomotion [18]. The barb angle variations [19, 20] and length [3] were assumed to be responsible for the vanes' morphology. Two regions along the barb were observed by Robert Hooke [21], and details of barbules were described [19]: the distal part with hooks that interlock with grooves on the proximal part.

Previous research has studied the properties and mechanisms related to the interlocking of the zipped barbs and their potential application [14, 22-26]. The barb's interlocking is reversible and can be quickly reestablished after separation, and the separation force of the hooklets was investigated [22]. The robustness and flaw-tolerance of the barb-barbule structure were explained by an analytical model [23]. It was assumed that the membranous flaps of overlapping barbules of feathers are impervious to air [27]. The vane's permeability is based on the effect of barb dimensions and the degree of their mechanical interlocking [28]. Damping of feather vibrations could be affected by the vanes supported by reversible hooklets,

cooperative effects of neighboring hooklets groups, and overlapping barbules [29].

In this study, the damping behavior and the underlying damping mechanisms of the zipped and unzipped vanes were examined at two types of deflection under atmospheric conditions, in order to show the functional significance of zipping structures in damping. Air is considered a viscous media in our experiments. Therefore, the energy dissipation of feathers vibrating in air occurs due to the viscous airflow caused by the vibrating structure [30]. Experiments were also carried out in vacuum, to decrease the effect of the friction between feathers and air and the associated aerodynamic damping. Three damping mechanisms were discussed based on the feather morphology and obtained experimental data.

4.2 Materials and methods

4.2.1 Feather preparation and morphology observations

The outermost primary feathers (Fig. 1A, Nos. 1-5) of an adult male rock pigeon (*Columba livia*) were taken from the Zoological Institute of Kiel University, Germany. An iPhone X camera (Apple, California, USA) and a scanning electron microscope (SEM) Hitachi S-4800 (Hitachi, Chiyoda, Japan) were used to explore the hierarchical structure of the feathers (Fig. 1). For SEM, the middle section of the vanes was sectioned, glued, and mounted on an SEM stub, coated with 8 nm gold-palladium using a sputter coater EM SCD500 (Leica, Wetzlar, Germany), and examined at an acceleration voltage of 3.0 kV.

4.2.2 Damping test at the atmospheric pressure and in the vacuum condition

Damping tests were performed at ambient conditions (room temperature of 18°C to 20°C and relative humidity of 40%-45%). The specimens (primary feathers Nos.1-5) were fixed at the calamus with the vane oriented horizontally. The feather oscillations were excited by a step deflection of 10 mm in horizontal (parallel to the vanes, from the leading edge to the trailing edge, x-axis) or vertical (perpendicular to the vanes, from the ventral to the dorsal side, y-axis) direction. The tips of the feathers were marked using a small white paint point (the mass could be ignored compared to the

mass of the feathers) to increase the tracking efficiency. The vanes' unzipping was performed by treating the feather with an air gun for 1 min with a pressure of 1.7 atm (Fig. 1B).

Damping tests in vacuum were performed inside a glass bell at 10 mbar pressure, to decrease the effect of air friction. Oscillations of the feathers fixed at their calamus on a 3D micro-manipulator were excited by the 10 mm tip deflection.

The decaying vibrations were recorded using a high-speed digital video (HSV) camera (I-Speed 3, Olympus, Tokyo, Japan) focused on the tip of the feathers with a focal plane parallel to the oscillation plane at 3000 fps, shutter time of 0.667 μ s, and resolution of 1280 \times 1024 pixels.

The tracking data (horizontal position X and vertical position Y) were extracted by Tracker (OSP, Massachusetts, USA) and plotted in the orthogonal coordinate system (Fig. 2). Fast Fourier Transform (FFT) in Origin software (OriginLab, Massachusetts, USA) was performed for determination of the fundamental frequencies in X - and Y -directions separately. Damping ratios were obtained using the fitting procedure in Origin software (OriginLab, Massachusetts, USA).

It is challenging to predict orders of frequencies and mode shapes that do not have uniform cross-section areas or constant elastic moduli [31]. A related aspect of flutter in airflows was described. Feathers may exhibit several oscillation modes and abruptly switch from one mode to another [32]. The first main frequencies of the vibrations in horizontal (f_x) and vertical (f_y) directions in the air and vacuum were determined to simplify the analysis. The equation for under-damped vibrations was employed to define vibrations of the first main (fundamental) frequency. The displacement X and the decay time t satisfy the under-damped condition according to the following equation [33]:

$$X = Ae^{-\beta t} \cos(\omega t + \varphi), \quad (1)$$

where β is the damping coefficient, A is the initial amplitude, e is Euler's number, ω is the frequency, and φ is the phase angle. The damping coefficient β was obtained by curve fitting with initial boundary conditions for A being the peak value of the oscillation, ω being the frequency gained by FFT analysis, and φ initially set to zero.

To compare the present data with results gained from earlier studies, the damping coefficient was converted to the damping ratio ζ using the equation below:

$$\zeta = \frac{\beta}{\omega}. \quad (2)$$

For statistical analysis, two-way ANOVA was used for normalized data, including the Turkey test for multiple comparisons by the software SigmaPlot 12.0 (SPSS Inc, Chicago, USA).

4.3 Results

4.3.1 Morphology

The primary feathers are shown in Fig. 1A. In the primaries, the shaft is surrounded by the zipped asymmetrical vanes (Fig. 1B). A feather with unzipped vanes after treatment with the air gun is shown in figure 1B. Barbules and hooklets could be visualized using SEM. The barbs are arranged at some angle towards the tip. They are interlocked with the adjacent barbs via the overlapping barbules in a uniform direction (Fig. 1C). The barbules can be subdivided into two distinct regions, the distal part that branches out at the tip having hooklets and the proximal one towards the base (Fig. 1D) The hooklets overlap at the adjacent barb and keep neighboring barb in parallel (Fig.1D). The simplified cross-section of the feathers shaft (dot) with zipped vanes (full line) and unzipped vanes (dotted line) under 2 deflections is presented in the right image (Fig. 1E).

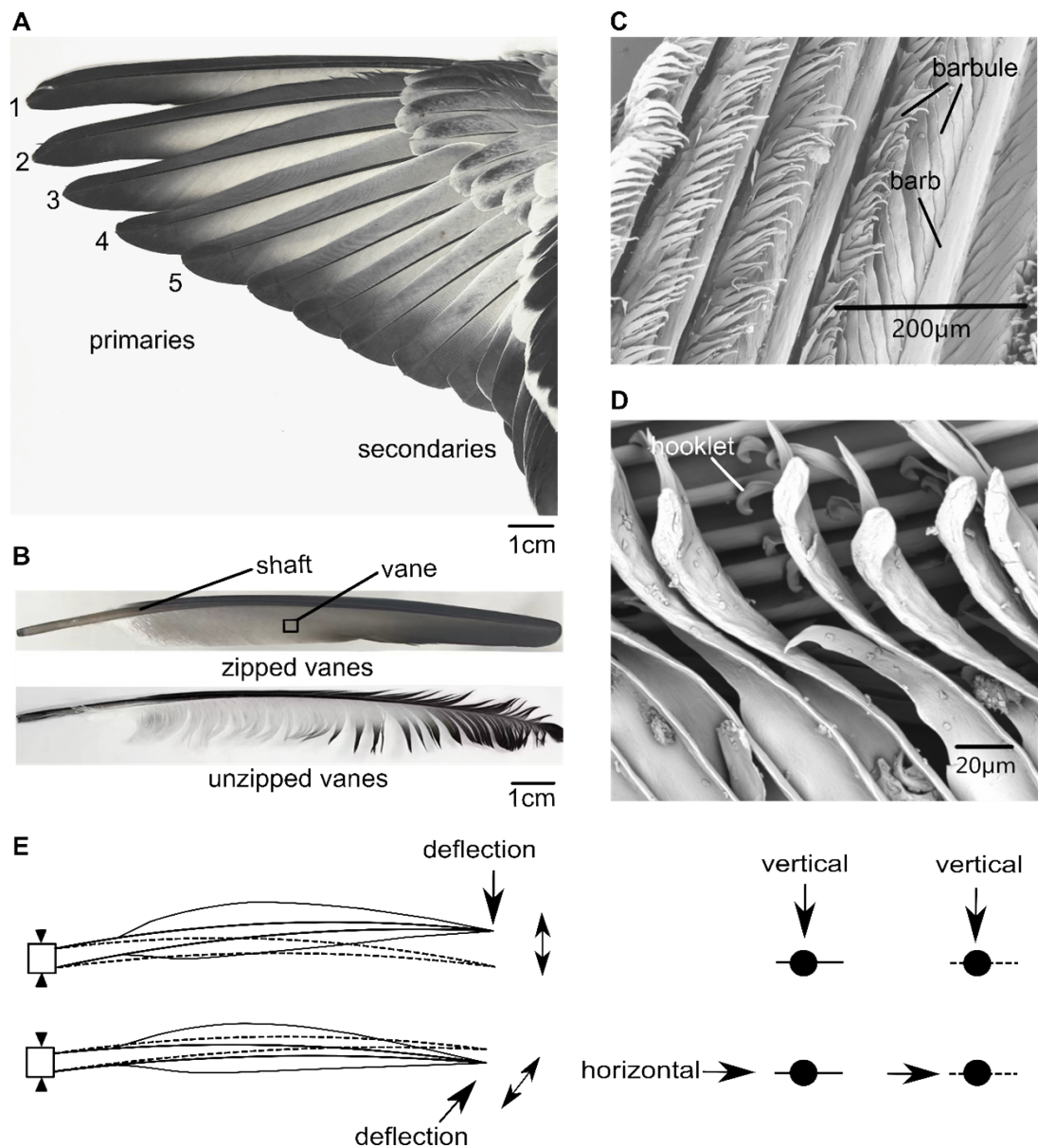


Fig. 1. Morphology of the primary flight feathers. (A) Wing of the pigeon with numbered primary feathers. (B) Primary flight feather (PFF No.1) is composed of the shaft and asymmetric vanes (upper image). Lower image represents unzipped vanes after air gun treatment. (C) Hooked barbules are interlocking with the neighboring barbs within the vane. (D) Hooklets at the tip of the barbules interlocking with the barbules. (E) The damping oscillation of the feather specimen was measured by two excitations and release vertically (upper panel) perpendicularly to the vane and horizontally in the plane of the vane (lower panel). The right image shows the simplified cross-section of the feathers shaft (dot) with zipped vanes (full line) and unzipped vanes (dotted line) under 2 deflections

4.3.2 Damping behaviors

Damping tests were conducted to investigate the damping property of the feathers with both zipped and unzipped vanes at ambient conditions (atmospheric pressure) and in vacuum. In the air, the shapes of the trajectories, excursion amplitudes, and the

directionality of the vibrations varied depending on the zipping state of the vanes and initial deflection direction (Fig. 2 A-D). The vibrations of feathers in the vacuum differed in their tip trajectory shapes and amplitude decay speed (Fig. 2 E-H). The oscillations of the primary feathers with the zipped vanes and unzipped vanes in the atmosphere and the vacuum are shown in Figs. 3 and 4. The oscillations of all feathers decayed in an under-damped regime. The oscillations in vacuum decayed slower.

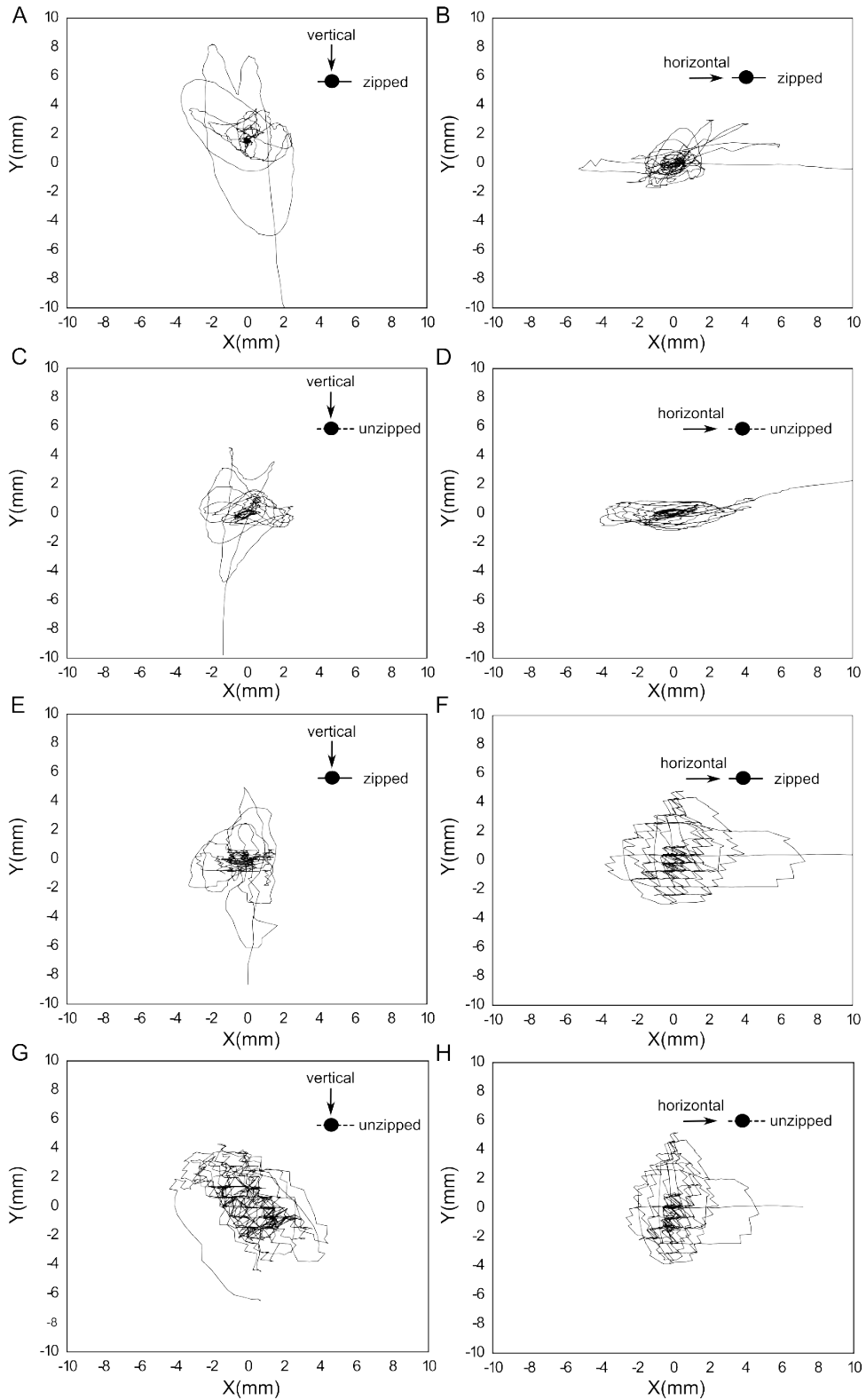


Fig. 2. Trajectories of the decaying vibrations of the primary feathers no. 1 with zipped and unzipped vanes in vertical (Y) direction after vertical (left) and horizontal (right) deflections at atmospheric pressure (A–D) and in vacuum (E–H)

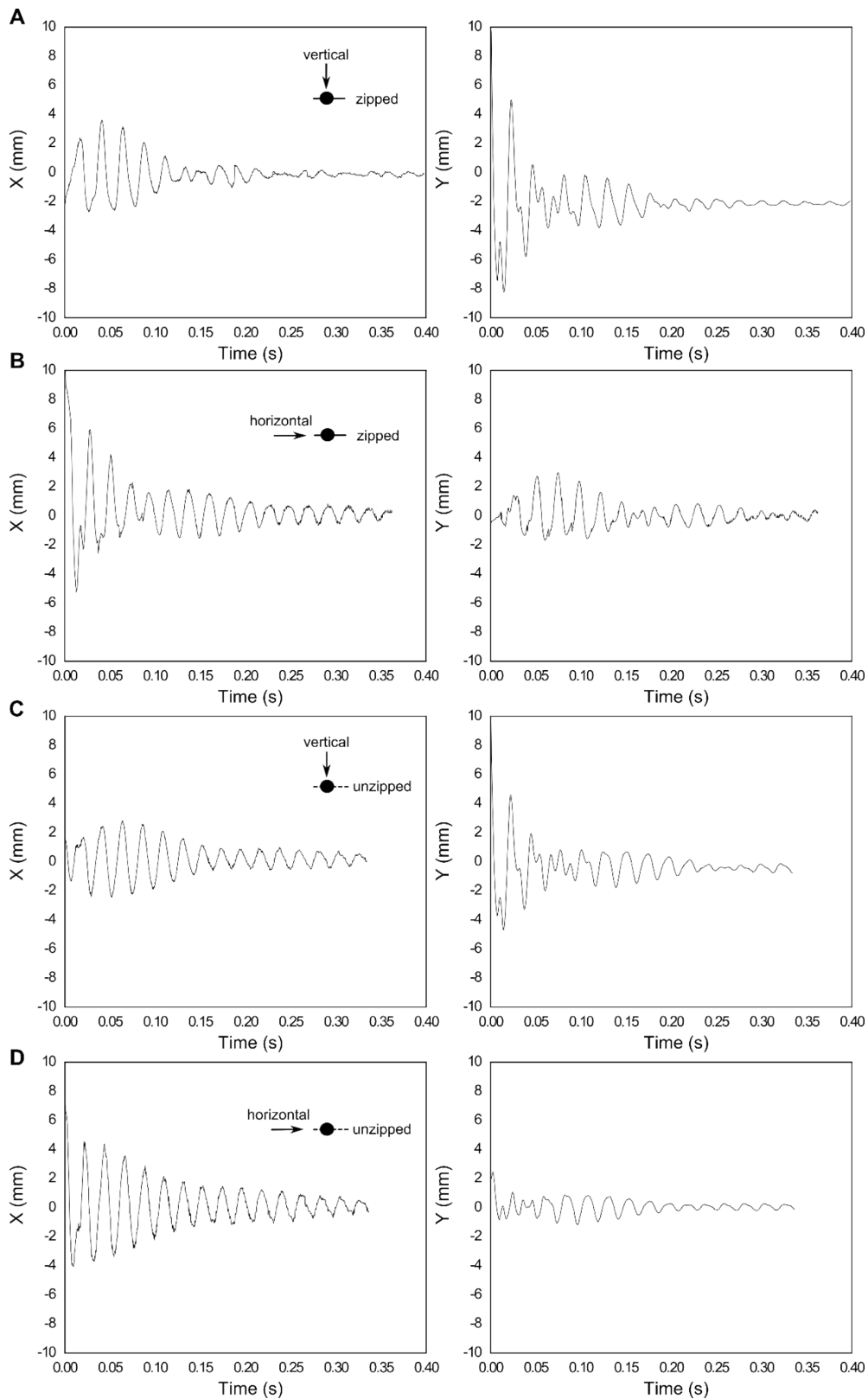


Fig. 3. Feather oscillation decay in X- and Y-directions at atmospheric pressure. (A) Zipped vane after vertical (along the y-axis) deflection, (B) zipped vane after horizontal (along the x-axis) deflection, (C) unzipped vane after vertical deflection, (D) unzipped vane after horizontal deflection

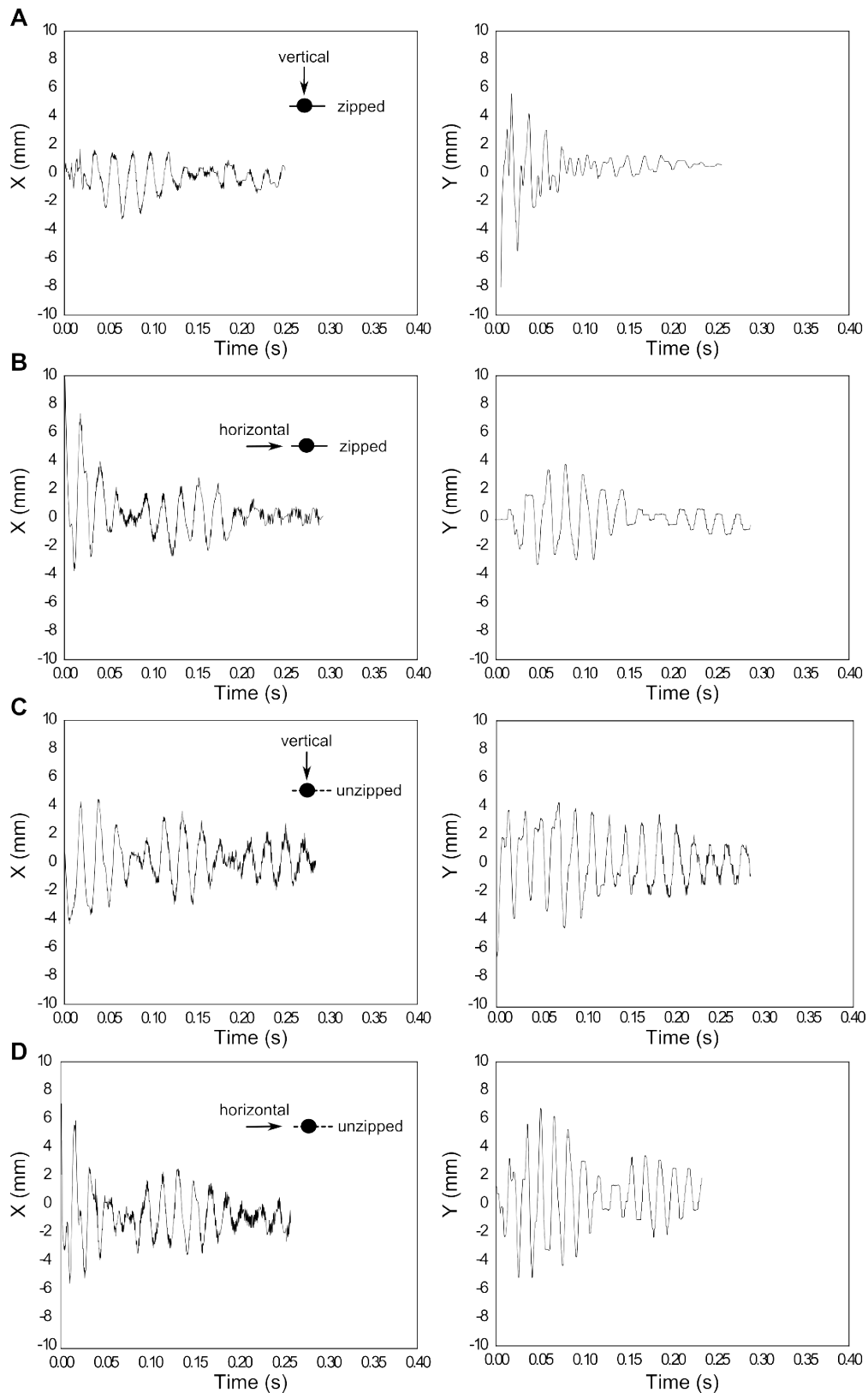


Fig. 4. Feather oscillation decay in X- and Y-directions in vacuum. (A) Zipped vane after vertical deflection, (B) zipped vane after horizontal deflection, (C) unzipped vane after vertical deflection, (D) unzipped vane after horizontal deflection.

4.3.3 Vibration frequency

The frequency spectra were obtained using FFT of the $X(t)$ and $Y(t)$ curves. To simplify the analysis, the first main frequencies of the vibrations in horizontal (f_x) and vertical (f_y) directions at ambient atmospheric conditions and the vacuum condition are summarized in Tables 1 and 2.

Table 1. First main frequencies of feathers in atmosphere (n=60)

feather state	deflections/ relative to the vanes	f_x / Hz	f_y /Hz
zipped vanes	vertical/ perpendicular	39.59 ± 1.26	39.86 ± 2.85
zipped vanes	horizontal/ parallel	39.80 ± 3.26	39.89 ± 1.39
unzipped vanes	vertical/ perpendicular	45.95 ± 3.63	44.80 ± 2.47
unzipped vanes	horizontal/ parallel	47.31 ± 5.29	45.11 ± 4.33

In the atmosphere, the feathers with zipped vanes had significantly lower fundamental vibration frequencies $f(x)$ and $f(y)$ than the unzipped vanes at both horizontal ($P < 0.001$) and vertical deflections ($P < 0.001$). The possible reasons for the higher vibration frequencies of the unzipped vanes could be the effective rigidity and its distribution, which may affect the vibration modes and damping ratios. In zipped feathers, the innumerable barbules and hooklets interact during vibrations. Since the hooklets interlocking and overlap of barbules are influenced by the external force, the sliding, unzipping and new hooking may change the temporary microstructure.

Table 2. First main frequencies of feathers in vacuum (n=60)

feather status	deflections/ relative to the vanes	f_x / Hz	f_y /Hz
zipped vanes	vertical/ perpendicular	50.73 ± 2.20	51.75 ± 3.83
zipped vanes	horizontal/ parallel	46.42 ± 4.61	49.70 ± 3.19
unzipped vanes	vertical/ perpendicular	53.81 ± 3.63	54.45 ± 4.64
unzipped vanes	horizontal/ parallel	46.88 ± 3.74	47.77 ± 4.16

In vacuum, only under vertical deflection, the frequencies of vibration $f(x)$ and $f(y)$ of the zipped vanes were significantly lower than that of the unzipped vanes ($P=0.021$ and $P=0.041$, correspondingly). $f(x)$ was significantly different between the two

deflection directions ($P=0.013$ and $P < 0.001$, for feathers with zipped/unzipped vanes). The possible reason for the absence of a significant difference between zipped and unzipped vanes at horizontal deflection in vacuum could be the following. The influence of the barbs' interlocking in vertical deflections still works, even though the hooks were partly unzipped. These barbs overlapping and interlocking hinder the barb separation (vane extension) but allow the vane compression. This overlapping barb property could affect the effective feather stiffness and distribution at horizontal deflection.

4.3.4 Damping in air

For comparative aspects, the damping characteristics of the vanes were analyzed using the damping ratios determined for the first natural frequency. Under vertical deflections, the damping ratios of feathers with the zipped vanes were $\zeta_x = 0.368 \pm 0.068$ and $\zeta_y = 0.477 \pm 0.213$, and the values of unzipped vanes were $\zeta_x = 0.297 \pm 0.042$, $\zeta_y = 0.248 \pm 0.092$. Under horizontal deflection, the damping ratios of the zipped vanes were $\zeta_x = 0.628 \pm 0.110$ and $\zeta_y = 0.272 \pm 0.026$, while with the unzipped vanes were $\zeta_x = 0.330 \pm 0.083$ and $\zeta_y = 0.219 \pm 0.044$ (Fig. 5).

For vibrations in the horizontal direction, the highest damping ratio ζ_x was observed in feathers with zipped vanes under horizontal deflection ($P < 0.001$). At vertical deflections, ζ_x decreased by 20%, and ζ_y decreased by 50% after unzipping. At horizontal deflections, the ζ_x decreased by 48%, and ζ_y decreased by 20% after unzipping. There was no difference in the damping ratio between zipped and unzipped vanes under vertical deflection ($P=0.295$). In the feathers with zipped vane, a significant difference was found between the two deflection directions ($P < 0.001$). In contrast, no difference was present in the damping ratio between the two deflections in the feathers with unzipped vanes ($P=0.758$).

For vibrations in the vertical direction, significant differences in the damping ratios ζ_y were found in zipped and unzipped vanes under vertical deflection ($P < 0.001$). In zipped vanes, damping ratios for the two deflection directions showed a statistically significant difference ($P=0.002$). However, no statistically significant difference was found in the unzipped feathers.

In summary, the zipped vanes had a higher damping capacity along the direction of deflections. For both ζ_x and ζ_y from unzipped vanes, no significant difference was found between the two deflection directions. The unzipping changed the damping of vanes under two deflections by affecting their integrity, partly weakening the hooklets-mediated interactions between barbs and reducing the coupling between vibrations perpendicular and parallel to the vane plane.

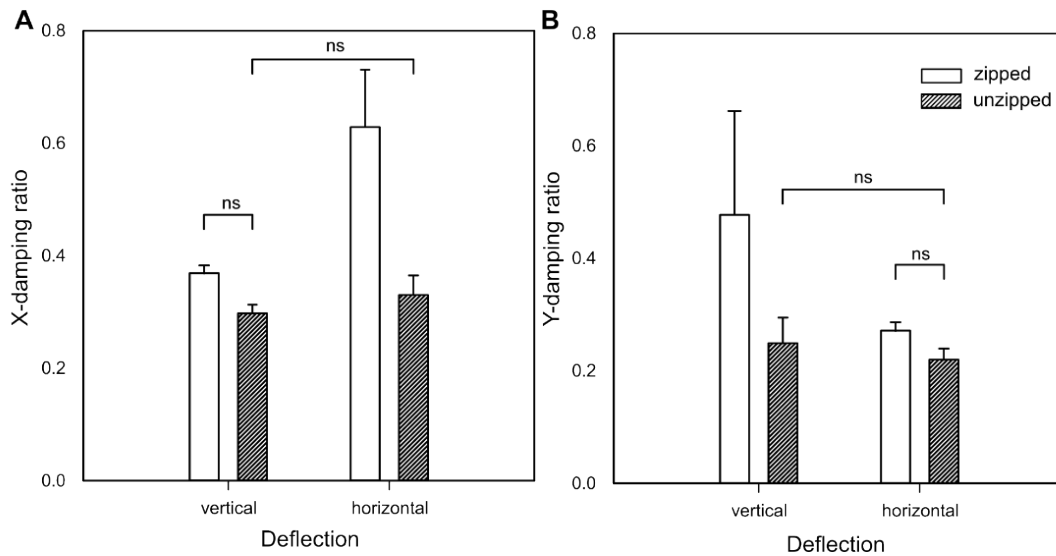


Fig. 5. Damping ratios of feathers with zipped (empty bars) and unzipped (hatched bars) vanes in air in (A) X- and (B) Y-direction corresponding to the main natural frequency after vertical and horizontal deflections. Ns indicates no significant difference

4.3.5 Damping in vacuum

In vacuum, the damping ratios of feathers with the zipped vanes under vertical deflections were $\zeta_x = 0.216 \pm 0.051$ and $\zeta_y = 0.341 \pm 0.049$, and the values for unzipped vanes were $\zeta_x = 0.096 \pm 0.009$, $\zeta_y = 0.075 \pm 0.013$. Under horizontal deflection, the damping ratios of feathers with zipped vanes were $\zeta_x = 0.353 \pm 0.140$ and $\zeta_y = 0.252 \pm 0.097$, whereas those of feathers with unzipped vanes were $\zeta_x = 0.131 \pm 0.012$ and $\zeta_y = 0.135 \pm 0.005$ (Fig. 6).

First, in both ζ_x and ζ_y , the damping ratios of the zipped vanes were significantly higher than those of unzipped vanes ($P < 0.001$). Respectively, at vertical deflections, ζ_x decreased 66%, and ζ_y decreased 79% after unzipping. At horizontal deflection, the decrease was 63% in ζ_x and 46% in ζ_y . Second, in zipped vanes, both damping ratios

ζ_x and ζ_y at horizontal and vertical deflection were higher than ζ_x and ζ_y by perpendicular deflection (vertical and horizontal, correspondingly) ($P < 0.001$, $P=0.001$). Third, in unzipped feathers, the damping ratio ζ_y at horizontal deflection was higher than ζ_y at vertical deflection ($P=0.014$; $P<0.001$).

In vacuum conditions, the contributions of the structural and material damping of the zipping structure of vanes are distinguishable. Compared to vacuum conditions, feather oscillations decay faster and have higher damping ratios in the atmosphere.

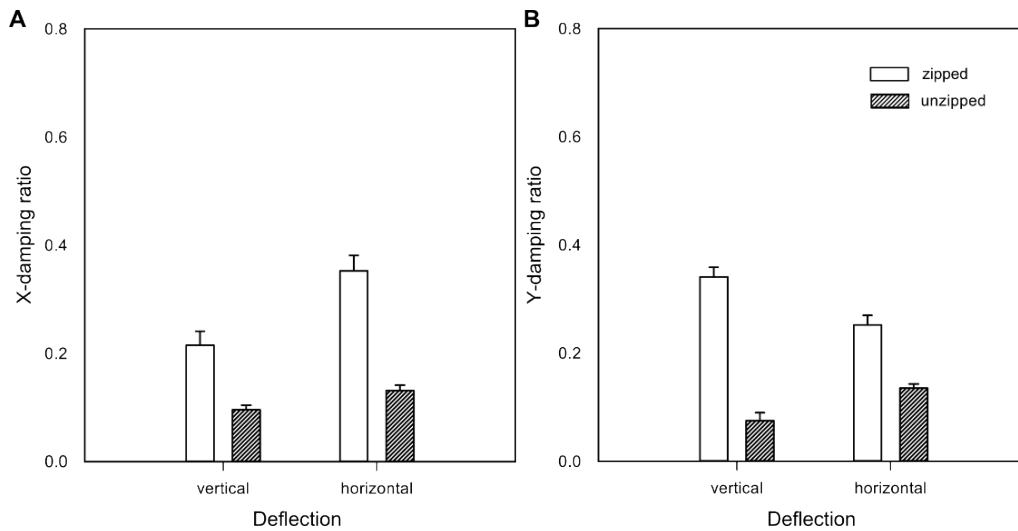


Fig. 6. Damping ratios of feathers with zipped (empty bars) and unzipped (hatched bars) vanes in vacuum conditions in (A) X- and (B) Y-direction corresponding to the main natural frequency after vertical and horizontal deflections. All data show significant differences

4.4 Discussion and conclusion

Our results show that the feathers with zipped vanes have a higher damping capacity in the atmosphere and vacuum in comparison to those with unzipped vanes. The damping ratios of the feathers at deflections within the vane plane and perpendicular to it are different. The mechanisms contributing to damping are the following:

I. *Aerodynamic damping.* Aerodynamic damping is related to the effect of the air on vibrating structures [34]. Feathers are practically air-impermeable during flight [35], and the airflow interacting with feathers could aerodynamically dampen their vibrations [34]. The intact planar shape and the air-valved hooked structure in the zipped vane help to enhance the damping ratios of feathers. This could help explain why the feather damping in the air decreases from 20% to 50% after unzipping. In

addition, the feathers with intact zipped vanes had lower fundamental frequencies at both deflections. However, in vacuum, there is no difference between zipped and unzipped vanes at horizontal deflection. The influence of the barbs' interlocking in vertical deflections still works, even if the hooks are partly unzipped. Such overlapping and interlocking of barbs hinder the barb separation (vane extension) but allow the vane compression.

II. *Structural damping.* Structural damping is another factor demonstrating a 3.3 times and 2.3 times difference in damping ratio between zipped and unzipped feathers in vacuum (0.278 vs. 0.085 at vertical deflections, 0.303 vs. 0.133 at horizontal deflections, the corresponding mean values). Under feather deformation, the barbules and hooklets undergo relative displacements. The barbules and hooklets are assumed to encounter moving, sliding, anchor-breaking, twisting, uncoupling, and recoupling: all these actions lead to energy dissipation. The resulting friction leads to energy dissipation and, consequently, to structural damping. Besides, the extension of a zipped vane is irregular because of the collective effect in hooklets' separation [22], which facilitates the oscillation energy transfer from natural frequency to higher harmonics. The energy dissipation is typically higher at higher frequencies.

III. *Material damping.* Material damping, as an inherent energy dissipation mechanism during material deformation, is another source of feather damping. The most efficient is the material damping in the basal part of the shaft medulla, since the damping ratio measured in vacuum is lower than the damping ratio measured for the base of a feather shaft. The interior part of the barbs is filled with gradient foams [18]. This foam structure undergoes plastic deformation, which contributes to energy dissipation, similar to the damping in the shaft medulla [15]. However, the contribution of the material damping is the lowest if compared to the two mechanisms mentioned above.

Future studies may investigate other sources of damping, such as acoustic vibration, i.e., the transfer of vibrations to the surrounding feathers and tissues (skin, bones). Sound is classified as pressure waves generated by vibrating structures [36]. The sound damping related to the zipping structure is also an interesting mechanism that may contribute to the overall damping of the feather.

In conclusion, our research suggests that the interlocking in the zipped vanes increases the damping ratio of feathers and transfers oscillations perpendicular to the vane into oscillations parallel to the vane plane. This effect shortens the decay time and dampens the oscillations by friction. The damping capability in the vanes can potentially contribute to the bird's flight efficiency. The zipped vanes features can inspire efficient, lightweight aerospace materials with tailored damping properties. The vibration behavior and damping ratio of artificial wings or other parts in unmanned aerial vehicles could be adjusted by varying the number of zipped structures.

Higher damping in the zipped vanes of primary feathers, compared to unzipped ones, is confirmed in the atmospheric and vacuum conditions. Possible damping mechanisms and their relation to feather morphology are discussed. In ambient condition, the planar surface and the interlocked one-way barbs in the vane improves its aerodynamic damping. The experiments in vacuum showed that the vane microstructure significantly contributes to its high damping due to the cooperative effect of overlapping barbs in zipped vanes helping the energy dissipation. Finally, the shaft and barbs filled with the gradient foam are thought to improve the damping in the feather further.

The magnified mimic vanes mode could be printed and matched in a 3D printer. It is possible to adjust the hooked and overlapped layers to control the damping properties and develop flexible damping structures. These bioinspired composites could improve the stability of flapping robots or other shock absorption applications with energy conservation and make less noise.

Acknowledgments. The authors would like to thank Dr. Oleksii Vodka (National Technical University, Ukraine) for separating the vibration modes. They also thank the members of the Department of Functional Morphology and Biomechanics at Kiel University and the Institute of Bioinspired Structure and Surface Engineering at Nanjing University of Aeronautics and Astronautics.

Authors' contributions. S.N.G. designed and coordinated the study; K.D., A.K., H.R., C.F.S., and S.N.G. designed the experiment; K.D. performed the experiment,

carried out the statistical analysis, and wrote the manuscript; All authors analyzed the data, discussed the results, edited the manuscript, and gave final approval for publication.

Funding. This work was financially supported by Sino-German Center for Research Promotion (Grant no. GZ1154 to SNG and ZDD).

Data availability statement. The data supporting this study's findings are available from the corresponding author upon request.

Declarations

Conflict of interests. The authors declare that there is no conflict of interest regarding the publication of this paper.

Open Access. This article is licensed under a Creative Commons Attribution 4.0 International License, which permits use, sharing, adaptation, distribution and reproduction in any medium or format, as long as you give appropriate credit to the original author(s) and the source, provide a link to the Creative Commons licence, and indicate if changes were made. The images or other third party material in this article are included in the article's Creative Commons licence, unless indicated otherwise in a credit line to the material. If material is not included in the article's Creative Commons licence and your intended use is not permitted by statutory regulation or exceeds the permitted use, you will need to obtain permission directly from the copyright holder. To view a copy of this licence, visit <http://creativecommons.org/licenses/by/4.0/>.

References

1. Alexander, D. E. On the wing. Insects, pterosaurs, birds, bats, and the evolution of animal flight. Oxford, UK: *Oxford University Press* (2015)
2. Clarke, J. Feathers before flight. *Science* 340, 690-692 (2013)
3. Feo, T. J., Field, D. J. and Prum, R. O. Barb geometry of asymmetrical feathers reveals a transitional morphology in the evolution of avian flight. *Proc. R. Soc. B.* 282: 20142864 (2015)
4. Bragulla, H. and Hirschberg, R. M. Horse hooves and bird feathers: Two model systems for studying the structure and development of highly adapted integumentary accessory organs - the role of the dermo-epidermal interface for the micro-

-
- architecture of complex epidermal structures. *J Exp Zool B Mol Dev Evol* 298 (1): 140-151(2003)
5. Hieronymus, T. L. Flight feather attachment in rock pigeons (*Columba livia*): covert feathers and smooth muscle coordinate a morphing wing. *J. Anat.* DOI: 10.1111/joa.12511 (2016)
6. Greenewalt, C. H. The wings of insects and birds as mechanical oscillators. *Proc. Amer. Phil. Soc.* 104, 6, 605-611 (1960)
7. Speck, O. and Spatz, H. S. Damped oscillations of the giant reed *Arundo donax* (Poaceae). *Am. J. Bot.* 91, 789-796 (2004)
8. Rajabi, H., Shafiei, A., Darvizeh, A., Dirks, J. H., Appel, E. and Gorb, S. N. Effect of microstructure on the mechanical and damping behaviour of dragonfly wing veins. *R. Soc. Open Sci.* 3, 160006 (2016)
9. Lietz, C., Schaber, C. F., Gorb, S. N. and Rajabi, H. The damping and structural properties of dragonfly and damselfly wings during dynamic movement. *Commun. Biol.* 4, 737 (2021)
10. Rajabi, H., Shafiei, A., Darvizeh, A., Gorb, S. N., Dürr, V., & Dirks, J. H. Both stiff and compliant: morphological and biomechanical adaptations of stick insect antennae for tactile exploration. *J. R. Soc. Interface*, 15(144), 20180246 (2018)
11. De Silva, C. W. *Vibration: fundamentals and practice*. Boca Raton, USA (1999)
12. Hansen, C. *Foundations of vibroacoustics*. Boca Raton, USA (2018)
13. Bonser, R. H. C and Purslow, P. P. The Young's modulus of feather keratin. *J. Exp. Biol.* 198, 1029-1033 (1995)
14. Gao, J. L., Chu, J. K., Guan, L., Shang, H. X. and Lei, Z. K. Viscoelastic characterization of long-eared owl flight feather shaft and the damping ability analysis. *Shock Vib.* 709367 (2014)
15. Deng, K., Kovalev, A., Rajabi, H., Schaber, C. F., Dai, Z. D. and Gorb, S. N. The damping properties of the foam-filled shaft of primary feathers of the pigeon *Columba livia*. *Sci. Nat.* DOI:10.1007/s00114-021-01773-7 (2022)
16. Liu, Z. Q., Jiao, D., Meyers, M. A. and Zhang, Z. F. Structure and mechanical properties of naturally occurring lightweight foam-filled cylinder: The peacock's tail coverts shaft and its components. *Acta Biomater.* 17, 137-151 (2015)
17. Prum, R. O. Development and evolutionary origin of feathers. *J. Exp. Zool.* 285, 291-306 (1999)
18. Sullivan, T. N., Pissarenko, A., Herrera, S. A., Kisailus, D., Lubarda, V, A. and Meyers, M. A. A lightweight biological structure with tailored stiffness: the feather vane. *Acta Biomater.* 41, 27-39 (2016)
19. Ennos, A. R., Hickson, J. R. E. and Roberts, A. Functional morphology of the vanes of the flight feathers of the pigeon *Columba livia*. *J. Exp. Biol.* 198, 1219-1228 (1995)

-
20. Prum, R. O. and Williamson, S. Theory of the growth and evolution of feather shape. *J. Exp. Zool.*, 291, 30-57 (2001)
 21. Hooke, R. *Micrographia: or some physiological descriptions of minute bodies made by magnifying glasses with observations and inquiries thereupon*. London, UK (1665)
 22. Kovalev, A., Filippov, A. E and Gorb, S. N. Unzipping bird feathers. *J. R. Soc. Interface* 11, 20130988 (2013)
 23. Chen, Q., Gorb, S. N., Kovalev, A., Li, Z. and Pugno, N. An analytical hierarchical model explaining the robustness and flaw-tolerance of the interlocking barb-barbule structure of bird feathers. *Europhys. Lett.* 116, 24001 (2016)
 24. Zhao, J., Zhang, J., Zhao, Y., Zhang, Z. and Godefroit, P. Shaking the wings and preening feathers with the beak help a bird to recover its ruffled feather vane. *Mater. Design* 187, 108410. (2020)
 25. Matloff, L. Y., Chang, E., Feo, T.J., Jeffries, L., Stowers, A. K., Thomson, C. and Lentink, D. How flight feathers stick together to form a continuous morphing wing. *Science* 367, 293-297 (2020)
 26. Wang, Y., Mu, Z., Zhang, Z., Song, W., Zhang, S., Hu, H., Ma, Z., Huang, L., Zhang, D., Wang, Z., Li, Y., Zhang, B., Li, B., Zhang, J., Niu, S., Han, Z. and Ren, L. Interfacial reinforced carbon fiber composites inspired by biological interlocking structure. *iScience* 25, 4, 104066 (2022)
 27. Dyck, J. The evolution of feathers. *Zoologica Scripta.* 14, 2, 137-154 (1985)
 28. Sullivan, T. N., Chon, M., Ramachandramoorthy, R., Roenbeck, M. R., Hung, T., Espinosa, H. D. and Meyers, M. A. Reversible attachment with tailored permeability: The feather vane and bioinspired designs. *Adv. Funct. Mater.*, 1702954 (2017)
 29. Deng, K., Rajabi, H., Kovalev, A., Schaber, C. F., Dai, Z. D. and Gorb, S. N. The role of vanes in the damping of bird feathers. *J. Bionic Eng.*, 20, 1646-1655 (2023)
 30. Bao, M., Yang, H., Yin, H. and Sun, Y. Energy transfer model for squeezed-film air damping in low vacuum. *J. Micromech. Microeng.* 12, 341-346 (2002)
 31. Clark, C. J., Mountcastle, A. M., Mistick, E. and Elias, D. O. Resonance frequencies of honeybee (*Apis mellifera*) wings. *J. Exp. Bio.* 220, 2697-2700 (2017)
 32. Clark, C. J., Elias, D. O., Girard, M. B. and Prum, R. O. Structural resonance and mode of flutter of hummingbird tail feathers. *J. Exp. Bio.* 216, 3404-3413 (2013)
 33. Rao, S. S. *Mechanical vibrations*. New Jersey, USA (2010)
 34. Akay, A. and Carcaterra, A. Damping mechanisms. In: Hagedorn P., Spelsberg-Korspeter G. (eds) *Active and passive vibration control of structures*. CISM International Centre for Mechanical Sciences, 558, 259-299. Springer, Vienna (2014)
 35. Mueller, W. and Patone, G. Air transmissivity of feathers. *J. Exp. Biol.* 201, 2591-2599 (1998)

36. Gao, J. L., Chu, J. K., Shang, H. X. and Guan, L. Vibration attenuation performance of long-eared owl plumage. *Bioinspired, Biomim. Nanobiomaterials*, 4, BBN3 (2015)

Publisher's Note Springer Nature remains neutral with regard to jurisdictional claims in published maps and institutional affiliations.

CHAPTER 5

General discussion

5.1. Relationship between material structure and damping properties in the shaft

The damping properties of different shaft parts resulted from their differences in morphology and material structure. In the shaft, the gradient damping properties are related to the observed structural gradients (Deng et al., 2022). Both the cortex and internal foams contribute to the shaft damping properties. In the cortex, friction between multiple layers of aligned fibers is presumably responsible for damping (Deng et al., 2022; Liu et al., 2015). In addition, the ridges interconnecting the cortex and foam have presumably higher internal friction due to an increased cortex-foam interface. In the foam-filled parts of the shaft, the larger foam cells, the higher filling percentage, and the higher area-ratio of foam and cortex lead to a higher damping ratio. The main deformation modes in these foams are bending, shear, and buckling (Vincent and Owers 1986; Gibson et al. 1989; Gibson and Ashby 1997). When the shaft is under bending, the cells remote from the central axis have higher stress. At strains, the cell walls bend elastically. These cells undergo shear deformations, and their walls may have no stretching. However, at large strains, cells may collapse by elastic buckling, and plastic yielding happens. Finally, the stiffness of cell arrays may increase rapidly after the densification due to the plastic yielding (Triantafillou et al. 1989; Gibson and Ashby 1997).

Energy dissipates during the deformation of foams across layers, reducing crack propagation and delaying the local buckling (Vincent and Owers 1986; Bonser 2001). In addition, energy is absorbed by weaving fibrils of the cell walls, causing an intrinsic damping and possible fiber pullout (Andersson et al. 2010).

The difference in damping properties under the two deflection directions may rely on the anisotropy of the cortex and foam structure in the shaft. The cell sizes, their relative density, and anisotropy in their shape may also influence the foam's mechanical properties and damping.

In conclusion, the combined cortex and gradient foam contribute to a lightweight shaft's specific graded damping properties. Especially the highly-damped shaft base anchored to the wing bone assures stability during flapping flight.

5.2. Damping properties of vanes

As shown in this study, the significance of vanes for reducing feather vibration was confirmed by the higher damping ratios of the feathers with vanes. Under both excitation directions, the damping ratios of feathers with the vanes were significantly higher than those without the vanes. Compared to the intact feathers, the damping ratios decreased by 38-60% after trimming the vanes (Deng et al., 2022).

For the feathers with vanes, the damping ratios for different excitation directions differed considerably. For shafts without vanes, the damping ratios significantly differed only for vibrations perpendicular to the vane plane. In the feathers with vanes and without vanes, the damping ratio perpendicular to the vane plane was the highest at the vertical excitation. Possible damping mechanisms of the vanes are listed below.

Three damping mechanisms of vanes were discussed.

Aerodynamic damping. Feathers are practically air-impermeable by the pressure gradient in the overlapping inner and outer vanes during the flapping (Mueller and Patone, 1998). Airflow could dampen the vibrations of an airfoil (Akay and Carcaterra, 2014). In wingbeat, the air friction affects the damping of feathers.

Structural damping. Structural damping is also a significant factor at low speeds (Sun, 2012). Under loading, the barbules and hooklets deform; their relative movements cause interfacial friction, and the bending leads to the storage of elastic energy. Furthermore, when anchored hooks separate, the stored energy in deformation is released and dissipated. The collective effect of neighboring barbs accumulates more elastic energy and dissipates energy (Kovalev et al., 2013). Vibrations excited perpendicular to the vanes are partially transferred to the vane plane.

Material damping. It refers to the inherent dissipation of energy in material deformation (Akay and Carcaterra, 2014). Both the shaft and barbs of the feathers are

filled with foam and can effectively contribute to the damping of vibrations (Deng et al., 2022).

5.3. Damping of zipped vanes and unzipped vanes

Our investigation of vanes confirmed the higher damping capacity in the feathers with zipped vanes compared to those with unzipped vanes in the atmosphere and vacuum. The damping ratios of the feathers at deflections within the vane plane and perpendicular to it are different. The contributing mechanisms are discussed as follows:

Aerodynamic damping. Due to the effect of the air on vibrating feathers, the friction between the airflow and feather surface could dampen vibrations (Akay and Carcaterra, 2014). The planar shape of the vane and the hooked microstructure in the zipped vane enhance the damping ratios, explaining why, in the air, the feather damping decreases from 20% to 50% after unzipping (Deng et al., 2023). In addition, the feathers with zipped vanes had lower fundamental frequencies in both deflection directions. In vacuum, however, the only difference between zipped and unzipped vanes was observed in the vertical deflection. This may be explained by the fact that the overlapping and interlocking of barbs in the vertical deflection still works, even if they are unzipped, hindering the barb separation and allowing the vane compression (Deng et al., 2023).

Structural damping. The structural damping is responsible for 3.3 times (at vertical deflections) and 2.3 times (at horizontal deflections) difference in damping ratio between zipped and unzipped feathers in vacuum. Under deformation, the barbules and hooklets undergo relative displacements and cause moving, sliding, anchor-breaking, twisting, uncoupling, and recoupling. The resulting friction, caused by structural damping, leads to energy dissipation in the system. Besides, the extension of a zipped vane is irregular because of the collective effect in hooklets' separation (Kovalev et al., 2013), which facilitates the oscillation energy transfer from natural frequency to higher harmonics. The energy dissipation is typically higher at higher frequencies.

Material damping. As an inherent energy dissipation during material deformation, it is the lowest if compared to the two mechanisms mentioned above.

In summary, higher damping in the zipped vanes of primary feathers, compared to unzipped ones, is confirmed in the air and vacuum. In the air, the planar surface and the interlocked barbs in the vane improve its aerodynamic damping. In vacuum, the vane microstructure significantly contributes to its high damping due to the cooperative effect of overlapping barbs in zipped vanes, helping the energy dissipation. Finally, the shaft and barbs filled with the gradient foam are thought to further improve the feather's damping.

5.4 Outlook

In this study, we investigated the damping behavior of shafts and vanes in a single primary feather. Two possible directions for future research are worth following.

First, future research could track changes in the groups of the adjacent 3 or 5 feathers to investigate how damping behavior changes and how a varied damping system develops in the overlapping feathers. In addition, these quantitative data on specific locations from pigeons' feathers might help interpret the significance of overlapping feathers in the wing.

Second, three-dimensional printing of different feather-like systems (with vane, without vane, with different internal structures, etc.) might be further performed in the lab. Those upscaled biomimetic systems could also be printed with barbs and barbules (interlocking with hooks or not interlocking without hooks). Then, by adjusting their hooked numbers or overlapped layers, it is possible to control the damping properties at different states. Future research in the field of engineering could use the data from this study to develop more enhanced damping systems. Such bioinspired systems could improve the wing stability in flying robots with flapping wings or might be used for various shock-absorption applications in the technology. Flying robots with more stable wings could benefit from energy conservation and make less noise.

References

-
- Akay, A., & Carcaterra, A. (2014). Damping mechanisms. In Hagedorn P., Spelsberg-Korspeter G. (Eds) *Active and passive vibration control of structures*, 259-299. CISM International Centre for Mechanical Sciences, Springer, Vienna.
- Deng, K., Kovalev, A., Rajabi, H., Schaber, C. F., Dai, Z. D., & Gorb, S. N. (2022). The damping properties of the foam-filled shaft of primary feathers of the pigeon *Columba livia*. *Science of Nature*, 109(1). 10.1007/s00114-021-01773-7.
- Deng, K., Rajabi, H., Kovalev, A., Schaber, C. F., Dai, Z. D. & Gorb, S. N. (2023). The role of vanes in the damping of bird feathers. *J. Bionic Eng.*, 20, 1646-1655.
- Deng, K., Schaber, C. F., Kovalev, A., Rajabi, H., Dai, Z. D. & Gorb, S. N. (2023). Aerodynamic vs. frictional damping in primary flight feathers of the pigeon *Columba livia*. *Applied Physics A*, 129, 121.
- Gibson, LJ, Ashby, MF, Zhang, J, & Triantafillou, TC. (1989). Failure surfaces for cellular materials under multiaxial loads - I. Modeling. *Int. J. Mech. Sci.* 31 (9), 635-663.
- Gibson, LJ, & Ashby, MF (1997) *Cellular solids: Structure and properties*. Cambridge, UK.
- Kovalev, A., Filippov, A. E., & Gorb, S. N. (2013). Unzipping bird feathers. *Journal of Royal Society Interface*, 11, 20130988.
- Liu, Z. Q., Jiao, D., Meyers, M. A., & Zhang, Z. F. (2015). Structure and mechanical properties of naturally occurring lightweight foam-filled cylinder: The peacock's tail coverts shaft and its components. *Acta Biomaterialia*, 17, 137-151.
- Mueller, W., & Patone, G. (1998). Air transmissivity of feathers. *J. Exp. Biol.*, 201(18), 2591-2599.
- Vincent, JFV, & Owers, P (1986) Mechanical design of hedgehog spines and porcupine quills. *J. Zool.* 210 (1), 55-75.
- Sun, J. (2012). *Vibration characteristics and structural damping of rotating compressor blades*. KTH Royal Institute of Technology, Stockholm, Sweden.

CHAPTER 6

Conclusions

Unwanted vibrations in the bird wings and feathers may lead to potential instability during flight. Therefore, high damping is desirable for low vibration and noise reduction. This study was devoted to studying the damping mechanisms underlying various kinds of microstructure of primary feathers. Based on the obtained data, the following conclusions can be drawn.

- i. Although feathers of wings, in particular primaries, undergo vibrations, they are capable of damping properties, decreasing vibrations and reducing their negative impact on flight stability.
- ii. The feather shaft represents a natural gradient material with different damping properties depending on its microstructure. This study provides the first indication of the graded damping properties in the shaft. Under horizontal and vertical deflections, the damping ratio at the base is highest in 1st mode, whereas the maximum values were observed in the middle of the shaft in 2nd mode. The higher damped base and middle of the shaft close to the bone assure strong wing stability.
- iii. In the shaft, the medulla cells are based on the weaving of keratin fibrils with hierarchical porosity. The higher damping properties are influenced by the morphology of the foam, such as the size of foam cells, the foam density, and the area ratio between the foam and cortex. The deformation and densification of the foam cause energy dissipation. This spectrum of structural features offers different possibilities to design technical structures with adjustable damping properties by varying and combining different foam cell sizes, cell porosity, and distribution of cells.
- iv. Compared to the bare shaft, the presence of vanes has been confirmed to enhance the damping properties of feathers by decreasing the number of vibration modes, lowering the first frequency, and increasing the damping ratios.

-
- v. In the atmosphere, the zipped vanes had higher damping ratios along the direction of excitations. No significant difference was found in both ζ_x and ζ_y in the unzipped vanes at two deflection directions; ζ_x and ζ_y were calculated for vibrations in X (parallel to the vane) and Y (perpendicular to the vane) directions. The unzipping changed the directional damping of vanes, possibly affecting the integrity, decreasing the hooked interactions between barbs, and reducing the vibrations transferred between the perpendicular and parallel directions to the vane plane.
 - vi. In vacuum, the damping ratios of the zipped vanes were higher than that of unzipped vanes. In the zipped vanes, the damping ratios of the direction, same as the excitation, were higher than the damping ratios of the perpendicular direction. In unzipped feathers, the damping ratio under horizontal deflection was higher than under vertical deflection.
 - vii. Three mechanisms mainly contribute to the damping of the vanes. First, aerodynamic damping is related to the effect of the air. Airflow could aerodynamically dampen the vibrations of the feathers. The intact zipped planar shape and the hooked structure enhance damping ratios. Second, structural damping is related to the energy dissipation from the displacements, uncoupling, and recoupling from barbules and hooklets. Third, material damping is an inherent energy dissipation mechanism during material deformation.
 - viii. The design strategy of foam medulla and zipped vanes in feathers can inspire efficient, lightweight engineering materials with tailored damping properties for various applications in aerospace technology and other fields.

Declaration

Hereby I declare that the present dissertation, apart from the supervisor's guidance, is all my own work. The thesis has not been submitted either partially or wholly as a part of a doctoral degree to another examining body. The essential parts of the work are published in scientific journals. The thesis is in compliance with the Rules of Good Scientific Practice of the German Research Foundation. I also declare that no academic degree has ever been withdrawn from me.

Kiel, *Kai Deng*